

IS-T- 858

Effect of backmixing on pulse column performance

Yen-Wu Miao

MASTER

M. S. submitted to Iowa State University

Ames Laboratory, DOE

Iowa State University

Ames, Iowa 50011

Date Transmitted: May 1979

PREPARED FOR THE U. S. DEPARTMENT OF ENERGY
UNDER CONTRACT NO. W-7405-eng-82

— NOTICE —
This report was prepared as an account of work sponsored by the United States Government. Neither the United States nor the United States Department of Energy, nor any of their employees, nor any of their contractors, subcontractors, or their employees makes any warranty, express or implied, or assumes any legal liability or responsibility for the accuracy, completeness or usefulness of any information, apparatus, product or process disclosed, or represents that its use would not infringe privately owned rights

DISTRIBUTION OF THIS DOCUMENT IS UNLIMITED

DISCLAIMER

Portions of this document may be illegible in electronic image products. Images are produced from the best available original document.

— NOTICE —

This report was prepared as an account of work sponsored by the United States Government. Neither the United States nor the United States Department of Energy, nor any of their employees, nor any of their contractors, subcontractors, or their employees, makes any warranty, express or implied, or assumes any legal liability or responsibility for the accuracy, completeness, or usefulness of any information, apparatus, product or process disclosed, or represents that its use would not infringe privately owned rights.

Available from: National Technical Information Service
U. S. Department of Commerce
P.O. Box 1553
Springfield, VA 22161

Price: Microfiche \$3.00

Effect of backmixing on pulse column performance

by

100

Yen-Wu Miao

A Thesis Submitted to the
Graduate Faculty in Partial Fulfillment of
The Requirements for the Degree of
MASTER OF SCIENCE

Department: Chemical Engineering
and Nuclear Engineering
Major: Chemical Engineering

Approved:

Lawrence Burkhardt
In Charge of Major Work

George Burnetts
For the Major Department

Dr. Jacobson
For the Graduate College

Iowa State University
Ames, Iowa

1978

1172526

TABLE OF CONTENTS

	Page
NOMENCLATURE	iii
ABSTRACT	vii
INTRODUCTION	1
Pulse Column	1
Dispersed Phase Holdup	6
Backmixing	9
Backmixing Model	16
LITERATURE REVIEW	18
Dispersed Phase Holdup	18
Backmixing	29
DEVELOPMENT OF PROPOSED DISPERSED PHASE HOLDUP CORRELATION	41
DEVELOPMENT OF PROPOSED BACKMIXING CORRELATION	59
PULSE COLUMN MODEL	69
SIMULATION STUDIES	74
RESULTS	79
CONCLUSIONS AND RECOMMENDATIONS	97
LITERATURE CITED	98
ACKNOWLEDGMENTS	103
APPENDIX: SIMULATION PROGRAM	104

NOMENCLATURE

a	Amplitude, inches/cycle
\bar{a}	Specific interfacial area, cm^2/cm^3
A	Pulse amplitude, cm/cycle
$(Af)_E$	Pulse velocity at emulsion region, cm/sec
$(Af)_M$	Pulse velocity at mixer-settler region, cm/sec
$(Af)_T$	Pulse velocity at transition region, cm/sec
α	Backflow ratio, $\alpha = \text{interstage mixing flow rate}/\text{main flow rate}$
3_d or L	Bottom disengagement section of pulse column
s	Miyauchi's backmixing correlation factor relates to the liquid motion instability
β_c	Constant for calculating ψ , $\beta_c = s^2/((1 - s)(1 - s^2))$
C_s	Hundredth concentration stage
d_p	Drop diameter
\bar{d}_p	Mean drop diameter
Δ	Difference symbol
Δt	Time interval for digital simulation calculations, sec
ΔZ	Interval of finite difference equation
D_h	Plate hole diameter, cm
D_t	Pulse column internal diameter, cm
E	Dispersion coefficient, cm^2/sec
ϵ	Holdup fraction
E_x	Distribution coefficient of solute X, $E_x = X_d/X_c$
f	Pulse frequency, cycle/sec
F	Superficial flow rate, cm/sec

F	Interstage mixing flow rate, $F = Af\epsilon_i$, cm/sec
$\phi(1-\epsilon_d)$	A function of holdup which accounts for the effect of adjacent drops on one another
f_H	Transition frequency, cycle/sec
f_r	Drag coefficient for spheres, dimensionless
f_T	A function of extraction factor
γ	Interfacial tension, dynes/cm
h	Dispersed phase volume holdup, cm ³
H	Continuous phase volume holdup, cm ³
H_t	Pulse column effective height, cm
H.T.U.	Overall transfer unit height, cm
K, K_1, K_2	Constants
K_d	Dissociation constant for PuNO_3^{+3}
K_{oi}	Overall interphase mass transfer coefficient, cm/sec
Λ	Extraction factor $\Lambda = E_x F_c / F_d$
λ_0	Principal length of turbulence, cm
ρ	Liquid density, grams/liter
N	Last stage number
N_F	Feed stage number
n	Total stage number
N.T.U.	Number of transfer units
N_{oi}	Overall number of transfer units for phase i
N_{oi0}	Single stage number of transfer units for phase i
OP	Interstage pseudoorganic phase flow rate, liter/sec
P_e	Peclet number
$P_i B$	Peclet number of phase i, $P_i B = F_i H_t / E_i$; i = c, or d

P_0	Mean rate of energy dissipation, cm^2/sec^3
ψ	Miyauchi's holdup correlation constant relates to the energy
Rxn 1 to Rxn 5	Chemical reaction in material balance, mole/liter
s	Plate free area fraction
σ^2	Variance of tracer residence distribution, sec^2
S_p	Pulse column plate spacing, cm
T	Pulse column plate thickness, cm
T_d	Top disengagement section
\bar{u}_t	Terminal velocity of droplet relative to the continuous phase, cm/sec
v	Volume velocity, liter/sec
V	Volume of a single state, liter, or volume velocity, $1/\text{sec}$
\bar{v}	Actual linear flow rate of a phase, cm/sec
\bar{v}_0	Characteristic velocity of droplet, cm/sec
\bar{v}_r	Velocity of the dispersed phase relative to the aqueous phase, cm/sec
v_s	Slip velocity (average velocity of the dispersed phase droplets), cm/sec
X or $[X]$	Concentration of solute X , mole/liter, in continuous phase or dispersed phase
$[X]^t$	Solute X concentration before time Δt , mole/liter
$[X]^{t+\Delta t}$	Solute X concentration after time Δt , mole/liter
X^*	Equilibrium concentration of solute X , between the two phases, mole/liter

Subscripts

c	Continuous phase
cf	Continuous phase at flooding point

d	Dispersed phase
df	Dispersed phase at flooding point
E	Extractant
F	Feed
i	Stage number or number index
j	Stage number or number index
m	Constant or mixed phase
o	Initial condition
R	Raffinate
S	Stripping

ABSTRACT

A critical survey of the published literature concerning dispersed phase holdup and longitudinal mixing in pulsed sieve-plate extraction columns has been made to assess the present state of the art in predicting these two parameters, both of which are of critical importance in the development of an accurate mathematical model of the pulse column. Although there are many conflicting correlations of these variables as a function of column geometry, operating conditions, and physical properties of the liquid systems involved it has been possible to develop new correlations which appear to be useful and which are consistent with much of the available data over the limited range of variables most likely to be encountered in plant sized equipment.

The correlations developed were used in a stagewise model of the pulse column to predict product concentrations, solute inventory, and concentration profiles in a column for which limited experimental data were available. Reasonable agreement was obtained between the mathematical model and the experimental data. Complete agreement, however, can only be obtained after a correlation for the extraction efficiency has been developed. The correlation of extraction efficiency was beyond the scope of this work.

INTRODUCTION

Pulse Column

Credit for the invention of the pulse column is usually given to Willhem Van Dijck. The equipment described in his 1935 patent (55) is for a countercurrent extraction column which contains sieve plates spaced at intervals along a central shaft. The two liquids are dispersed by a motor which moves the plate assembly up and down. Although such a column is now marketed commercially by the Chem-Pro Equipment Corporation, this is not the basic operating principle of what has come to be known over the last 30 years as a "pulse column." His patent also mentions the possibility of pulsing the liquid in a column with stationary plates.

Carl Groot, as cited by Sege and Woodfield (46), who worked on the early development of liquid-liquid contactors for use in nuclear fuel reprocessing, first suggested that a unit similar to the one patented by Van Dijck be used in fuel reprocessing. He proposed that the two liquid phases be dispersed by pulsing the contents of the column up and down. Although this required a greater power input than the moving plate technique, it permitted the pulsing equipment to be placed some distance from the column. For processing highly radioactive materials, this meant that the pulse generator could be remotely located in a shielded area away from the column and attached to the column by a large pipe. The use of air in the pulse leg then served to isolate the radioactive material in the column and thus permitted easier maintenance of the pulse generator since it was in an area of low level radioactivity.

The pulse column as we know it today uses the idea of pulsing the liquids in the column. It has been used widely in the nuclear industry because of its ease of maintenance, high mass transfer efficiency, and short residence time and is now finding application in other areas of the chemical process industry.

A functional diagram of the pulse column is shown in Figure 1. Perforated plates are spaced at intervals up the column. Heavy liquid enters from the top of the column and light liquid enters from the bottom. Ordinarily the size of the holes in the perforated plates is small enough that no countercurrent flow occurs through the column due to gravity alone. The pulse generator at the bottom serves to disperse or mix the two liquid phases and also to pump the liquids through the column.

In Figure 1 the light phase is the dispersed or discontinuous phase and the heavy phase is the continuous phase. The light phase is present in the smaller quantity, as is customary for the discontinuous phase, and the principal interface is located in the top end-section of the column. If the heavy phase were the discontinuous phase then heavy phase would be present in the smaller quantity and the principal interface would be in the bottom end-section of the column.

Figure 2 shows the operating characteristics of a pulse column. The curve was presented by Sege and Woodfield (46) to illustrate the various types of dispersion obtained as a function of the flow rates and the pulse frequency. The curve only shows general trends and has no numerical values along its axes.

Choose an arbitrary total flow rate and follow a horizontal line across the figure. Region A is a flooding region in which the column will

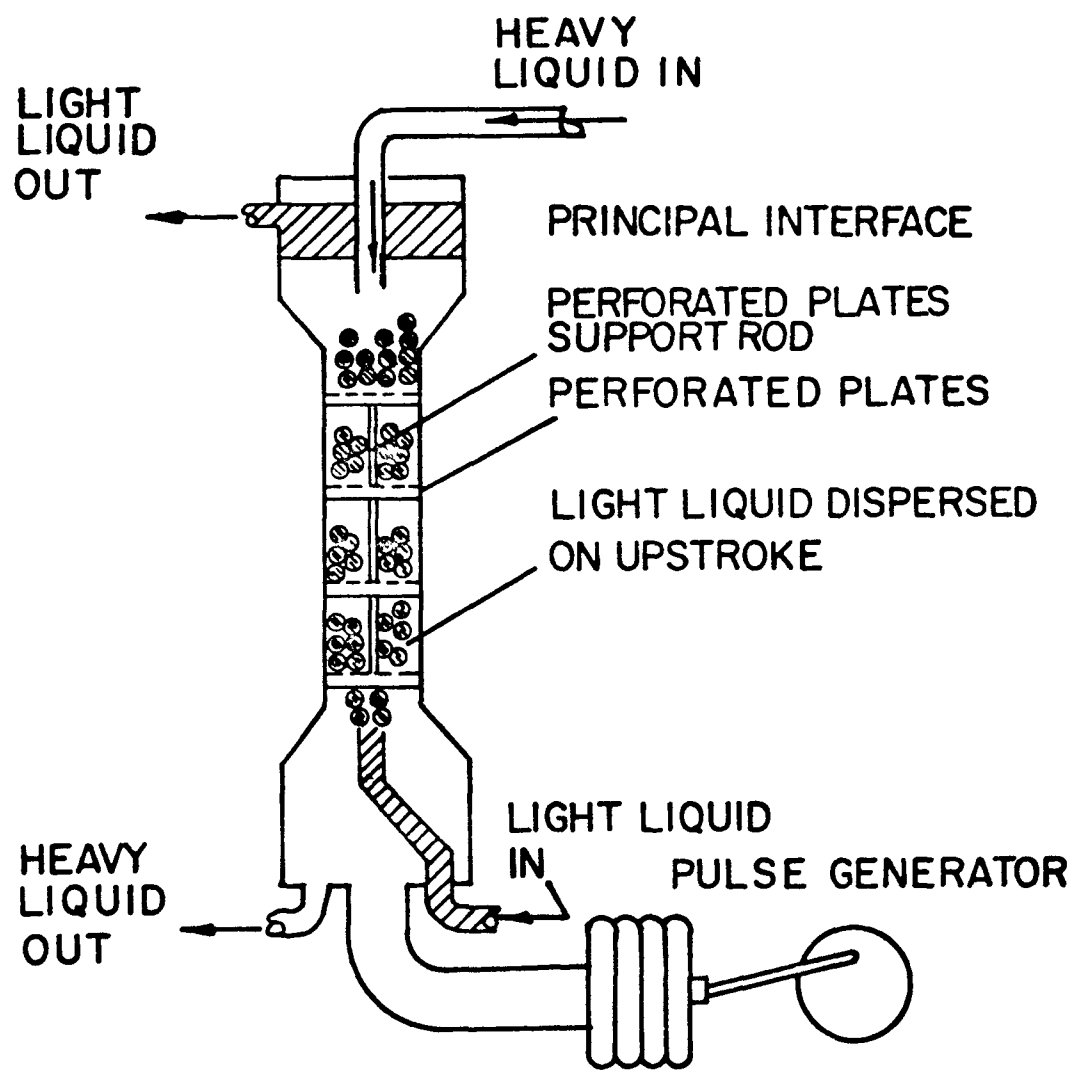


Figure 1. Diagram of perforated plate pulse column.

INCREASING THROUGHPUT —
GAL/(HR.)(SQ.FT.), SUM OF BOTH PHASES
FLOW RATE:

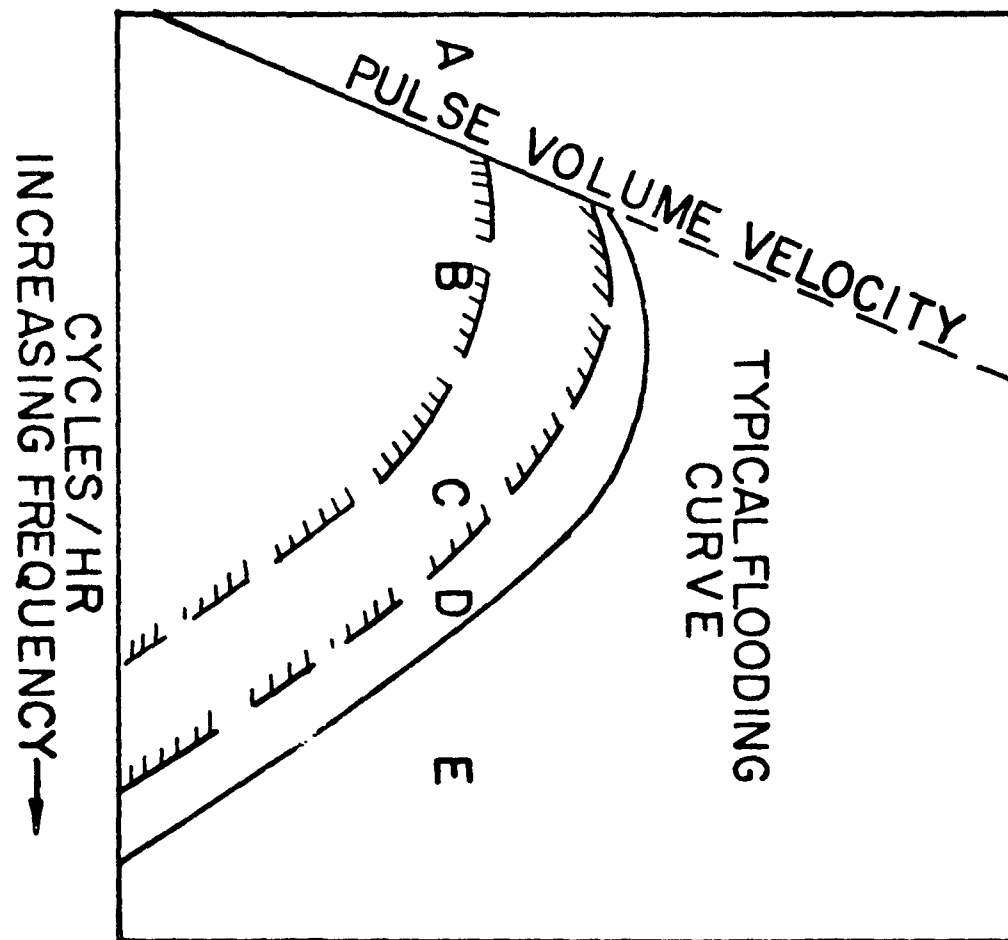


Figure 2. Operating characteristics of a pulse column at constant amplitude.

not operate because the amount of pulsation is too small to pump liquid through the column as fast as it is fed at each end. At a point on the line marked "pulse volume velocity," the pulsation applied to the column is just enough to maintain a net flow equal to the superficial flow rates, or the rates at which the two liquids are being fed to the column. This point is called the lower flooding limit or the point of incipient flooding due to insufficient pulsation.

When the pulse frequency is increased so that the column operates in area B, mixer-settler operation is obtained. The two phases settle out completely between pulses; thus there is an alternating sequence of mixing and settling in each portion of the column between two adjacent perforated plates. When a pulse column is operated in region C, the two phases in the column give the appearance of an homogeneous emulsion at all times and so the area is called the "emulsion region."

Increasing the pulse frequency still further causes the dispersion to become irregular and nonuniform. Large globules of the liquid begin to appear and local flooding, or reversal of the dispersion, may occur. This unstable region is indicated by area D in Figure 2. The transitions between regions B and C, and between regions C and D are gradual and not well-defined.

The flooding curve which separates regions D and E represents the locus of points at which the net flow of liquids through the column is again just equal to the superficial flow rates. This time the trouble is not too little pulsation but too much pulsation. Hindered settling has reduced the net flow of liquid through the column. A point on this line

is often referred to as the upper flooding point or the point of incipient flooding due to excessive pulsation.

The pulse column thus has two flooding points. Both are sharply defined and the permissible operating range of the column is sandwiched between these two flooding points. The extraction efficiency varies throughout this range and the resulting degree of separation obtained depends on the net effect of two opposing phenomena. Ideally, increasing the pulsation applied to the extractor produces better dispersion of the phases and creates more interfacial area for mass transfer. Turbulence within the column is increased, tending to improve the rate of extraction. On the other hand, backmixing, or recycling, is present throughout the operating range of the column. This decreases the local concentration gradient and reduces the extraction efficiency.

Dispersed Phase Holdup

The amount of dispersed phase present in the column is an important parameter and is called the "holdup." The residence time distribution, the interphase mass transfer rates and the degree of backmixing are all a function of the holdup. Dispersed phase holdup in the pulse column is defined as the percent of total volume occupied by the dispersed phase between all the sieve plates when the column is operating at steady state conditions.

During column operation dispersed phase is pushed up through the holes in the perforated plates on an upstroke of the pulse generator. Liquid jets issuing from the plate perforations constitute a kind of

couette type of shear-flow field between the expanding jets in the direction of pulsation and globules form. The pressure distribution on the globule causes it to deform into an ellipsoid. After sufficient elongation, breakup may occur (21) and smaller droplets may form.

In the mixer-settler region the holdup decreases as the amplitude or frequency of pulsation increases, as shown in Figure 3. Holdup goes through a minimum at the transition point between mixer-settler and emulsion operation. As the pulsation is increased further, the droplets become smaller and, because of their slower rise time, the holdup in the column increases and reaches a maximum at the upper flooding point.

Holdup has been measured both directly and indirectly using the techniques listed below:

(1) Indirect methods:

- (a) Measurement of electrical resistance between the plates (Defives and Schneider (14)).
- (b) Measurement of the effective specific gravity of the contents of the column (Jones (23)).

(2) Direct methods:

- (a) Analysis of the relative phase volumes in a sample of the column contents removed from the column very rapidly (Wilburn, as cited by Bell and Babb (3)).
- (b) Direct measurement of total relative phase volumes in the column after it is shut down (Graham (19)).
- (c) Utilization of the change in the water-organic interface at the top of the column while the column is running after all inlet flows have been stopped (Sehmel and Babb (47)).

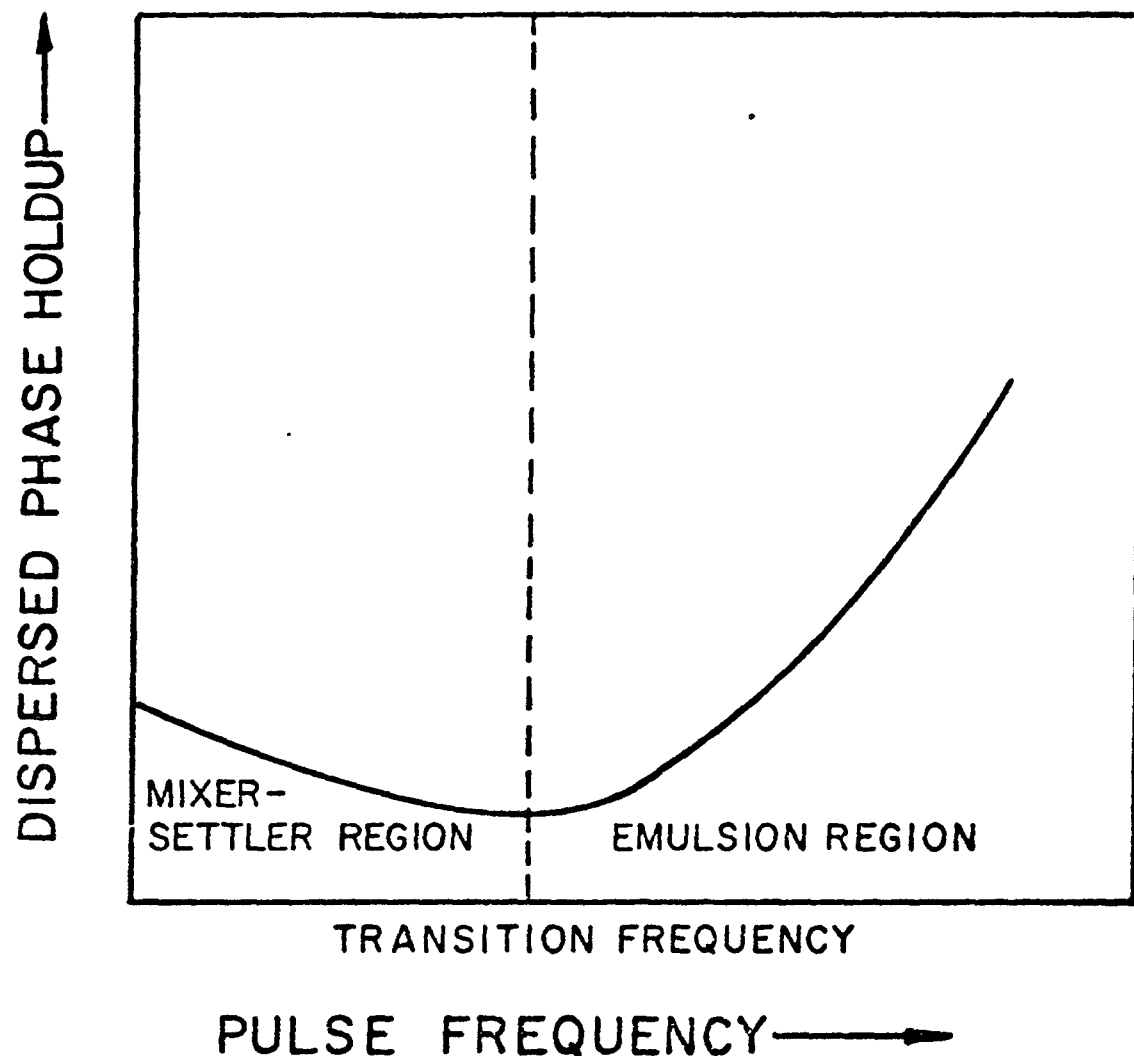


Figure 3. Dispersed phase holdup characteristics of a pulse column at constant amplitude.

(d) A shutter plate technique by which the active portion of the column can be quickly isolated (Bell and Babb (3)).

Table 1 shows that the direct measurement methods have been most widely used. Also, see Figure 6, herein.

The dispersed phase holdup of a pulse column has the following characteristics:

- (1) It is a function of the geometry of column, the pulse amplitude, and pulse frequency, the dispersed phase flow rate, the surface properties of the plate materials, and the physical properties of the liquids involved.
- (2) The continuous phase flow rate has little effect.
- (3) It is uniform throughout the column for a column having more than 23 cells.
- (4) It increases with increasing plate spacing, plate hole diameter and dispersed phase flow rate.
- (5) Dispersion is governed by the ratio of viscosity of the two phases.
- (6) Interfacial tension is important in determining the size of the droplets.

Backmixing x

Backmixing in cylindrical flow is a nonideal flow pattern that is intermediate between the two ideal cases of plug flow and perfect mixing. It implies a backflow against the direction of the main stream so that some parts of the liquid actually move backwards relative to a fixed

Table 1. Dispersed phase holdup in pulse column measurement experimental details

Investigator	Column geometry					Operating variables			
	D _t cm	H _t m	S _p cm	D _h cm	s	A cm/ cyc	f cyc/ sec	F _c cm/ sec	F _d cm/ sec
Arthayukti et al. (2)	5.0	2.0	5.0	0.2	0.2	1.0 ~ 9.0	2.0 ~ 0.3	0.014 ~ 0	0.014 ~ 0.042
Bell and Babb (3)	5.08		5.59	0.32	0.23	0 ~ 12.7	0.3 ~ 3.3	0 ~ 0.54	0.12 ~ 0.58
Biery (4)	7.62	6.1	5.71	0.16	0.23	0.3 ~ 3.6	0.4 ~ 3.5	0.1 ~ 0.2	0.25 ~ 0.45
Cohen and Beyer (11)	2.54		5.08	0.32	0.09	0.38 ~ 1.14	0.28 ~ 1.2	0.03 ~ 0.16	0.03 ~ 0.16
Eguchi and Nagata (15)	5.8		5.2	0.15	0.08	0.1 ~ 0.85	0.5 ~ 3.3	0.14 ~ 0.44	0.18 ~ 0.38
Kagan et al. (25)	5.6	4.0	5.0	0.2	0.08	0.5 ~ 1.5	0.8 ~ 1.67	0.15 ~ 0.5	0.3 ~ 1.0
Miyauchi and Oya (36)	3.2 5.4	3.7 7.8 8.6	1.0 ~ 10.0	0.15 ~ 0.30	0.09 ~ 0.19	0 ~ 1.5	0.4 ~ 3.0	0.03 ~ 0.27	0.03 ~ 0.26
Sato et al. (45)	3.5	0.69	2.5	0.1 ~ 7.0	0.081 ~ 0.33	0.6 ~ 2.0	0.3 ~ 3.3	0.1 ~ 1.0	0.1 ~ 0.5
Sehmel and Babb (47)	5.05	2.2	5.03	0.32	0.23	0.64	0.3	0	0.174
						5.2	3.5	0.43	0.43

System H_2O and	Method of measurement	ϵ_d range
CC ₁₄	Draining the column and measuring the volume	0.01 ~ 0.12
M.I.B.K. Hexane	Shutter plate technique	0.01 ~ 0.08
50% TBP kerosene	Suddenly stopped and measured the dispersed phase layer height on each stage	0.08 ~ 0.25
Isoamyl alcohol	Draining to a graduated cylinder and measured	0.1 ~ 0.26
Ketone	Not mentioned	0.03 ~ 0.15
Kerosene	Not mentioned	0.03 ~ 0.21
M.I.B.K.	Measured volumetrically by closing all inlet and outlet at upper disengaging section	0.005 ~ 0.34
M.I.B.K.	Not mentioned	0.025 ~ 0.23
Hexane Benzene M.I.B.K.	Closed inlet and outlet valve and measure the ratio at contacting section	0.02 ~ 0.26

point. From the viewpoint of a differential process, backmixing means a random axial flow superimposed on the main flow and leads to the axial eddy diffusion concept. These same basic concepts also apply to the flow of each phase in the pulse column.

For pulse column operation in the mixer-settler region, a layer of the lower specific gravity organic phase forms from the rising organic droplets and collects below each plate at the end of each pulsation half cycle. The continuous water phase is backmixed principally during the upstroke. The organic layer is first forced through the plate and the remaining volume of liquid displaced during an upstroke then consists of the continuous water phase as a backmix stream.

As the pulse frequency is increased through the mixer-settler region all of the organic droplets do not have sufficient time between pulsation cycles to collect under the plates. Hence, the thickness of the organic layer decreases under each plate and results in an increased amount of water backmixed across a plate during each cycle (48). As the pulsation intensity increases, the effect of the distribution of droplet velocities becomes more important. The jetting of the continuous phase through the plates forms vortices and eventually the vortex fields become so strong that the dispersed phase backmixes through the holes in the plate owing to the strong drag forces. The axial mixing in the dispersed phase becomes truly diffusive owing to increased droplet interactions and can be treated as a second continuous phase.

Backmixing increases the residence time of fluid elements and the small droplets increase the interphase mass transfer contact area. Also,

backmixing reduces the local concentration gradients and decreases the extraction efficiency. In some production sized extraction columns, 60 to 75% of the necessary effective height of the column may be accounted for by the effects of backmixing (32).

Figure 4 gives a graphical comparison of the typical concentration profiles in a pulse column with and without backmixing. Both the true driving force, taking backmixing into account and the apparent driving force, without making such allowance, can be seen.

Backmixing is evaluated by measuring its effect on the distribution of a solute concentration in the column. The methods that have been used are listed below:

(1) Model comparison method (concentration profile)

This method uses the concentration profiles of the transferring solute. The experimental profile is compared with concentration profiles calculated from a one-dimensional backmixing steady state model, and using a two-dimensional search technique, values of both the longitudinal dispersion coefficient, E , and the product of the mass transfer coefficient, times the interfacial area, $K_{0i}\bar{a}$, are found which provide the best fit between the experimental and the calculated concentration profiles. The one-dimensional backmixing steady state diffusion model shown below is used to compute the theoretical profiles.

$$E_c \frac{d^2X_c}{dZ^2} - F_c \frac{dX_c}{dZ} - K_{0c}\bar{a}(X_c - X_c^*) = 0 \quad (1)$$

$$E_d \frac{d^2X_d}{dZ^2} - F_d \frac{dX_d}{dZ} + K_{0c}\bar{a}(X_c - X_c^*) = 0 \quad (2)$$

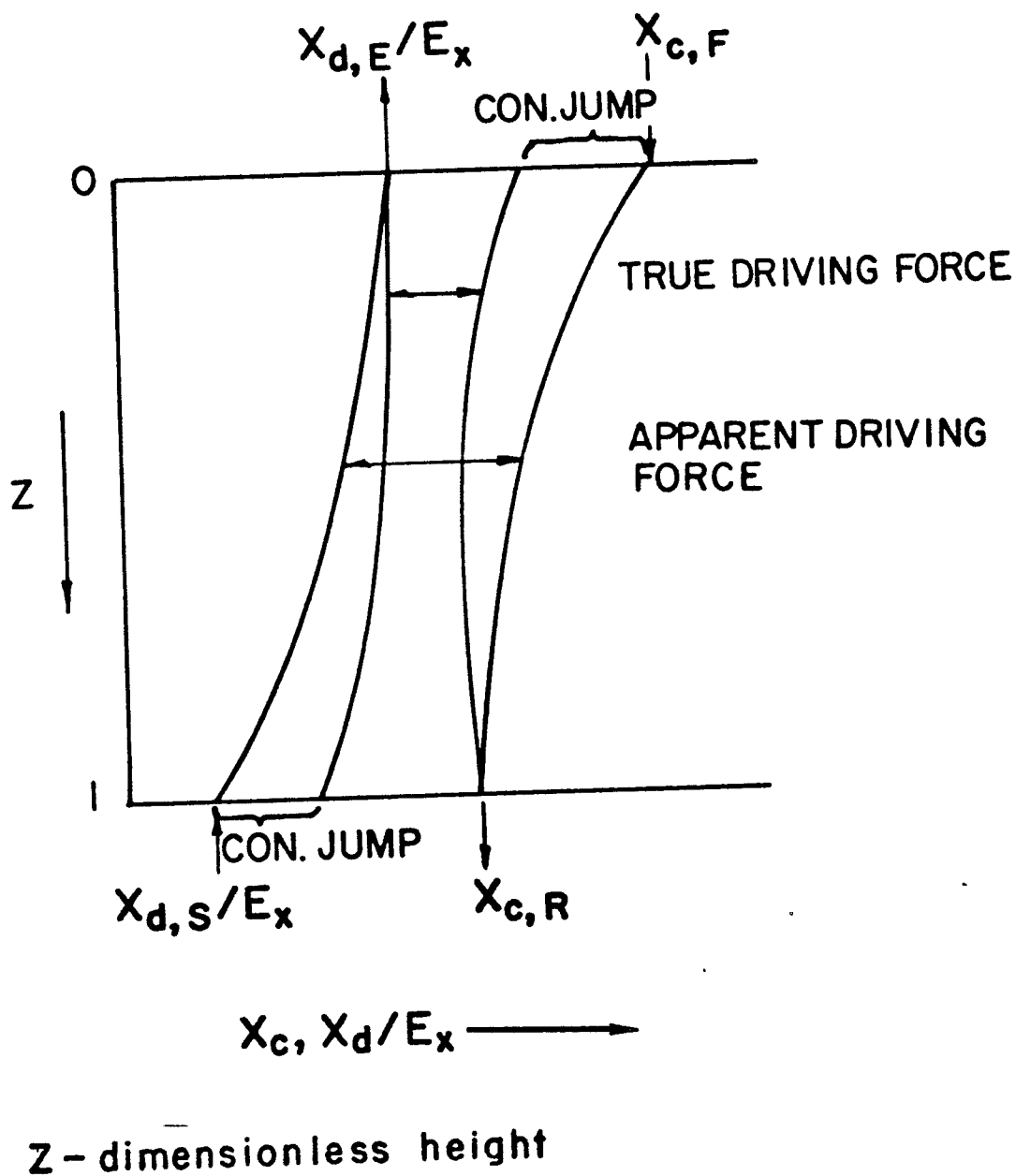


Figure 4. Concentration profiles in the column.

(2) Stimulus-response techniques (tracer techniques)

Because of experimental difficulties in measuring solute concentrations, a more widely used method involves the injection of a tracer into the system. The tracer used in backmixing experiments has many forms, but it should be soluble in only one of the two phases. Typical tracer experiments include the use of ionization-current counting of radioactive materials, the measurement of electrical conductivity or electrode potential and the absorption of ultraviolet or visible light. The most popular method with regard to aqueous phase determinations, however, is to use a salt tracer and measure its concentration by electrical conductivity. Radioactive tracers have the advantage that their concentrations can be detected from the outside of the column continuously, thus avoiding measurement lags in the system and interference with the liquid flow pattern.

Backmixing evaluation methods by using tracer techniques are:

(1) Steady state method

The tracer is injected continuously into the column and the steady state tracer concentration profile is measured along the column upstream from the injection point. By comparison of the concentration versus column height with the right mathematical model, the backmixing coefficient can be evaluated.

(2) Dynamic method

A tracer is injected into the column and the time dependence of the tracer concentration is measured at a fixed point downstream from the injection point. A breakthrough curve is obtained. The stimulus injection of the tracer is usually an impulse input. The tracer concentration

profiles are compared with the profiles calculated by the appropriate mathematical model and the backmixing coefficient determined.

(3) Two detection point technique (radioactive tracer method)

The dynamic method needs a perfect pulse input of tracer, which is difficult to obtain in practice. Aris (1) and Bischoff and Levenspiel (6) have developed a method which avoids the mathematical requirement for perfect pulse injection. In this method tracer concentration measurements are taken at two points within the test section of the column, the variances are calculated from the two experimental breakthrough curves, and the backmixing coefficient calculated from the relation:

$$\Delta\sigma^2 = \sigma_2^2 - \sigma_1^2 = 2/P_i B = 2E_i/F_i H_t \quad (3)$$

The backmixing of both phases has the following characteristics:

- (1) It is a function of the geometry of column, the pulse amplitude, and pulse frequency, the phase flow rate, the phase holdup fraction and the physical properties of the liquids involved.
- (2) It is independent of column diameter.
- (3) It increases with increasing plate spacing, plate hole diameter, phase flow rate, and phase holdup.
- (4) Interfacial tension is important in determining the size of the droplets.
- (5) Viscosity and density have little effect.

Backmixing Model

There are two models that have been widely used for describing mass transfer with backmixing in a countercurrent extractor. These models have

been identified by various names in the literature. The first, derived from a differential material balance on the column is called a differential, diffusion, or distributed-parameter model. The quantity of interest in this model is called the axial diffusion coefficient or the longitudinal dispersion coefficient. The second, derived from a stagewise concept of the column is called a discrete, backflow, or lumped parameter model. The parameter of interest in this second type of model is called the backmixing or backflow coefficient defined as the ratio of the linear flow rate of the backflow stream to the main flow stream.

In the limit as the number of stage becomes large the two models approach each other, and in fact, it is the relation between the two models that forms the basis of a method for computing a backmixing coefficient for the stagewise model from data taken on a continuous system.

The primary purpose of this work was to evaluate the vast body of literature on dispersed phase holdup and on backmixing, and to determine the best method for estimating these parameters for pulse columns of the size usually encountered in chemical plants. A final parameter of great importance in column design and performance evaluation is the mass transfer coefficient. This is discussed briefly but is largely considered beyond the scope of the present effort.

LITERATURE REVIEW

Dispersed Phase Holdup

Cohen and Beyer (11) reported some of the earliest data on dispersed phase holdup in pulse columns. They measured the ratio of isoamyl alcohol dispersed in water in a one inch diameter column by stopping the flow into the column after it had reached steady state operation and then draining the contents of the column into a graduated cylinder. Since the volume drained also contained the liquid in both disengagement sections, there was some error inherent in their data. The holdup values reported ranged from 0.10 to 0.26.

Li and Newton (27) studied the extraction of benzoic acid from water into toluene and found that the holdup increased with increasing flow rate of the discontinuous phase but was essentially independent of the flow rate of the continuous phase. Only a limited number of holdup measurements were given in these two early papers and no attempt was made to obtain any type of correlation by which the holdup could be predicted.

In an extended series of fourteen papers, the first of which appeared in 1951, Thornton and co-workers reported on a lengthy series of investigations covering holdup, flooding, and extraction efficiency for a variety of different types of extraction columns. The first series of papers, published in 1951 were concerned with packed columns. Then in 1953 they published the results of additional work on rotary annular columns. Finally, in 1957 he presented the results of their work on rotary disc

contactors and pulse columns. In all cases they used a similar approach to the correlation of dispersed phase holdup data.

The work on pulse columns is described in the paper by Logsdail and Thornton (28). The velocity of the dispersed phase relative to the stationary column was written as

$$\bar{v} = F_d/\epsilon_d \quad (4)$$

The velocity of the dispersed phase relative to the moving continuous phase was written as

$$\bar{v}_r = F_d/\epsilon_d + F_c/(1 - \epsilon_d) \quad (5)$$

Then, \bar{v}_r was expressed in terms of a modified form of the Stokes law expression in which the buoyancy force is assumed proportional to the difference between the densities of the mixed phases and the dispersed phase.

On this basis, the relative velocity of a droplet of diameter d_p is

$$\bar{v}_r = 2 d_p^2 g (\rho_m - \rho_d) \phi(1 - \epsilon_d) / 36 \mu_c \quad (6)$$

where $\phi(1 - \epsilon_d)$ is a function of holdup which allows for the effect of adjacent drops on one another. The value of ρ_m is

$$\rho_m = \epsilon_d \rho_d + (1 - \epsilon_d) \rho_c \quad (7)$$

Using this definition, Equation 6 becomes

$$\bar{v}_r = 2 d_p^2 g (\rho_c - \rho_d) (1 - \epsilon_d) \phi(1 - \epsilon_d) / 36 \mu_c = \bar{v}_o (1 - \epsilon_d) \phi(1 - \epsilon_d) \quad (8)$$

where \bar{v}_o is the mean Stokes law velocity of isolated droplets. Combining Equations (5) and (8) gives

$$F_d/\epsilon_d + F_c/(1 - \epsilon_d) = \bar{v}_o (1 - \epsilon_d) \phi(1 - \epsilon_d) \quad (9)$$

When data were plotted as

$$F_d/\epsilon_d (1 - \epsilon_d) + F_c/(1 - \epsilon_d)^2 \text{ vs. } (1 - \epsilon_d)$$

the result was a straight line, indicating that $\phi(1 - \varepsilon_d)$ was a constant. When $F_c = 0$ and F_d approaches zero then $(1 - \varepsilon_d)$ approaches 1.0. Under these conditions the droplets in the column are isolated and have no effect upon one another and $\phi(1 - \varepsilon_d)$ is unity so that

$$\bar{v}_0 = \lim_{\substack{F_d \rightarrow 0 \\ \varepsilon_d \rightarrow 0}} (F_d/\varepsilon_d) \quad (10)$$

Thus the term \bar{v}_0 is the limiting mean droplet velocity at zero continuous phase flow rate and very low dispersed phase flow rate and has been named the "characteristic velocity." Equation (9) becomes, after some rearranging,

$$F_d + (\varepsilon_d/(1 - \varepsilon_d))F_c = \bar{v}_0 \varepsilon_d (1 - \varepsilon_d) \quad (11)$$

If \bar{v}_0 , the characteristic velocity, is known, then Equation (11) can be used to calculate the holdup in the column as a function of the rates of the two phases. Working from previous experience with rotary annular columns and rotating disc columns, Logsdail and Thornton assumed that, as with other mechanically agitated columns, the mean droplet size and its associated characteristic velocity was a function of column geometry, energy input, and system physical properties but independent of the phase flow rates. They developed a correlation involving power functions of the appropriate dimensionless groups. A similar approach correlated their characteristic velocity data to within $\pm 15\%$ for rotary disc contactors and rotary annular columns. But curiously, no indication of the success of the correlation was given for the work on pulse columns.

Two important conclusions can be drawn from their work. First, the holdup was relatively insensitive to continuous phase flow rate as

reported earlier by Li and Newton. Second, the general theory seems applicable to a variety of mechanically agitated columns.

Thornton's approach assumes some importance because it has been used by several other investigators in correlating holdup data for pulse columns. Actually, the correlations were originally developed as an aid in design calculations in order to predict the upper flooding point for a pulse column. To do this one differentiates Equation (9) with respect to ϵ_d first considering F_d as the dependent variable and then considering F_c as the dependent variable and then setting the derivatives equal to zero to obtain

$$F_{df} = 2 \bar{v}_0 \epsilon_{df}^2 (1 - \epsilon_{df}) \quad (12)$$

$$F_{cf} = \bar{v}_0 (1 - \epsilon_{df}^2) (1 - 2\epsilon_{df}) \quad (13)$$

The f subscript indicates flooding since at the upper flooding point $dF_d/d\epsilon_d = 0$ and $dF_c/d\epsilon_d = 0$. Combining Equation (12) and (13) gives the holdup at flooding

$$\epsilon_{df} = 2/(3 + (1 + 8F_{cf}/F_{df})^{1/2}) \quad (14)$$

which shows that the holdup at the flooding point is a function only of the flow rate ratio and is independent of physical properties of the system, the column geometry, and the pulsing conditions.

Nicholson (39) used Equation (14) together with a large compilation of flooding point data assembled by Groenier et al. (20) to estimate the holdup in a pulse column. He chose, from the tables of Groenier et al., an experimental point which gave the flooding conditions for a column and a system similar to the one he was considering. Then, using the values of F_{cf} and F_{df} so obtained, he computed ϵ_{df} from Equation (14). This value

of ε_{df} , along with the values of F_{cf} and F_{df} , were then substituted into Equation (9) to find \bar{v}_0 , the characteristic velocity. In principle \bar{v}_0 is the same for less-than-flooding rates and so with \bar{v}_0 known he estimated ε_d for the conditions under which he was operating. This approach depends upon access to valid experimental flooding data or else an accurate flooding correlation. Although acceptable in principle, the method seems a very indirect way of obtaining holdup data unless no better way can be found. It would probably be most accurate if actual flooding data were available on a similar column.

The best generalized flooding correlation to use if this technique were to be employed in the absence of experimental flooding data on the column would be that of Groenier et al. who analyzed about 2200 data points representing over 20 different chemical systems having a wide range of physical properties and included mass transfer in both directions. Their correlation was, on the average, 8.6% higher than the experimental values.

Eguchi and Nagata (15) used a 2.28 inch diameter column with the methyl isobutyl ketone-water system to study holdup in a pulse column and gave as their correlation the equation

$$\varepsilon_d = 0.23 (F_d/Af)^{0.8} (1/(1 + F_d/F_c)^{0.8}) \quad (15)$$

and reported an error of 20%. If F_c is large this equation reduces to the form

$$\varepsilon_d = 0.23 (F_d/Af)^{0.8} \quad (16)$$

and if F_d is very small, ε_d approaches zero. According to this equation the holdup is a function of the dispersed phase flow rate and the pulsing

conditions. The holdup would decrease with increasing pulsation, in agreement with mixer-settler type operation. It thus appears that the work was done at low pulse amplitude and frequency. However, the fact that ϵ_d approaches zero at zero continuous phase flow rate is at odds with physical reality.

The work of Thornton and his associates represents the first extended study of holdup in pulse columns. The second major effort was carried out by Babb and his students at the University of Washington (Seattle). In the first of a series of papers, Sehmel and Babb (47) reported on their holdup studies using a 2 inch diameter pulse column with hexane, benzene, and methyl isobutyl ketone as solvents. They studied the effects of pulse amplitude, phase flow rates, and pulse frequency. Their experimental method did not permit determination of the axial variation in holdup but they observed visually that in a column with 43 plates spaced 2 inches apart that the dispersed phase, which entered at the bottom of the column, continued to break up into smaller droplets with a corresponding increase in local holdup for about seven to eleven plates above the inlet distributor. Above that point the local holdup appeared to remain reasonably constant.

They also observed that the holdup was practically independent of the continuous phase flow rate and that, as the pulsation was increased, the total holdup first decreased then went through a minimum at the transition point between mixer-settler and emulsion operation, after which it continued to increase up to the flooding point. The transition frequency could be predicted by the equation

$$f_H = 40(0.3 + 9 \times 10^{-8} \mu_d \gamma \Delta \rho - \ln a) \quad (17)$$

where the empirical constants are functions of the column geometry.

In a later paper, Bell and Babb (3) measured both the total holdup and the axial distribution of the holdup in a pulse column. For a 2 inch diameter column with a 2.2 inch plate spacing they found that the local holdup passed through a maximum near the middle of a column containing less than 24 plates but that it was uniformly distributed in the axial direction for longer columns. Their data also showed that the average holdup increased as the number of plates increased (at fixed plate spacing) for columns with less than about 20 plates and remained constant for longer columns. Their holdup correlation was based upon their observations that:

1. The effects of amplitude and frequency were accounted for by the amplitude-frequency product.
2. The effect of dispersed phase flow rate can be accounted for by an organic flow rate ratio.

The final correlation presented was

$$\epsilon_d = F_d / 28.2 (K_1 + (1.25 \times 10^{-5} + 2.42 \times 10^{-7} F_c) (Af - K_2)^2) \quad (18)$$

where the ratio $F_d/28.2$ is the organic flow rate ratio based upon a reference flow rate of 28.2 ft/hr, and the constants are functions of the column geometry and the physical properties of the system.

In a final paper from Babb's group, Foster et al. (17) investigated the transient holdup behavior in a pulse column operating in the emulsion region. They wrote unsteady state material balances for the change in holdup in each stage following a hydrodynamic upset. During an upset, the

superficial velocity of the dispersed phase is not known but the slip velocity defined as the average velocity of the dispersed phase droplets relative to the continuous phase can be determined as a function of the pulse volume velocity and the holdup by the relation

$$v_s = F_d/\epsilon_d + F_c/(1 - \epsilon_d) \quad (19)$$

Thus, from a correlation of slip velocities it was possible to write the material balance for $d\epsilon_d/dt$ in terms of quantities which could be measured. A simultaneous solution of these equations for each stage then gave the transient holdup response. The initial solution of these equations produced a curve which led the experimentally determined curve and so a first order lag was introduced into the equations to allow for coalescence time of the droplets. Using a coalescence time constant of 0.1 minute gave a theoretical curve which matched the experimental one much more closely. Use of the equations require that the steady state holdup characteristics be known in the form of a slip velocity correlation at the pulse volume velocities to be used.

Sato et al. (45) used the methyl isobutyl ketone-acetic acid-water system in a 1.38 inch diameter column to measure the holdup in all operating regions. Three correlations were presented, one for each of the three different regions. The pulse volume velocity range for each region was also given. For the mixer-settler region, the pulse velocity range and the holdup correlation were

$$(Af)_M < 1.3F_d^{0.22}S_p^{-0.32}D_h^{-0.37}$$

$$\epsilon_d = 0.52(Af/F_d)^{-0.7}(1 + F_d/F_c)^{-0.7}S_p^{-1.2}D_h^{-0.26} \quad (20)$$

This equation is very similar to that of Eguchi and Nagata. It shows that

the holdup will decrease with an increase in pulse volume velocity (Af), but it also includes a functional dependence on plate spacing and hole diameter. In the mixer-settler region the equation predicts that holdup varies inversely with plate spacing and hole diameter.

For operation in the transition region, the pulse volume velocity range and holdup correlation were given as

$$1.3F_d^{0.22}S_p^{-0.32}D_h^{-0.37} \leq (Af)_T \leq 0.8F_d^{0.22}S_p^{0.35}D_h^{-0.37}$$

$$\epsilon_d = 0.42 Af F_d^{0.33}(1 + F_d/F_c)^{-0.7}S_p^{-0.68}D_h^{0.37} \quad (21)$$

From their experimental data plot there is a minimum point of holdup at the transition region.

For emulsion operation region, the corresponding pulse volume velocity and holdup correlation were

$$(Af)_E \geq 0.8F_d^{0.22}S_p^{0.35}D_h^{0.37}$$

$$\epsilon_d = 0.54(Af)^{2.4}(1 + F_d/F_c)^{-0.7}S_p^{-1.2}D_h^{0.89} \quad (22)$$

This equation shows that the holdup in the emulsion region will increase linearly with an increase of pulse velocity. The larger exponent on the pulse volume velocity term (2.4) indicates that holdup is very sensitive to the energy input into the column.

The third major effort in the study of holdup in pulse columns is represented by the work of Miyauchi and Oya (36) who correlated their own data as well as that of Cohen and Beyer (11), Li and Newton (27), Sehmel and Babb (47), and Shirotuka et al. (49). They first attempted the use of the "characteristic velocity" concept introduced by Thornton, but found that at high pulsation the correlation so obtained diverged significantly

from their experimental data. Their final approach to holdup correlation, carried out as part of an extensive backmixing study, was to measure drop sizes photographically and to correlate them by a semi-theoretical relationship first introduced by Endoh and Oyama (16) which employs the application of Kolmogoroff's local isotropy concept to drop dispersion in a mixing vessel. Their equation for the mean drop size in dilute liquid suspension is

$$\bar{d}_p = 1.73 \times 10^{-2} \lambda_0 (\gamma \lambda_0 \rho / \mu^2)^{0.6} \quad (23)$$

where

$$\lambda_0 = (\mu_c^3 / \rho_c^3 P_0)^{1/4} \quad (24)$$

The variable P_0 is the mean rate of energy dissipation per unit mass of column fluid and, for the pulse column, has been determined by Jealous and Johnson (22) to be

$$P_0 = (Af)^3 / (\beta_c \times S_p) \quad (25)$$

where

$$\beta_c = s^2 / (1 - s)(1 - s^2) \quad (26)$$

The droplets of dispersed phase of mean diameter \bar{d}_p were considered to move at a terminal velocity relative to the continuous phase of

$$\bar{u}_t = F_d / \epsilon_d + F_c / (1 - \epsilon_d) \quad (27)$$

where the terminal velocity was represented by spheres travelling freely through a continuous medium, given by the equation

$$\bar{u}_t = (4 g \bar{d}_p \Delta \rho / 3 f_r \rho_c)^{1/2} \quad (28)$$

Equations (23) through (28) were then combined to form a holdup correlation of the form

$$\epsilon_d = 0.66 F_d^{2/3} \psi^{0.84} \quad \psi < 0.21 \quad (29)$$

$$\epsilon_d = 6.32 F_d^{2/3} \psi^{2.4} \quad \psi > 0.30 \quad (30)$$

$$\psi = ((Af)/(\beta_c S_p)^{1/3})(\mu_d^2/\gamma \Delta \rho)^{1/4} \quad (31)$$

The semi-theoretical derivation shows that ϵ_d should be a function of F_d , but the data were fit best by using $F_d^{2/3}$. The authors postulated that the 2/3 power dependence arose either from unsteady drop dispersion or from coalescence as the dispersed phase traveled through the column.

Biery (4) studied the performance of a 3 inch diameter pulse column using the system (50% TBP-kerosene)-nitric acid-water and, although no holdup correlation was attempted, the data he obtained are especially useful because the column used was about 30 feet long and thus represents one of the larger experimental columns for which information is available.

Rouyer et al. (43) collected holdup data on larger diameter columns using 30% TBP in dodecane as the organic phase. They studied mass transfer, holdup, and longitudinal dispersion in thirty 4 inch diameter columns having a variety of different geometries, in several 12 inch diameter columns, and in one 24 inch diameter column. Unfortunately, the specific geometric details of each column were not given. However, of the details that were provided, the amplitude-frequency products and the flow rates were typical of many commercial installations and were similar to those used by Biery. Their holdup values fell in the 10% to 20% range, as did those of Biery.

Arthayukti et al. (2) measured the holdup in a 2 inch diameter column using the system CCl_4-H_2O . The dispersed phase flow rate used was low compared with other investigators and the pulse velocity was high. The

holdup range reported was 0.01 to 0.12. They showed that the measured holdup did not coincide with the value calculated from the residence time calculations using the volumetric flow rate of the dispersed phase in a piston flow diffusion model.

Backmixing

In 1950, Morello and Poffenberger (37) and Geankoplis and Hixson (18) noted the existence of backmixing in extraction columns, especially in spray towers, but its significance was not clearly stated until two years later, by Newman (38). Thornton (54) also noted the influence of axial mixing on pulsed column behavior and over the years the actual extent of longitudinal mixing has been determined in a number of different studies. Experimental details of the various investigations are tabulated in Table 2. What has been missing is a critical review and evaluation of this work.

Burger and Swift (8) were the first to investigate backmixing in a pulse column. They used a 2 inch diameter column with water and a kerosene-like solvent, supersol, as the liquid system. They found that considerable backmixing occurred in the continuous phase and also, from visual observation, that some droplets of dispersed phase were also transported backwards through the column. They concluded that backmixing was quite insensitive to pulse frequency, plate spacing, flow rate ratio, and total throughput over the operating range which they studied. The two most important variables were continuous phase flow rate and pulse amplitude. The order of magnitude of the longitudinal dispersion coefficient

Table 2. Backmixing in pulsed columns: experimental details

Investigator	Operating variables							
	Column geometry				A cm/cyc	f cyc/sec	F _C cm/sec	F _d cm/sec
	D _t cm	H _t cm	S _p cm	D _h cm	s			
Burger and Swift (8)	5.08	70	2.54	0.32	0.25	1.3 - 2.9	1.2 - 1.5	0.07 - 0.33
Mar and Babb (29)	5.08	153	7.6	0.16	0.23	1.3 - 2.5	0.5 - 1.0	0.17 - 0.6
Eguchi and Nagata (15)	5.8	55	5.2	0.15	0.08	0.1 - 0.9	0.5 - 3.3	0.1 - 0.4
Kagan et al. (25)	5.6	400	5.0	0.2	0.08	0.5 - 1.5	0.3 - 2.5	0.7
Kagan et al. (26)	5.6 30.0	-	5 - 15	0.2	0.08	0 - 2.4	0 - 2.5	0.1 - 0.5
Sehmel and Babb (48)	5.1	220	5.0	0.3	0.2	0.6 - 5.2	0.3 - 2.5	0.1 - 0.4
Miyauchi and Oya (36)	3.2 5.4	37	10	0.15	0.09	0 - 1.5	0.4 - 3.0	- - -
Rozen et al. (44)	10	160	3.75	0.15 to 8.0	0.1 to 0.32	1.45 - 2.0	1.0 - 1.0	0.14 0.14
Smoot and Babb (52)	5.08	122	0.18	0.01	0.23	1.28 - 2.54	3.0 - 9.0	0.23 - 0.58
Arthayukti et al. (2)	5.0	200	5.0	0.2	0.2	2 - 4.1	0.9 - 2.1	0.01 0.57

System	Method of analysis	Range	
		E_c cm ² / sec	E_d cm ² / sec
Supersol H ₂ O	Tracer: MnSO ₄ , steady state technique	6.17 to 11.18	No
Hexane Benzene CCl ₄ ; H ₂ O	Tracer: Fe(NO ₃) ₃ , steady state technique	1.29 to 10.32	No
Ketone H ₂ O	Tracer: acetone acid, steady state technique	0.4 to 6.0	No
Kerosene CCl ₄ H ₂ O	Tracer: dye stuff steady state and pulse input of dye tracer	7.0 to 18.0	No
CCl ₄ H ₂ O	Tracer: methyl blue dye and KCl, impulse method	2.0 to 15.0	No
Hexane Benzene MIBK	Tracer: CuSO ₄ , steady state technique	0.57 to 2.6	No
MIBK H ₂ O	Tracer: red color dye stuff, impulse technique	0.3 to 12.0	0.3 to 2.0
Kerosene H ₂ O	Tracer: methyl blue and sudan brown, impulse method	3.0 to 18.0	9.0 to 35.0
MIBK 1,1,2-C ₂ HCl ₃ , H ₂ O	Tracer: acetic acid, acetone steady state technique	0.7 to 2.6	0 to 0.99
CCl ₄ H ₂ O	Tracer: ICH ₂ CH ₃ or NaI, two detection point technique	No	0.9 to 2.1

in the continuous phase as measured in their experiments was about 10 cm²/sec.

Attempts have been made to correlate backmixing as a function of column geometry, pulse conditions, flow rates and physical properties of the liquid system. Mar and Babb (29) proposed the first correlation for the longitudinal dispersion coefficient in a pulse column based on experimental data using the system hexane-water, benzene-water, and carbon tetrachloride-water. By using dimensional analysis, logarithmic transformation and multiple regression they obtained the following relation, for which a 17% deviation from the experimental data was claimed,

$$E_c = K S_p^{0.68} A^{0.07} f^{0.36} F_d^{0.3} D_h^{0.3} \gamma^{0.42} / (F_c^{0.45} T^{0.05}) \quad (32)$$

This correlation shows a fairly strong dependence on the pulse frequency and only a small effect of pulse amplitude, which conflicts with the findings of Burger and Swift. According to this equation, an increase in the continuous phase flow rate will decrease backmixing in the continuous phase and an increase in the dispersed phase flow rate will increase backmixing in the continuous phase. Density and viscosity was found to have a minor effect but interfacial tension was important because it controlled the size of the droplets. The equation shows a high dependence on interfacial tension. Plate spacing was also an important variable. It should be noted that the correlation of Mar and Babb shows no effect of column holdup on backmixing.

Kagan et al. (25) pointed out that the dependency of the longitudinal dispersion coefficient on pulse frequency and pulse amplitude is too small in the correlation of Mar and Babb. According to their own experiments

they proposed the equation

$$E_C = 1.2 \times 10^5 (A^{1.2} f^{1.35}) / F_C^{1.4} \quad (33)$$

The units used in Equation (33) were not clearly stated in the original paper. Nevertheless, this equation shows a greater dependence on amplitude and frequency which seems reasonable in light of other investigations to be discussed.

Sehmel and Babb (48) presented a correlation based on the use of their correlation for the transition frequency between mixer-settler and emulsion operation. The two equations presented were

$$E_C = 4.18 - 1.64 \times 10^{-5} \times F_C (f - f_H)^2 + 0.19 \Delta \rho \quad (f < f_H; \text{ mixer-settler operation}) \quad (34)$$

$$E_C = 6.97 - 9.08 \times 10^{-9} \times F_C (f - f_H)^2 + 0.166 \Delta \rho - 4.8 a + 2.49 a^2 \quad (f > f_H; \text{ emulsion operation}) \quad (35)$$

These two equations also show that backmixing tends to decrease with increasing continuous phase flow rate. In the mixer-settler region backmixing was independent of amplitude and dependent on continuous phase flow rate, and on the square of the frequency difference from the transition frequency. A density difference increase also increased the backmixing. In the emulsion region backmixing decreased more rapidly with an increase in the continuous phase flow rate, and also with an increase in the pulse amplitude.

The constants in these equations were obtained for a single liquid system and for a single column geometry, hence its use is limited. Holdup did not appear in their correlations.

Miyauchi (33), early in 1957, worked on the backmixing problems theoretically by using a simplified diffusion model. The extent to which extraction was influenced by backmixing was investigated, but no experimental work was done. The following year, McMullen et al. (31) worked on the solution of the diffusion model with backmixing in both phases, and solved it numerically for a large number of conditions.

In 1963, Myauchi and Vermeulen (34) presented the diffusion and backflow models for two-phase axial dispersion. They wrote the diffusion model for the two phases over a differential length of column as

$$(1/P_c B) d^2 X_c / dZ^2 - dX_c / dZ - N_{oc} (X_c - X_c^*) = 0 \quad (36)$$

$$(1/P_d B) d^2 X_d / dZ^2 - dX_d / dZ + N_{od} (X_c - X_c^*) = 0 \quad (37)$$

where $N_{oi} = K_{oi} \bar{a} H_t / F_i$ (overall number of transfer unit); $i = c, d$ and then a finite difference approximation of Equation (36) using central order differences as

$$(1/P_c B) (X_{c,i+1} - 2X_{c,i} + X_{c,i-1}) / (\Delta Z)^2 - (X_{c,i+1} - X_{c,i-1}) / 2\Delta Z = N_{oc} (X_{c,i} - X_{c,i}^*) \quad (38)$$

Then they wrote a material balance over component i of a typical stage, j , of a stagewise model as

$$(1 + \alpha_c) (X_{c,i-1} - X_{c,i}) - \alpha_c (X_{c,i} - X_{c,i+1}) = N_{oc0} (X_{c,i} - X_{c,i}^*) \quad (39)$$

$$(1 + \alpha_d) (X_{d,i} - X_{d,i+1}) - \alpha_d (X_{d,i-1} - X_{d,i}) = N_{od0} (X_{c,i} - X_{c,i}^*) \quad (40)$$

where $\alpha_i = \bar{F}_i / F_i$; $N_{oi0} = K_{oi} \bar{a} S_p / F_i$ (single stage number of transfer unit).

Upon examining Equations (38) and (39) they noted that, if the number of stages to which Equation (39) applied became large, then Equation (36) tended to approach Equation (38). Specifically, if the difference

approximation to the differential model is divided into n segments, then the size of each segment ΔZ was equal to $1/n$, which could be used to transform Equation (38) into

$$(n/P_c B + 1/2)(x_{c,i-1} - x_{c,i}) - (n/P_c B - 1/2)(x_{c,i} - x_{c,i+1}) = N_{oc0}(x_{c,i} - x_{c,i}^*) \quad (41)$$

and Equation (41) would be the same as Equation (36) if the following relation were satisfied:

$$1/P_c B = 1/2n + \alpha_c/n \quad (42)$$

Then, in the limit as n becomes very large,

$$\lim_{n \rightarrow \infty} (P_c B) = n/\alpha_i \quad (43)$$

Equation (42) might thus serve as a basis for providing a link between the differential and the stagewise models of the column. However, Equation (42) applies only for $n \gg 1$. The preceding outline shows only one approach to linking the two models. Miyauchi and Vermeulen used a different linking mechanism. They chose to equate the limiting extents of mass transfer for each model. The diffusion model was solved for mass transfer at an infinite number of transfer units ($NTU \rightarrow \infty$), and the stagewise model was solved with each stage assumed to be an equilibrium stage. The results were then equated to obtain the expression

$$1/P_i B = 1/2(n - 1)f_T + \alpha_i/(n - 1)f_T \quad (44)$$

where f_T is a function of the extraction factor $\Lambda = E_x F_c / F_d$. They found that for $(\Lambda\alpha_c + \alpha_d) > 0.5$ the value of f_T was very nearly equal to 1.0 irrespective of Λ .

As a severe test of the linking relationship, calculations were made for $n = 2$ over the wide range of variables,

$$1 < N_{oc} < \infty$$

$$0.56 < (\Lambda \alpha_c + \alpha_d) < 32$$

$$0.0625 < \Lambda < 16$$

and the fraction of solute unextracted from the two models when the linking conditions were satisfied generally agreed to within $\pm 5\%$. If f_T were set equal to 1.0 in the same calculations, agreement to within 10% was obtained. At increasing n , α_i , and N_{oc} the approximation improved rapidly.

It is also of interest to note that Equation (44) can also be obtained if the variance for the residence time distribution of fluid elements was used to develop a link between the two models.

In applying these results to the pulse column Miyauchi and Vermeulen considered that the rate of interstage mixing could be considered to be equal to the pulse volume velocity for each phase, or

$$\bar{F}_i = A f \epsilon_i \quad (45)$$

They also drew upon information obtained from the work of Miyauchi and Oya (36) which showed that, hydrodynamically, a single cell or stage (the volume between two perforated plates) may behave as some fractional number of perfectly mixed stages, β , where β normally has a value between one and two and whose value can be obtained from the correlation

$$\beta = 0.57 (D_t^2 S_p)^{1/3} / (D_h s) \quad (46)$$

Thus, the variable n in Equation (44) should be replaced by βn , the effective number of stages. So, expanding Equation (44), neglecting the terms $1/n$ and $1/2$, in comparison with n , and replacing n by βn in the remaining

terms gives

$$1/P_i B = 1/(2\beta n - 2) + \alpha_i/n \quad (47)$$

Finally, for column operation in the "emulsion" region the backmixing coefficient can, if the assumption of Equation (45) is accepted, be written as

$$\alpha_i = \bar{F}_i/F_i = Af\epsilon_i/F_i \quad (48)$$

which is physically the volume of phase i moved by the pulse generator divided by the flow rate of phase i . Substituting $P_i B = H_t F_i/E_i = n S_p F_i/E_i$, where S_p is the height of an individual stage and H_t is the column height, gives

$$E_i/(Af\epsilon_i S_p) = (1/\alpha_i)(1/(2\beta - 2/n)) + 1/\beta \quad (49)$$

If one neglects the term $2/n$, which is usually very small, and plots Equation (49) with Equation (46) substituted for β , then measured values of the longitudinal dispersion coefficient should fall on the line represented by the equation.

Miyauchi and Oya (36) have done this and found good agreement for pulse columns. Now, the important result of their work is that, if longitudinal dispersion coefficients are measured for the continuous phase and if they fit a plot of Equation (49), then one has a means of computing values of α_i (for a stage-wise model) from values of E_i obtained by standard tracer injection techniques in the laboratory. Further, as long as relation (49) holds, then α_i can be computed from Equation (48) which involves only pulse amplitude, pulse frequency, holdup fraction and superficial flow rate and does not require that the dispersion coefficient be known. Two other points add importance to this result. First, α_i cannot

be measured directly in the pulse column and second, for multicomponent systems involving chemical reaction a differential model of the column is not feasible. Therefore, to include backmixing in multicomponent calculation for reacting systems there must be a means of obtaining α_i . The work of Miyauchi and Vermeulen potentially provides an elegant and simple solution to the problem.

In addition to providing verification of Equation (49) for backmixing in the continuous phase, Miyauchi and Oya (36) also studied backmixing in the dispersed phase, a subject which had not yet been dealt with quantitatively. They tested the validity of Equation (49) for both phases in the pulse column. Although the backmixing equation of Miyauchi and Vermeulen uses the subscript i indicating that the equations may be applied to either phase, their plots of Equation (49) for the dispersed phase show a significant deviation from the theory at low pulsing conditions. However, as pulsation was increased, the theory was found to hold. Thus, backmixing coefficients for both phases may be computed from Equation (49) if the column is operating in the emulsion region.

Support for the approach of Miyauchi comes from additional work by Kagan et al. (26). Kagan studied longitudinal mixing in 2.2 inch and 12 inch diameter pulse columns with holes approximately 3/32-inch diameter and with plate spacings of 2, 4, and 6 inches. Continuous phase flow rates ranged from 83 to 450 gal/hr-ft². These variable ranges are similar to those used by Rouyer et al. (43) and by Biery and Boylan (5) in their holdup measurements, and are also in the same range as can be expected in a commercial sized column.

Kagan found that, for single phase flow in the absence of pulsation, the longitudinal dispersion coefficient, E_c , was a linear function of the flow rate and as the column diameter and the plate spacing increased the value of the dispersion coefficient also increased. The variation of E_c with diameter was due to transverse nonuniformities (channeling, etc.). However, when pulsation was applied to the column at a constant plate spacing the value of E_c varied linearly with the expression $(Af + F_c)$, which is the effective velocity of the continuous phase under pulsation, and was independent of the column diameter.

For two phase flow, such as occurs in an operating pulse column, Kagan found that above an effective velocity $(Af + F_c)$ of 1.8 cm/sec the presence of the second phase had little effect upon longitudinal dispersion in the continuous phase since at higher pulsation intensities the dispersed phase droplets become smaller and their velocity approaches the pulsation velocity. Experimental data for E_c was fitted to the equation

$$E_c = 0.49 S_p^{0.76} (Af + F_c) \quad (50)$$

which held for single phase flow over the entire range of their experimental data and, for $(Af + F_c) > 1.8$ cm/sec, it also fit their data for the continuous phase in two-phase flow. Now, Miyauchi's equation for the longitudinal dispersion coefficient is

$$E_c = ((Af S_p \epsilon_c) / \beta) (1 + F_c / (2Af \epsilon_c)) \quad (51)$$

and, by some algebraic manipulation, it can be rewritten as

$$E_c = (S_p / \beta) (Af \epsilon_c + 0.5F_c) \quad (52)$$

which is similar to Kagan's correlation, Equation (50). Further, in the variable ranges of interest the pulse velocity (Af) is 1.0-2.0 cm/sec

while the range of F_c is 0.1-0.2 cm/sec. In other words, (Af) is about 10 times as large as F_c . Thus to a good approximation Kagan's equation is

$$E_c = 0.49 Af S_p^{0.76} \quad (53)$$

And Miyauchi's equation is

$$E_c = (\varepsilon_c/\beta) Af S_p \quad (54)$$

So the basic structure of the two correlations is consistent. Further, ε_c has a value of 0.8 to 0.9, while β , according to Miyauchi should be between 1 and 2. Therefore, ε_c/β should be approximately $0.85/\beta$. So for a 2 inch plate spacing the two approximate equations would be

$$E_c = 1.69 Af \quad (\text{Kagan}) \quad (55)$$

$$E_c = (4.32/\beta) Af \quad (\text{Miyauchi}) \quad (56)$$

DEVELOPMENT OF PROPOSED DISPERSED PHASE HOLDUP CORRELATION

Typical experimental data and calculated values from the correlations of various authors are shown in Table 3.

The most important results are found in the comparison of the experimental work of Biery and Boylan (4,5) with calculated values of holdup from the correlations of Miyauchi and Oya (36), Sato et al. (45), and Sehmel and Babb (48). Biery's work assumes importance because it was taken on a pulse column of sufficient length and diameter that approaches the dimensions of plant-size columns. Also, sufficient details of the measurement conditions were given to permit comparison. As can be seen from Figure 5, the correlation of Miyauchi and Oya (36) is significantly better than the others in agreement with Biery's experimental data. Closer examination of these nine points shows that the agreement is best when values of ψ (the major parameter used in Miyauchi's correlation) is in the range of 0.1 to 0.3. The predicted values of holdup from the correlation also agrees best with the experimental work of other investigators when the value of ψ is in the range of 0.1 to 0.3. This parameter (ψ) is a measure of the column geometry, pulsing conditions, and physical properties of the fluid system, as can be seen from its definition:

$$\psi = ((Af/(\beta_c S_p)^{1/3})(\mu_d^2/\gamma\Delta\rho)^{1/4}) \quad (31)$$

To evaluate the usefulness of Miyauchi's correlation in a pulse column the information in Tables 4 and 5 was prepared. Table 4 describes the pulse columns used in the Purex plant at Richland, Washington and also those used in other plants around the world since many of the other plants were designed from the same data. The information was obtained from the

Table 3. Comparison of hold-up correlations with experimental data from various investigators

A (1/sec)	Operating variables			Geometry			Physical properties			Experimental data for hold-up fraction						Hold-up fraction from correlation								
	F _c (cyc/min)	F _c (gal/hr-ft ²)	F _c (gal/hr-ft ²) ^a	D _c (in)	S _c (in)	S _c (in)	W _c (dyn/cm)	W _c (dyn)	W _c (dyn/cm)	Solvent	Satoh ^b	Bell ^b	Epstein ^b	Sato ^b	Arthukutti ^b	Miyachi ^b	Story ^b	Beynon ^b	Miyachi ^b	Sato ^b	Epstein ^b	Solvent	V (l/mole)	
0.50	154	236 ^b	236	1.97	1.97	0.125	23	30.7	0.660	0.21	0.033								0.042	0.296	0.017	0.056	Hexane	109
0.50	150	0	230								0.036								0.041	— ^c	—	0.048		197
1.00	80	230	230					10.3	0.796	0.55	0.080								0.058	0.163	0.021	0.065	MEK ^d	220
0.50	67	303	303								0.116								0.081	0.075	0.042	0.094		159
1.25	160	0	396	2.00	2.20	0.125	23	30.7	0.660	0.21	0.260								0.037	— ^c	—	0.057	Hexane	219
1.00	160	162	216								0.150								0.065	1.345	0.085	0.088		220
1.00	160	162	394					10.3	0.796	0.55	0.580								1.360	0.009	0.108	MEK		640
1.00	71	222	210								0.240								0.374	0.920	0.011	0.149		460
1.25	100	475	210								0.245								0.343	1.046	0.344	0.014		440
0.40	305	0	396					30.7	0.660	0.21	0.120								0.035	— ^c	—	0.094	Hexane	165
0.20	110	336	336	2.28	2.20	0.099	0.1	10.3	0.796	0.55	0.070								0.078	0.039	0.066	0.105	MEK	161
0.25	35	177	177								0.090								0.020	0.058	0.096	0.052		955
0.00	120	265	265	1.38	2.05	0.099	0.1				0.150								0.710	0.128	0.021	0.063		56
0.25	80	265	265								0.040								0.041	0.053	0.008	0.081		994
0.40	60	265	88								0.025								0.035	0.327	0.029	0.023		187
1.34	125	125	13	1.97	1.97	0.076	20	12.0	1.595	1.5	0.019								0.216	0.006	—	CCl ₄		800
0.55	125	125	13								0.009								0.025	0.136	0.012	—		130
1.00	120	265	38	2.13	0.40	0.099	19	10.3	0.796	0.55	0.255								0.556	4.440	0.005	0.011	MEK	570
1.00	29	151	394	3.00	2.25	0.025	22.5	10.3	0.992	1.73	0.209								0.169	0.021	0.028	—	90% TBP-hexane	776
1.00	19	164	394								0.153								0.073	0.036	0.051	—		130
0.34	24	169	394								0.241								0.034	0.068	0.107	—		956
0.12	210	163	394								0.125								0.037	0.030	0.043	—		171
1.00	44	87	210								0.082								0.147	0.022	0.017	—		307
1.00	44	88	394								0.169								0.206	0.020	0.019	—		302
1.00	44	168	394								0.152								0.209	0.020	0.020	—		302
1.03	48	156	394								0.191								0.278	0.039	0.024	—		300
1.03	36	152	394								0.145								0.130	0.022	0.030	—		715

^aCorrelation equation given only for hexane and MEK.

^bMultiply by 1.132 x 10⁻³ to convert to cm²/cm²-sec.

^cContinuous shear flow rate F_c = 0; correlation fails because of F_c in denominator.

^dMEK = methyl isobutyl ketone.

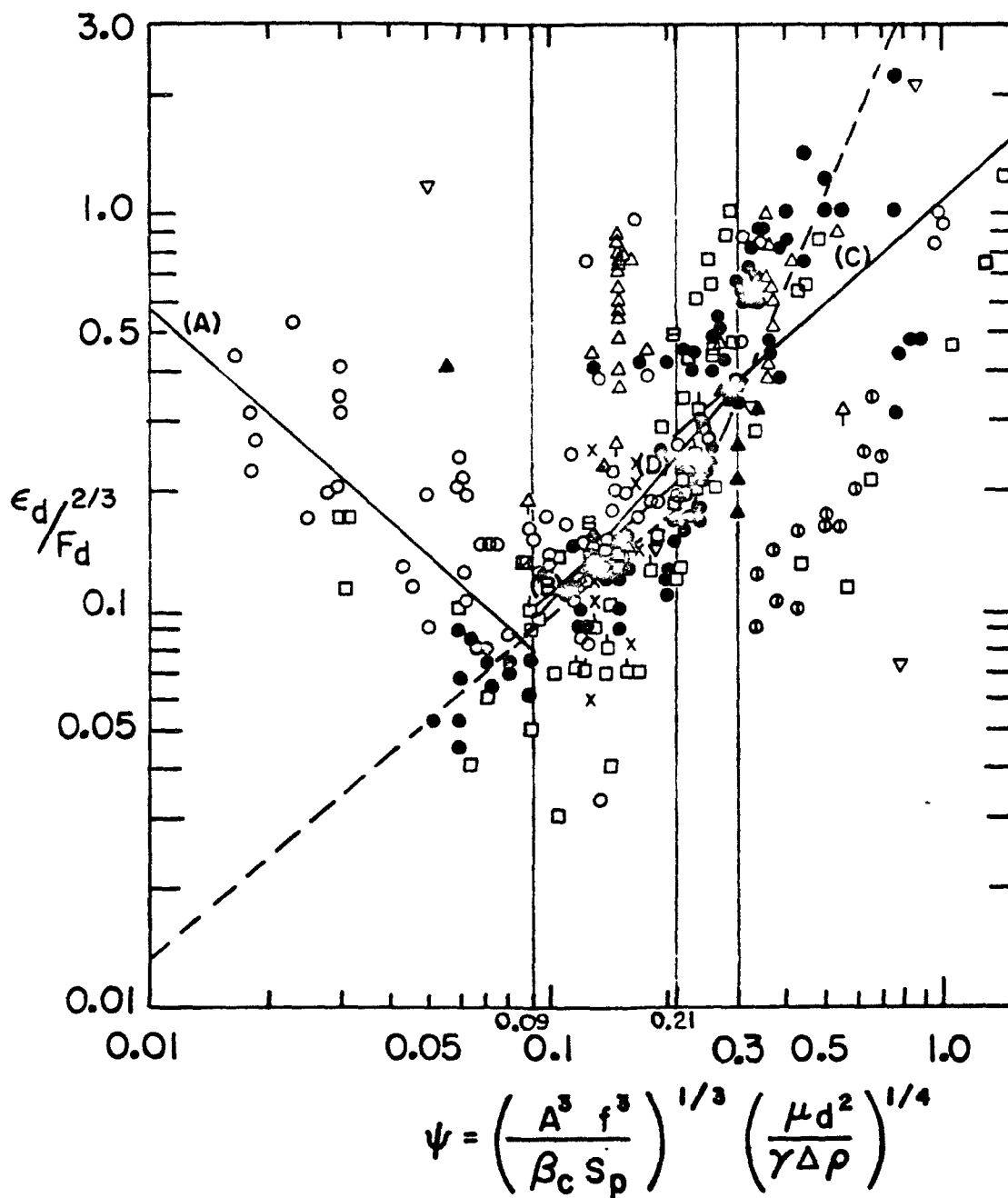


Figure 5. Comparison of the proposed holdup equation with Miyuchi's equation and experimental data.

Symbol	∅	▲	□	△	▲	X	⊕	●	▽	○	↑	□
By Dis. phase	Arthayukti CC1,	Biery 50% TBP-kero.	Bell Hexane MIBK	Cohen Isoamyl alcohol	Egauchi Ketone	Kagan Kerosene	Li ^a Toluene	Miyauchi MIBK	Sato MIBK	Sehmel Hexane Benzene MIBK	Sehmel ^a Hexane Benzene MIBK	Shirotuka ^a Benzene
D _t cm	5.0	7.62	5.08	2.54	5.8	5.6	~	3.2 5.4	3.5	5.05	5.05	~
S _p cm	5.0	5.71	5.59	5.08	5.2	5.0	~	1.0 ~ 10.0	2.5 ~ 7.0	5.03	5.03	~
D _h cm	0.2	0.16	0.32	0.32	0.15	0.2	~	0.15 ~ 0.30	0.1 ~ 0.33	0.3175	0.3175	~
s	0.2	0.23	0.23	0.09	0.081	0.082	~	0.095 0.19	0.081	0.23	0.23	~
A cm/cyc	1.0	0.3 ~ 3.6	0 ~ 12.7	0.38 ~ 1.14	0.1 ~ 0.9	0.5 ~ 1.5	~	0 ~ 1.5	0.6 ~ 2.0	0.64 ~ 5.2	0.64 ~ 5.2	~
f cyc/sec	2.0 ~ 9.0	0.4 ~ 3.5	0.3 ~ 3.3	0.28 ~ 1.2	0.5 ~ 3.3	0.8 ~ 1.7	~	0.4 ~ 3.0	0.3 ~ 3.3	0.3 ~ 3.5	0.3 ~ 3.5	~
F _d cm/sec	0.01 ~ 0.04	0.25 ~ 0.45	0.12 ~ 0.6	0.03 ~ 0.16	0.18 ~ 0.38	0.3 ~ 1.0	0.29~0.38	0.03 ~ 0.26	0.1 ~ 0.5	0.17 ~ 0.43	0.17 ~ 0.28	0.04
F _c cm/sec	0.01 ~ 0.04	0.1 ~ 0.2	0 ~ 0.54	0.03 ~ 0.16	0.14 ~ 0.44	0.15-0.5	~	0.03 ~ 0.27	0.1 ~ 1.0	0 ~ 0.43	~	~

^aData used in Miyauchi's plot; (A) $\epsilon_d = 0.0073 F_d^{2/3} \psi^{-0.9485}$; (B) $\epsilon_d = 0.738 F_d^{2/3} \psi^{0.8355}$; (C) $\epsilon_d = 1.058 F_d^{2/3} \psi^{0.856}$; (D) $\epsilon_d = 1.4703 F_d^{2/3} \psi^{1.1515}$; ----Miyauchi's correlation.

Figure 5. (Continued)

Table 4. Design and operating parameters of purex pulse columns at the Hanford plant^a

Column type	Active height (ft)	Inside diameter (in)	Amplitude (in)	Frequency (cyc/min)	Disp. phase flow (gal/hr-ft ²)	Cont. phase flow gal/hr-ft ²	Direction of transfer	Flow rate ratio ^b	Volume velocity gal/hr-ft ²	Cartridge type
HA,1A,2P	13.5 (Extr.) 13.2 (Scrub)	24 (Extr.) 32 (Scrub)	1.1 (Extr.) 0.6 (Scrub)	40-50	375 (0) 210 (0)	155 (A) 30 (A)	A 0 0 A	2.42 0.14	530 240	Standard ^c
HC,2E	18.0	34	0.53	40-50	330 (A)	180 (0)	0 A	1.83	510	Fluorothene ^d
1C	18.0	34	0.53	40-50	330 (A)	220 (0)	0 A	1.50	550	Fluorothene
1BX	28.0	27	0.84	40-50	355 (0)	25 (A)	0 A	0.07	380	Standard
1BS	13.3	8	0.84	40-50	550 (0)	275 (A)	A 0	2.00	820	Standard
2B	21	7	1.1	40-50	160 (0)	90 (A)	0 A	0.56	250	Standard

^aFrom information contained in HW-31000 (Del.), "Purex Technical Manual" (41).

^bBased on direction of transfer.

^cTwo inch plate spacing, one-eighth inch holes, 23 percent free area, stainless steel.

^dFour inch plate spacing, three-sixteenths inch holes, 23 percent free area, fluorothene.

Table 5. Parameters for Purex plant columns using Miyauchi's correlations

Column type	ψ	Hold-up fraction ϵ_d	E_c (ft ² /hr)	E_d (ft ² /hr)	α_c	α_d
HA, TA, 2D						
Extract	0.277	0.163	3.29 ^a	0.98 ^a	9.99 ^b	0.81
Scrub	0.151	0.052	1.62	0.26	31.92	0.25
HC, 2E	0.112	0.055	3.56	0.81	4.69	0.15
1C	0.112	0.055	4.24	0.95	3.83	0.15
1BX	0.211	0.082	2.39	0.53	51.89	0.33
1BS	0.211	0.110	5.87	1.81	4.57	0.28
2B	0.277	0.093	7.93	1.16	18.67	1.07

^aMultiply by 0.259 to convert to cm²/sec.

^bBackmixing coefficient, defined as backflow over main flow, \bar{F}_i/F_i .

Purex Technical Manual (41). The use of pulse columns in fuel reprocessing operations represents the most widespread application of these extractors and thus is the best source of data on large scale units. Although the information is about 20 years old it still contains the key elements of current pulse column design and operation.

The column diameters shown in Table 4 range from 7 to 34 inches and have processing capabilities of about 10 tons U processed per day. The columns built at the Nuclear Fuel Services plan at West Valley, New York range from 4 to 10 inches in diameter and will handle about 1 ton U/day. At the Eurochemic plant in Belgium (24) the columns are 4 to 6 inches in diameter (one column, the 1BS scrub column is only 2 inches). Thus, in a plant, column diameters over the tenfold range of about 3-30 inches are

to be expected. This conclusion will be important in discussing holdup and backmixing.

Using the data from Table 4, values of ψ and of holdup were calculated from the correlation of Miyauchi and Oya (36). Notice that, for actual plant columns, the values of ψ fall within the range of 0.1 to 0.3 which, according to the data in Table 3, is the range of greatest accuracy for the correlation. Figure 6, which is a plot of Miyauchi and Oya's correlation against the data they had available shows that much of the experimental data on holdup in the literature also fall in this range. However, although the correlation fits the data plotted in Figure 6 quite well, errors in using the correlation to predict the data of Biery and Boylan range from 4 to 40% over this same range of ψ . Although values of ψ from 0.1 to 0.3 provide the best fit to their data (which Miyauchi did not have available), the degree of fit is still not satisfactory.

A logical question at this point is, "In the face of a large amount of experimental data given in the literature and used by Miyauchi in developing his correlation, why should so much credence be given to the nine points reported by Biery and Boylan (5)? Three factors account for this. First, they used a three-inch diameter column, which is of sufficient magnitude that it borders on the lower range of diameters encountered in plant-sized columns. Second, their pulse amplitude, pulse frequencies, and amplitude-frequency products were similar to those used commercially and third, their dispersed phase flow rates (in gal/hr-ft²) were close to the values likely to be encountered in a plant.

In Table 5 and also in the last nine points of Table 3, Miyauchi's correlation tends to yield values that are lower than the experimental

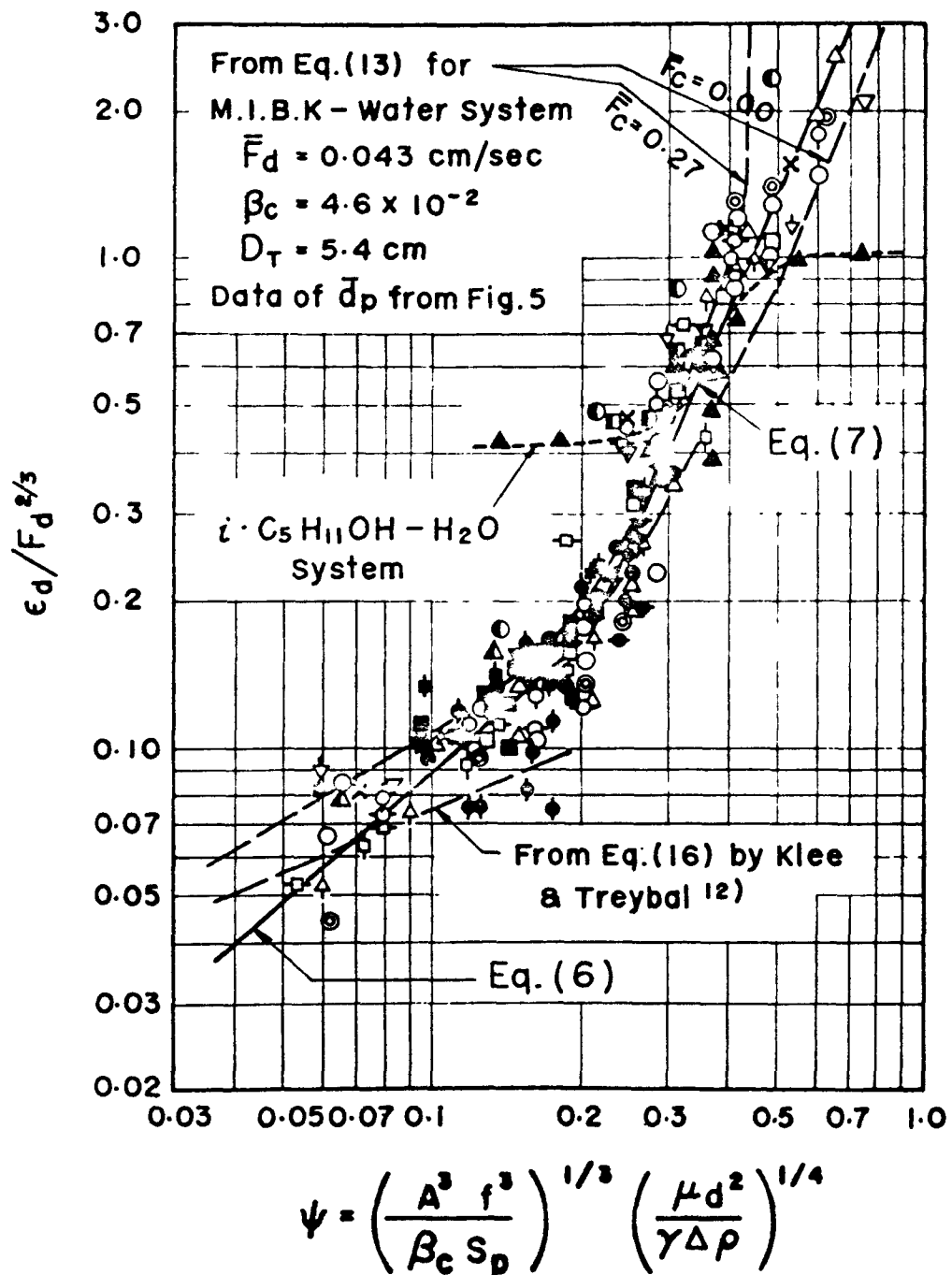


Figure 6. Holdup correlation of Miyauchi and Oya.

points of Biery and Boylan. But support for their higher values can be found in the results of work done in France by Rouyer et al. (43) on large diameter columns. They studied mass transfer, holdup, and longitudinal dispersion in thirty 4-inch diameter pulse columns having a variety of different geometries, in three 12-inch diameter columns, and in one 24-inch diameter column. Unfortunately the specific geometric details of each column were not given. However, of the details that were provided the amplitude-frequency products and the flow rates were similar to those given in Table 4 and also those used by Biery. Their data for a 4-inch diameter column are shown in Table 6. The values for dispersed phase holdup fall in the 10%-20% range, as do the data of Biery. The comparison is quite good. For example, Biery's sixth data point (Table 3) is for flow and pulsing conditions very close to entries four and five of Rouyer et al. Biery reports a holdup of 15% while Rouyer reports 16% and 17%. The comparison is even better when one considers that Rouyer used a slightly higher dispersed phase flow-rate. Other similar comparisons of the two sets of data are also consistent.

Rouyer et al. further studied holdup in twelve and twenty-four-inch diameter columns and concluded that, although a certain anisotropy in the emulsion region of the column could lead progressively to channeling, the effect for pulse columns does not appear at diameters up to 24 inches, as evidenced by the uniform holdup measured as a function of column radius. They did find some radial variation near the ends of a 24 inch diameter column but found it negligible at a distance of 4 meters from the inlet.

Table 6. Experimental and calculated holdup obtained by Rouyer et al. on a 4-inch diameter pulse column

Af (in/min)	F_c (gal/hr-ft ²)	F_d (gal/hr-ft ²)	Holdup (experimental)	Holdup ^a (calculated)
32.3	82.3	438	.143	.139
35.4	82.3	438	.153	.151
38.3	82.3	438	.154	.164
41.3	83.2	438	.159	.178
44.1	83.2	438	.172	.192
47.2	83.2	438	.191	.208
53.2	83.2	438	.227	.248
59.1	83.2	438	.310	.328
35.4	104.4	547	.182	.203
41.3	104.4	547	.229	.248
47.2	125	547	.362	.323
29.5	125	658	.232	.209
32.4	125	658	.257	.236

^aCalculated by Rouyer et al. using a correlation based on the work of Thornton.

They also found only a minor effect on mass transfer results as the columns were scaled up.

Similar conclusions on the effect of column diameter on scale-up are reported in the Purex Technical Manual (41) except for partition columns where only a small amount of excess extractant is available. In these cases, louver-plate redistributors were placed at selected locations along the length of the column to redistribute the flow and minimize channeling. Other than this, scale-up using data from 3-inch columns was straightforward. It thus appears that scale-up from 3-inch columns to

plant size columns can be carried out effectively. However, almost all of the data used in Miyauchi's correlation was obtained for pulse columns less than three inches in diameter, a number of the data points coming from columns 2-inches or less in diameter. One can thus conclude that Miyauchi's correlation is probably valid but that there are small-column effects which place a limit on the minimum size of an experimental column which should be used to take holdup data.

At present, then, the holdup correlation of Miyauchi and Oya (36) appears to be better than others which have been presented. This correlation is

$$\epsilon_d = 0.66 F_d^{2/3} \psi^{0.84} \quad \psi < 0.21 \quad (29)$$

$$\epsilon_d = 6.32 F_d^{2/3} \psi^{2.4} \quad \psi > 0.21 \quad (30)$$

where

$$\psi = (Af/\beta_c S_p)^{1/3} (\mu_d^2 / \gamma \Delta \rho)^{1/4} \quad (31)$$

In the mixer-settler region ($\psi < 0.21$) the dispersed phase holdup predicted by Equation (29) is in disagreement with the experimental data of Bell and Babb (3), Sehmel and Babb (47), and Eguchi and Nagata (15) as shown in Table 7. For a given system at a fixed value of the dispersed phase flow rate the holdup should decrease with increasing values of ψ in the mixer-settler region, passing through a minimum, and then as emulsion operation begins the holdup should increase with increasing pulsation.

In the emulsion region ($\psi > 0.21$) the dispersed phase holdup predicted by Equation (30) shows that the agreement is best when the value of ψ is in the range of 0.1 to 0.3 as discussed previously, but at higher values of ψ the predicted holdup is too large, as shown in Table 8. The slope of Equation (30) is too sharp. This means a small change in ψ will

Table 7. Comparison with Miyauchi's correlation of holdup with experimental data at low effective velocity ($A_f + F_d$)^a

f cyc/ sec	Operating variable			Pulse column Geometry				s	Experimental data ^b by					
	A cm/ sec	F_c cm/ sec	F_d cm/ sec	D_t cm	S_p cm	D_h cm	System		A	B	C	ψ	ϵ_d^c	
	cm/ sec	cm/ sec	cm/ sec	cm	cm	cm							ϵ_d^d	
0.367	1.27	0.261	0.261	5.05	5.029		0.23	Hexane H_2O	0.1			0.0183	0.009	0.132
0.5	1.27	"	"	"	"		"	"	0.07			0.025	0.012	0.099
0.33	0.635	"	"	"	"		"	MIBK H_2O	0.11			0.0181	0.009	0.134
1.13	0.635	"	"	"	"		"	"	0.045			0.0621	0.026	0.0415
0.33	2.54	0.183	0.245	5.08	5.59	-	0.23	Hexane H_2O		0.068		0.0318	0.014	0.075
0.33	2.54	"	0.576	"	"		"	"		0.12		0.0321	0.025	0.132
0.67	2.54	"	0.446	"	"		"	"		0.06		0.0647	0.038	0.0572
0.3	1.0	0.2	0.2	5.8	5.2	0.15	0.081	Ketone H_2O			0.09	0.048	0.017	0.045

^a $\psi < 0.09$, proposed correlation is: $\epsilon_d = 0.0073 F_d^{2/3} \psi^{-0.9485}$.

^bA = Sehmel and Babb; B - Bell and Babb; C - Eguchi and Nagata.

^c ϵ_d evaluated by using Miyauchi's correlation.

^d ϵ_d evaluated by using proposed correlation.

Table 8. Comparison with Miyauchi's correlation of holdup with experimental data at high effective velocity $(Af + F_d)^a$

f cyc/sec	Operating variables				Geometry			s
	A cm/cyc	F_c cm/sec	F_d cm/sec	D_t cm	S_p cm	D_h cm		
3	2.54	0.183	0.446	5.08	5.59	0.3175	0.23	
5.89	3.175	0.251	0.239	"	"	"	"	
4.95	"	"	"	"	"	"	"	
4.125	"	"	"	"	"	"	"	
2.475	"	"	"	"	"	"	"	
2	1.5	0.3	0.3	3.5	5.0	-	0.081	
1	7.2	0.014	0.042	5.0	5.0	-	0.2	
1	8.4	"	"	"	"	-	"	
1	8.8	"	"	"	"	-	"	

^aProposed correlation for $\psi > 0.3$, $\epsilon_d = 1.058 F_d^{2/3} \psi^{0.856}$.

^bA - Bell and Babb (3), B - Sato et al. (45), C - Arthayukti et al. (2).

^c ϵ_d evaluated by using Miyauchi's correlation.

^d ϵ_d evaluated by using proposed correlation.

Experimental data^b

System	A	B	C	ψ Miyauchi	ϵ_d^c	ϵ_d^d
MIBK-H ₂ O	0.58			0.64	1.26	0.42
"	0.48			1.56	7.1	0.59
"	0.29			1.31	4.7	0.51
"	0.18			1.1	3.01	0.44
"	0.09			0.66	0.88	0.28
"		0.15		0.56	0.71	0.28
CCl ₄ -H ₂ O			0.058	0.85	0.51	0.11
"			0.12	0.99	0.74	0.13
"			0.11	1.032	0.82	0.13

produce too great a change in the holdup. The power of ψ is 2.4 in Equation (30) is so large that the holdup is very sensitive to the value of ψ in their correlation.

Equations (29) and (30) were obtained by Miyauchi and Oya (36) from their own experimental data and from selected data of Cohen and Beyer (11), Sehmel and Babb (47), Li and Newton (27), and Shirotuka et al. (49). Toluene, benzene, methyl isobutyl ketone and isoamyl alcohol were used in their experiments. After studying the data of these authors carefully, it appears that Equations (29) and (30) should be modified since Miyauchi and Oya use only selected data points from the work of many of the authors cited.

The modified correlation was made using all the experimental data available and with the help of a statistical analysis program for regression. If one examines the experimental data points plotted in Figure 6, it can be seen that the data approximate a parabola. Therefore, an effort was first made to correlate the points by first, second and third order polynomial regression. Up to a fourth order polynomial regression only a flattened parabolic line was given but with fluctuation in it. It did not appear to fit the data well. Therefore, no further attempt was made to obtain a single correlation equation, and a separate regression was performed for each operating region.

The experimental data plotted on Figure 6 shows that the transition point from mixer-settler to emulsion operation occurs at a value of ψ equal to 0.09. By checking these equations on Figure 6 with the experimental data, a proposed dispersed phase holdup correlation was selected as follows:

$$\epsilon_d = 0.0073 F_d^{2/3} \psi^{-0.9485} \quad (\psi < 0.09, \sigma = 0.218) \quad (57)$$

$$\epsilon_d = 1.4703 F_d^{2/3} \psi^{1.1515} \quad (0.09 < \psi < 0.3, \sigma = 0.177) \quad (58)$$

$$\epsilon_d = 1.058 F_d^{2/3} \psi^{0.856} \quad (\psi > 0.3, \sigma = 0.249) \quad (59)$$

The equation for $\psi > 0.3$ shown in Figure 5 has a lower slope than Miyauchi's plot, hence this will correct the holdup calculated from the modified holdup correlation and also evaluated from the original correlation of Miyauchi and Oya. The new proposed holdup correlation is in good agreement with the experimental data. Table 9 shows the comparison of this new correlation with Biery's experimental data (4). The proposed correlation is also in good agreement with these data.

Table 10 shows the application of this proposed correlation to real plant operating columns at the Purex plant at Richland, Washington. The holdup values calculated from the new correlation are a little higher than the value calculated by using Miyauchi's correlation. This fits the holdup range as reported by Rouyer et al. (43) from their large scale pulse column experimental data.

By checking the holdup calculated from the proposed correlation with Rouyer's experimental data and with the only data set available from the Purex plant under the similar conditions, there is also good agreement, as shown in Table 11. According to Rouyer's investigation, channeling does not occur in columns up to 600 mm (23.6 inches). It thus appears that the new holdup correlation should provide a better means of predicting holdup in columns up to at least two feet in diameter and perhaps even larger diameters if redistributor plates are employed.

Table 9. Modified correlation comparison with Biery's experimental data^a

Biery's run No.	Operating variables				Biery's experimental data	ψ	ϵ_d	Proposed correlation
	f cyc/sec	A cm/cyc	F_c cm/sec	F_d cm/sec				
4	0.483	3.53	0.174	0.45	0.21	0.276	0.17	0.20
9	0.317	2.69	0.186	0.45	0.14	0.138	0.07	0.09
11	0.4	0.864	0.191	0.44	0.24	0.056	0.03	0.07
12	3.5	0.305	0.185	0.25	0.13	0.173	0.06	0.08
14	0.733	2.54	0.098	0.437	0.08	0.302	0.21	0.22
15	0.733	2.54	0.1	0.45	0.15	0.302	0.21	0.22
18	0.733	2.54	0.19	0.45	0.15	0.302	0.21	0.22
20	0.8	2.62	0.176	0.45	0.19	0.34	0.28	0.24
21	0.6	2.62	0.172	0.45	0.15	0.255	0.14	0.18

^a(1) pulse column geometries are: $D_t = 7.6$ cm, $S_p = 5.7$ cm, $D_h = 0.16$ cm, $s = 0.23$; (2) system physical properties are: 50% TBP, kerosene-H₂O, $\rho_d = 0.89$ g/cm³, $\mu_d = 0.17$ cp, $\gamma = 10.5$ dyne/cm, $\rho_c = 1.034$ g/cm³.

Table 10. Comparison of ϵ_d evaluated by Miyauchi's correlation and new correlation at Hanford plant

Column type	Diameter cm	Amplitude cm/cyc	Frequency cyc/sec	F_c cm/sec	F_d cm/sec	ψ	ϵ_d by Miyauchi's correlation	ϵ_d by new correlation
HA,1A,2D	60.96	2.79	0.75	0.18	0.42	0.28	0.16	0.19
HA,1A,2D	81.28	1.52	0.75	0.03	0.24	0.15	0.05	0.06
HC,2E	86.36	1.35	0.75	0.20	0.37	0.11	0.05	0.06
1C	86.36	1.35	0.75	0.25	0.37	0.11	0.05	0.06
1BX	68.58	2.13	0.75	0.03	0.40	0.21	0.08	0.13
1BS	20.32	2.13	0.75	0.31	0.62	0.21	0.11	0.18
2B	17.78	2.79	0.75	0.10	0.18	0.28	0.09	0.11

Table 11. Comparison of similar condition from Rouyer's et al. (43) data and from Purex plant data

	A _f (in/min)	F _c (gal/hr ft ²)	F _d (gal/hr ft ²)	ε _d	D _t (inch)
Rouyer's experimental data	35.4	104.4	547.0	0.182	4
Proposed correlation evaluated HW-31000 1BS column result	37.8	275	550.0	0.179	8

DEVELOPMENT OF PROPOSED BACKMIXING CORRELATION

The backmixing correlation presented by Miyauchi (33) which was derived from the backflow model shows that his correlation and the correlations suggested by Kagan et al. (26) and by Rozen et al. (44) have the same form. Kagan's correlation was limited to an effective velocity ($Af + F_c$) greater than 1.8 cm/sec and Rozen's correlation appeared to yield coefficients too high to fit the experimental data of other investigators (see Table 12). Also it was correlated from his own experimental data only. Miyauchi correlated continuous phase backmixing by using his own data plus some from Eguchi and Nagata (15) but by examination of Table 12, it can be seen that this correlation yields coefficients too low to fit the data of Burger and Swift (8), and of Kagan and Rozen, and too high to fit that of Smoot and Babb (52) and of Sehmel and Babb (47). According to several authors, Miyauchi's correlation fits best for operation at low pulse volume velocities. Therefore, a modification of Miyauchi's backmixing correlation is needed.

Based on Miyauchi's backmixing correlation and some experimental data of the other investigators (see Table 13), the modification was carried out by using a least square statistical analysis program. After regression on all of the available experimental data, the best continuous phase backmixing correlation was found to be

$$\epsilon_c = 1.3078 (S_p/D_t)^{2/3} (D_h/s) (Af\epsilon_c + F_c/2) \quad (\sigma = 3.4) \quad (60)$$

The physical constant also corrected as

$$\beta = 0.765 (D_t^2 S_p)^{1/3} (s/D_h) \quad (61)$$

Miyauchi's continuous phase backmixing correlation is

$$\epsilon_c = 1.75 (S_p/D_t)^{2/3} (D_h/s) (Af\epsilon_c + F_c/2) \quad (62)$$

Table 12. Comparison of E_c correlations with experimental data from various investigators

Column geometry					Operating variables				System ^a	ψ	E_c^b cm ² /sec	E_c^c cm ² /sec	E_c^d cm ² /sec	E_c^e cm ² /sec	E_c^f cm ² /sec	E_c^g cm ² /sec	Investigator
D_t cm	S_p cm	D_h cm	T cm	s	A cyc/sec	f cm/cyc	F_c cm/sec	F_d cm/sec									
5.08	5.08	0.32	0.3	0.25	2.86	1.17	0.27	0.5	30% Supersol	0.24	10.41	6.92	4.03	6.07	9.13	0.54	Burger & Swift (8)
-	-	-	-	-	-	1.5	0.28	-	-	0.31	10.16	7.79	4.32	7.69	11.4	0.97	
-	2.54	-	-	-	-	1.17	0.33	0.64	-	0.30	11.18	3.75	2.47	3.64	5.94	0.26	
5.09	5.6	0.16	-	0.23	2.54	-	0.23	0.36	MIBK	0.25	1.35	3.72	1.28	6.0	6.58	1.39	Smoot & Babb (52)
-	-	-	-	-	1.28	0.5	0.36	0.23	-	0.06	0.94	1.66	0.89	3.27	2.16	1.56	
-	-	-	-	-	2.54	0.83	0.23	-	-	0.18	1.81	5.41	1.71	4.24	5.94	1.69	
30	10	0.21	-	0.09	1.19	1.67	0.22	0.22	CCl ₄	0.34	6.9	3.56	2.99	6.2	3.75	1.61	Kagan et al. (26)
-	-	-	-	-	1.49	-	-	-	-	0.43	7.9	3.78	3.04	7.61	4.56	0.17	
5.6	5	-	-	-	1.23	-	0.34	0.34	-	0.45	9.2	5.19	1.75	3.99	2.63	0.95	
10	15	0.5	0.05	0.32	2.0	1.0	0.14	0.14	Kerosene	0.11	15.8	7.24	7.15	8.21	14.9	1.18	Rozen et al. (44)
-	-	-	-	0.1	2.0	1.0	-	-	-	0.28	10.5	23.18	7.16	8.21	12.7	1.18	
5.05	5.03	0.32	0.11	0.23	0.64	0.67	0.26	0.26	Benzene	0.03	0.86	1.326	2.35	-h	1.84	0.89	Sehmel and Babb (48)
-	-	-	-	-	2.54	1.75	0.44	0.44	Hexane	0.18	1.86	19.31	3.16	8.16	11.5	1.46	

^aDispersed phase physical properties: (continuous phase is water)

	γ dyne/cm	ρ_d g/cm ³	μ_d poise	μ_c poise	ρ_c g/cm ³
30% Supersol	44.0	0.754	0.009	0.01	1.0
MIBK	9.8	0.81	0.005		
CCl ₄	12.0	1.595	0.015		
Kerosene	25.0	0.74	0.014		
Benzene	34.28	0.97	0.006		
Hexane	38.7	0.65	0.003		

^bExperimental E_c data.

^c E_c evaluated by Miyauchi and Oya's correlation (36).

^d E_c evaluated by Mar and Babb's correlation (29).

^e E_c evaluated by Kagan's et al. (26) correlation.

^f E_c evaluated by Rozen's et al. (44) correlation.

^g E_c evaluated by Sehmel and Babb's correlation (48).

^h $A_f + F_c < 1.8$ cm/sec Kagan's et al. correlation cannot be used.

Table 13. Data used for modification of Miyauchi's E_c correlation

Data points used	Investigator	Column used				System
		D_t cm	S_p cm	D_h cm	s	
7	Burger and Swift (8)	5.08	2.54 to 5.08	0.3175	0.245	30% Supersol Water
32	Kagan et al. (26)	5.6 30	5 10 15	0.21	0.087	CCl_4-H_2O
113	Miyauchi and Oya (36)	3.2	1.0 10.0	0.15 0.30	0.095 0.19	MIBK Water
13	Rozen et al. (44)	10	3.75 7.5 0.5	0.15 0.3 0.23 0.32	0.095	Kerosene- H_2O
81	Sehmel and Babb (48)	5.055	5.029	0.3175	0.23	Hexane- H_2O Benzene- H_2O MIBK- H_2O
64	Smoot and Babb (52)	5.08	5.578 4.023	0.1585 0.3169	0.23	MIBK- H_2O ; 1,1,2, trichloroethane-acetone-water

Tracer and technique	Tracer concentration measured	E_c evaluated
MnSO ₄ , Steady state injection	2 pts. Take sample with S.S. Capillary with- draw	Diffusion model
Impulse injection, Methyl blue dye KCl	By photoelectric colorimeter	Diffusion model $\sigma^2 = \frac{2}{P_e} - \frac{2}{P_e^2} + \frac{2}{P_e^2} e^{-P_e}$
H ₂ O-KCl; MIBK - oil- soluble red dyestuff, Impulse injection	H ₂ O-phase-electrical con- ductivity; MIBK-photo- electrically measured	One dimension diffu- sion model $\frac{\partial X}{\partial t} = E_i \frac{\partial^2 X}{\partial Z^2} - F_c \frac{\partial X}{\partial Z}$
Impulse injection; H ₂ O- methylene blue Keroene-sudan brown	FEK-M photocalorimeters EPD-09 recording potentiometers	Not mentioned
Steady state injection, Copper sulfate	By hypodermic needles analyzed by colorimeter	Diffusion model $E_c = -F x S_p \times C_s / \ln(0.01)$
Acetic acid, Steady-state injection Acetone	Hypodermic needles Withdraw Direct titration	E_c by using Mar & Babb's correlation E_d by lab. study

$$\beta = 0.57 (D_t^2 S_p)^{1/3} (s/D_h) \quad (46)$$

It is seen that the proposed correlation will give a little lower value than Miyauchi's correlation. This is because the influence of the lower experimental data by Sehmel and Babb and of Smoot and Babb and also some of Rozen's data. Figure 7 shows the comparison of these two correlations with the experimental data.

Table 14 shows a comparison of the backmixing calculated by the proposed new correlation with the experimental data. The calculated values are in good agreement with the experimental data, especially that of Smoot and Babb and of Rozen.

It has been shown by Miyauchi that at high pulse volume velocities dispersed phase backmixing approaches an ideal backflow model and thus that the correlation should be of the same form as for the continuous phase:

$$E_d = 1.75 (S_p/D_t)^{2/3} (D_h/s) (Af\epsilon_d + F_d/2) \quad (63)$$

Table 15 shows a comparison of the dispersed phase backmixing coefficient from this correlation. It gives a very good agreement with Arthayukti's et al. (2) experimental data.

The backmixing correlation for both phases is thus proposed as:

For continuous phase

$$E_c = 1.3078 (S_p/D_t)^{2/3} (D_h/s) (Af\epsilon_c + F_c/2) \quad (60)$$

For dispersed phase

$$E_d = 1.75 (S_p/D_t)^{2/3} (D_h/s) (Af\epsilon_d + F_d/2) \quad (63)$$

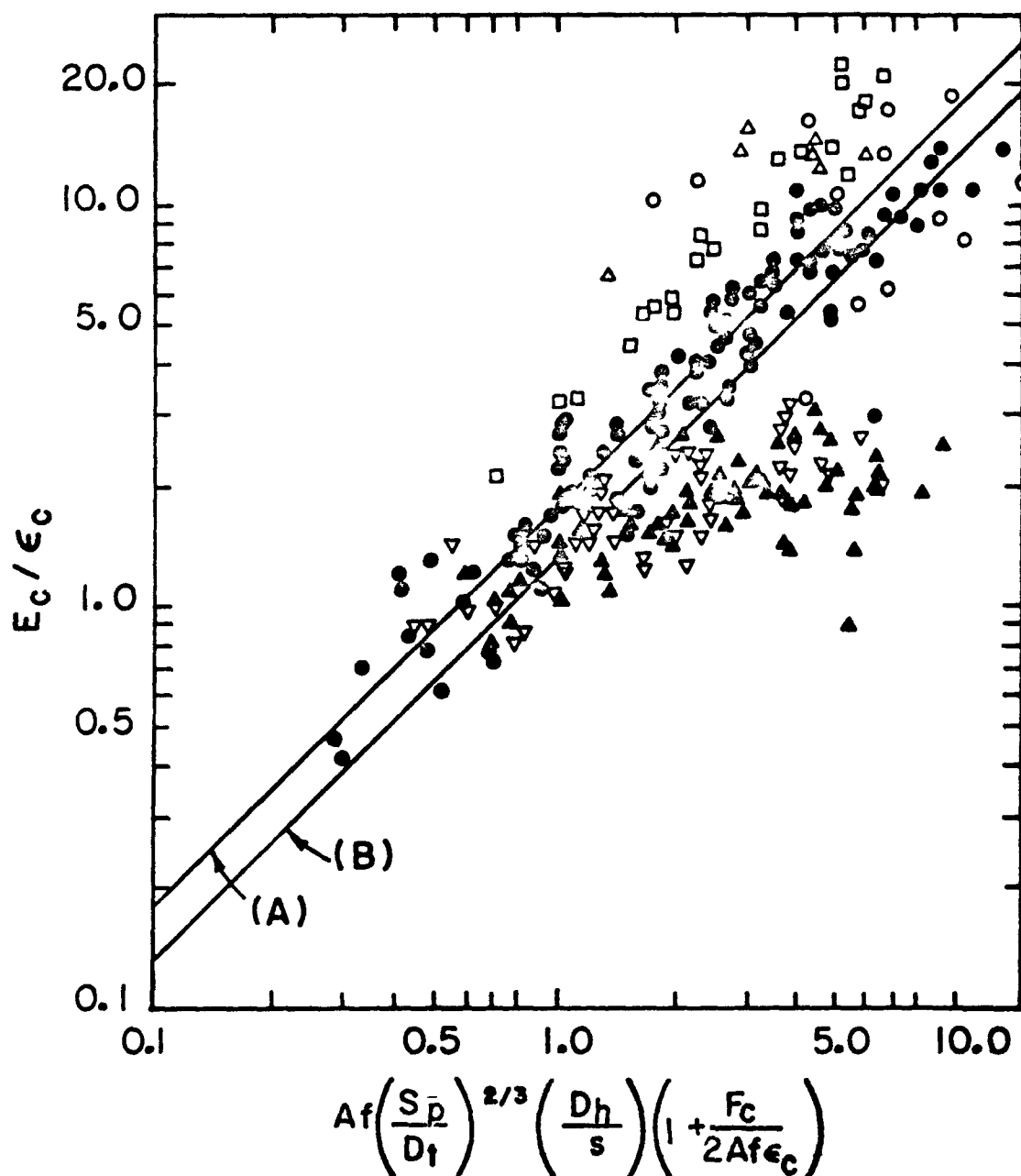


Figure 7. Comparison of proposed backmixing correlation with Miyauchi's correlation and experimental data.

Symbol used	△	□	●	○	▲	▽	
Investigator	Burger	Kagan	Miyauchi	Rozen	Sehmel	Smoot	
Dispersed phase	30% Supersol	CCL_4	M.I.B.K.	Kerosene	Hexane Benzene M.I.B.K.	M.I.B.K. 1,1,2 tri- chloroethane	
Column Dia. cm	5.08	5.6 30.0	3.2 5.4	10.0	5.05	5.08	
Spacing cm	2.54 5.08	5 10 15	1~10.0	3.75 7.5	5.029	5.58 4.02	
Hole dia. cm	0.3175	0.21	0.15 0.3 0.5	0.15 0.3 0.5	0.3175	0.159 0.32	
Free area fraction	0.245	0.087	0.095 0.19	0.095 0.23 0.32	0.23	0.23	96
Amplitude cm/cyc	1.27 2.86	0.635-5.156	0~1.5	1.45 2.0	0.635-1.27	1.28-2.54	
Frequency cyc/sec	1.5 1.167	0.33-3.5	0.4~3.0	1.0	0.3~3.5	0.5-1.5	
Dis. flowrate cm/sec	0.4~0.68	0.174~0.43	0.043	0.139	0.23~0.60	0.23~0.60	
Con. flowrate cm/sec	0.06~0.33	0.174~0.43	0.05~0.30	0.139	0.25~0.60	0.23~0.53	
(A) $E_c = 1.75 \left(\frac{S_p}{D_t}\right)^{2/3} \left(\frac{D_h}{s}\right)(Af\epsilon_c + F_c/2)$ (Miyauchi's correlation)							
(B) $E_c = 1.3078 \left(\frac{S_p}{D_t}\right)^{2/3} \left(\frac{D_h}{s}\right)(Af\epsilon_c + F_c/2)$ (proposed correlation)							

Figure 7. (Continued)

Table 14. Comparison of the E_C calculated by proposed correlation with the experimental data

Column geometry				Operating variables			
D_t cm	S_p cm	D_h cm	s	A cm/cyc	f cyc/sec	F_c cm/sec	F_d cm/sec
5.08	5.08	0.3175	0.25	2.86	1.17	0.067	0.68
"	"	"	"	"	1.5	0.28	0.5
5.09	5.578	0.1585	0.23	2.54	0.5	0.36	0.36
"	"	"	"	"	"	0.23	0.23
"	"	"	"	1.28	0.5	0.36	0.23
30	5.0	0.21	0.09	0.83	1.67	0.22	0.22
"	"	"	"	1.78	1.67	0.22	0.22
30	15.0	"	"	2.14	1.67	"	"
10	3.75	0.5	0.111	1.45	1.0	0.14	0.14
"	7.5	"	"	"	"	"	"
"	3.75	"	"	2.0	1.0	"	"
10	15	"	"	"	"	"	"
"	7.5	"	"	"	"	"	"

System	Experimental E_c data cm^2/sec	Proposed E_c data cm^2/sec	Investigator
30% H_2O Supersol	10.56	4.48	Burger & Swift (8)
"	10.16	5.78	"
MIBK;acetic H_2O	1.13	1.32	Smoot & Babb (52)
	1.21	1.27	"
	0.95	0.76	"
$\text{CCL}_4\text{-H}_2\text{O}$	2.9	1.25	Kagan et al. (26)
"	11.0	4.88	"
"	12.8	5.47	"
H_2O Kerosene	3.0	4.89	Rozen et al. (44)
"	5.8	7.9	"
"	4.8	6.3	"
"	10.5	17.1	"
"	8.0	10.43	"

Table 15. Comparisons of the correlation of E_d with Arthayaukti's experimental data^a

Operating variables		E_d ^b	E_d ^c	E_d ^d	E_d ^e	E_d ^f	ψ	ϵ_d ^g	ϵ_d ^h
A cm/cyc	f cyc/sec	cm ² /sec							
3.4	2.1	1.036	3.033	0.89	2.24	0.66	0.84	0.24	0.07
3.4	1.82	0.943	1.88	0.66	1.98	0.49	0.73	0.17	0.06
4.1	1.61	2.02	2.33	0.75	2.09	0.56	0.78	0.19	0.06
4.1	1.95	1.036	4.46	1.13	2.5	0.84	0.94	0.32	0.08
4.1	1.07	0.283	0.59	0.32	1.48	0.239	0.52	0.08	0.04
4.1	0.93	0.142	0.37	0.24	1.31	0.178	0.45	0.05	0.03

^aThe system is CCL_4-H_2O , and the column geometry is: $D_t = 5.0$ cm, $S_p = 5.0$ cm, $D_h = 0.2$ cm, $T = 0.1$ cm, $s = 0.2$, dispersed phase flow rate is: 0.57 cm/sec.

^bExperimental data.

^c E_d evaluated by using Miyauchi's holdup correlation and E_d correlation.

^d E_d evaluated by using proposed ϵ_d correlation and Miyauchi's E_d correlation.

^e E_d evaluated by using Rozen's correlation.

^f E_d evaluated by using proposed ϵ_d and E_d correlation.

^g ϵ_d evaluated by using Myiauchi's ϵ_d correlation.

^h ϵ_d evaluated by using proposed ϵ_d correlation.

From the above examination it is seen that Miyauchi's backflow model is valid and hence that for a stagewise model of a column, the backmixing coefficient may be calculated from the simple relation, $\alpha_i = Af\epsilon_i/F_i$.

PULSE COLUMN MODEL

Two pulse column models have been developed to describe mass transfer with backmixing in a countercurrent extraction process. They are often referred to as the diffusion model and the stagewise or backflow model. In the diffusion model mass transfer is based on the concentration gradient and the column is treated as a differential system approaching a packed column. Similar equations are written for each phase, and in these equations, backmixing is represented by longitudinal dispersion coefficients E_c and E_d which can be evaluated from the proposed backmixing correlation. Because the height of a transfer unit for each species in the column is different, and up to now the H.T.U. of the species in the column to be simulated cannot be estimated by the available information, the diffusion model will not be used in this work. Also, for nonlinear distribution coefficients, the equations must be solved numerically. Hence, little is gained by using this approach, as can be seen by comparing Equations (38) and (39).

The stagewise model is the simplest way of describing mass transfer with backmixing in pulse columns. The pulse column model used in this backmixing investigation was based on the following assumptions:

- (1) Each stage is assumed to be an equilibrium stage and interphase mass transfer depends on the equilibrium distribution.
- (2) Each stage is a perfect mixing stage and the concentration is uniform throughout the stage.
- (3) Backflow occurs between stages to account for backmixing effects.

(4) The backflow ratio used is calculated from the equation

$$\alpha_i = A_f \epsilon_i / F_i$$

(5) ϵ_i is evaluated from the proposed new holdup correlation.

(6) The volume of each equilibrium stage is assumed to be the same.

(7) The equilibrium stages are numbered from the top of the column.

(8) The first and last stage are disengagement sections which are assumed to have the same volume as the other equilibrium stage. No chemical reactions and no mass transfer occur in these sections.

The mathematical equation derived from a material balance for each stage is as follows:

Input - Output - (Lost to Reaction) + (Gained from Reaction) = Accumulation

Figure 8 shows the "Backflow Stagewise Model" schematically. For a typical stage i , the material balance equation is:

$$F_d((1+\alpha_{d,i-1})X_{d,i-1} - (1+2\alpha_{d,i})X_{d,i} + \alpha_{d,i+1}X_{d,i+1}) + F_c((1+\alpha_{c,i+1})X_{c,i+1} - (1+2\alpha_{c,i})X_{c,i} + \alpha_{c,i-1}X_{c,i-1}) + \sum \text{RXN gained} - \sum \text{RXN lost} = d(H_i X_{c,i} + h_i X_{d,i})/dt \quad (62)$$

The accumulation term can be written in the following form:

$$d(H_i X_{c,i} + h_i X_{d,i})/dt = H_i d(X_{c,i})/dt + X_{c,i} d(H_i)/dt + h_i d(X_{d,i})/dt + X_{d,i} d(h_i)/dt \quad (63)$$

For an equilibrium stage:

$$X_{d,i}/X_{c,i} = E_{x,i} \text{ hence } X_{d,i} = E_{x,i} X_{c,i} \quad (64)$$

where $E_{x,i}$ is the equilibrium distribution coefficient. Also,

$$H_i + h_i = V_i \quad (65)$$

$$h_i = V_i - H_i \quad (66)$$

$$-dH_i/dt = dh_i/dt \quad (67)$$

$$H_i = V_i(1 - \epsilon_{d,i})$$

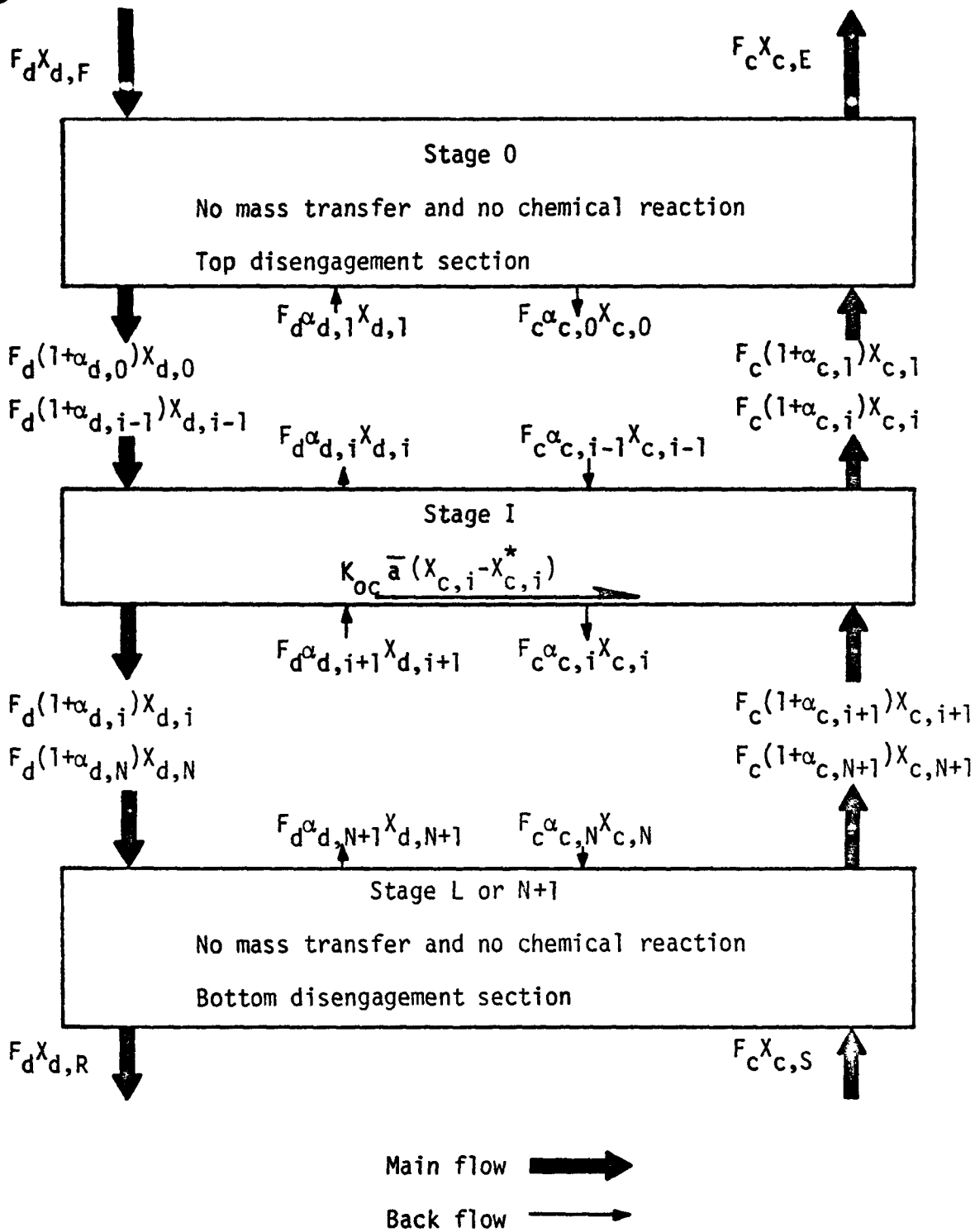


Figure 8. Backflow stagewise model.

By rearrangement, the accumulation term can be found as follows:

$$d(H_i X_{c,i} + h_i X_{d,i})/dt = H_i (1 + (V_i - H_i)) d(X_{c,i})/dt + (1 - E_{x,i}) X_{c,i} dH_i/dt \quad (68)$$

By using the new proposed holdup correlation for a value of ψ between 0.09 and 0.3 the holdup is:

$$\epsilon_d = 1.4703 F_d^{2/3} \psi^{1.1515} \quad (58)$$

Then,

$$H_i = V_i (1 - \epsilon_d) = V_i (1 - 1.4703 F_d^{2/3} \psi^{1.1515}) \quad (69)$$

$$d(H_i)/dt = -0.9802 F_d^{-1/3} \psi^{1.1515} V_i d(F_d)/dt \quad (70)$$

In order to use a digital computer for generation of the response data from the simulation model, the continuous derivatives must be approximated. A backward finite difference technique was assumed in this work. The approximation has the form:

$$d([X]_{c,i})/dt = ([X]_{c,i}^{t+\Delta t} - [X]_{c,i}^t)/\Delta t \quad (71)$$

Then the general concentration control equation of species X derived using Euler's integration formula is

$$\begin{aligned} [X]_{c,i}^{t+\Delta t} = & [X]_{c,i}^t + (\Delta t / (1 + ((V_i - H_i) / H_i) E_{x,i})) \left(\frac{F_c}{H_i} (\alpha_{c,i-1} [X]_{c,i-1}^{t+\Delta t} - (1 + 2\alpha_{c,i}) \right. \\ & [X]_{c,i}^t + (1 + \alpha_{c,i+1}) [X]_{c,i+1}^t) + (F_d / H_i) (E_{x,i-1} (1 + \alpha_{d,i-1}) [X]_{c,i-1}^t \\ & E_{x,i} (1 + 2\alpha_{d,i}) [X]_{c,i}^t + E_{x,i+1} \alpha_{d,i+1} [X]_{c,i+1}^t) + \Sigma \text{RXN gain} \\ & - \Sigma \text{RXN lost} - ((1 - E_{x,i}) / H_i) [X]_{c,i} (d(H_i)/dt) \end{aligned} \quad (72)$$

The basic model used in this simulation study is one developed by McCutcheon (30) for the separation of uranium from plutonium and was written to simulate a column in a scrap recovery plant for the recovery of unirradiated plutonium. Data on the operating column have been collected by Bruns (7). In the column there is an organic feed containing a mixture

of uranium and plutonium in a nitric acid solution. The plutonium in the feed stream is selectively reduced from Pu(IV) to Pu(III) by use of hydroxylamine nitrate. This reduction in the plutonium valence causes the plutonium to transfer into the aqueous phase, thus effecting the uranium-plutonium separation. So, one of the basic reactions in the column is the reduction of plutonium by hydroxylamine.

A second reaction concerns the re-oxidation of plutonium by the nitric acid in the column. This re-oxidation reaction is autocatalytic, with a nitrous acid catalyst being produced. To suppress the accumulation of the nitrous acid it is destroyed by adding hydrazine to the column. There are finite kinetics to each of the reactions among the various species in the column and these are accounted for by McCutcheon in the development of the basic model. Details are given in his thesis (30), as are the equations for the equilibrium distributions of each component. The model presented here is a modification of McCutcheon's work to include the effects of backmixing on column operation.

The number of equilibrium stages required in the basic simulation model was 20, as suggested by Bruns (7). The feed stream entered at stage four. These values were used so that a comparison of the piston flow model with the results from the backmixing model could be made. The effect of backmixing should be to increase the number of equilibrium stages necessary to give the same separation.

SIMULATION STUDIES

Figure 9 shows a diagram of the column and Table 16 gives the detailed conditions of operation. An equation for each specie in the column can be written in the general form of Equation (72). The results are:

Equation for Pu(IV)

$$\begin{aligned}
 [Pu(IV)]_{c,i}^{t+\Delta t} = & [Pu(IV)]_{c,i}^t + \frac{F_c}{H_i} [(1 + \alpha_{c,i+1})[Pu(IV)]_{c,i+1} + \alpha_{c,i-1} \\
 & [Pu(IV)]_{c,i-1} - (1 + 2\alpha_{c,i})[Pu(IV)]_{c,i}] + \frac{F_d}{H_i} [(1 + \alpha_{d,i-1}) \\
 & E_{Pu,i-1}[Pu(IV)]_{c,i-1} + \alpha_{d,i+1}E_{Pu,i+1}[Pu(IV)]_{c,i+1} \\
 & - (1 + 2\alpha_{d,i})E_{Pu,i}[Pu(IV)]_{c,i}] - Rxn\ 1 + Rxn\ 2 - Rxn\ 3 \\
 & - \frac{(1 - E_{Pu,i})}{H_i} [Pu(IV)]_{c,i} \frac{d}{dt} H_i \cdot \{\Delta t / [1 + E_{Pu,i}(\frac{V_i - H_i}{H_i})]\}
 \end{aligned}$$

Equation for Pu(III) (only present in aqueous phase)

$$\begin{aligned}
 [Pu(III)]_{c,i}^{t+\Delta t} = & [Pu(III)]_{c,i}^t + \frac{F_c}{H_i} [(1 + \alpha_{c,i+1})[Pu(III)]_{c,i+1} + \alpha_{c,i-1} \\
 & [Pu(III)]_{c,i-1} - (1 + 2\alpha_{c,i})[Pu(III)]_{c,i}] + Rxn\ 1 - Rxn\ 2 \\
 & + Rxn\ 3 - \frac{1}{H_i} [Pu(III)]_{c,i} \frac{d}{dt} H_i \cdot \Delta t
 \end{aligned}$$

Equation for U(VI) (no chemical reaction on U(VI))

$$\begin{aligned}
 [U(VI)]_{c,i}^{t+\Delta t} = & [U(VI)]_{c,i}^t + \frac{F_c}{H_i} [(1 + \alpha_{c,i+1})[U(VI)]_{c,i+1} + \alpha_{c,i-1}[U(VI)]_{c,i-1} \\
 & - (1 + 2\alpha_{c,i})[U(VI)]_{c,i}] + \frac{F_d}{H_i} [(1 + \alpha_{d,i-1})E_{U,i-1}[U(VI)]_{c,i-1} \\
 & + \alpha_{d,i+1}E_{U,i+1}[U(VI)]_{c,i+1} - (1 + 2\alpha_{d,i})E_{U,i}[U(VI)]_{c,i}]
 \end{aligned}$$

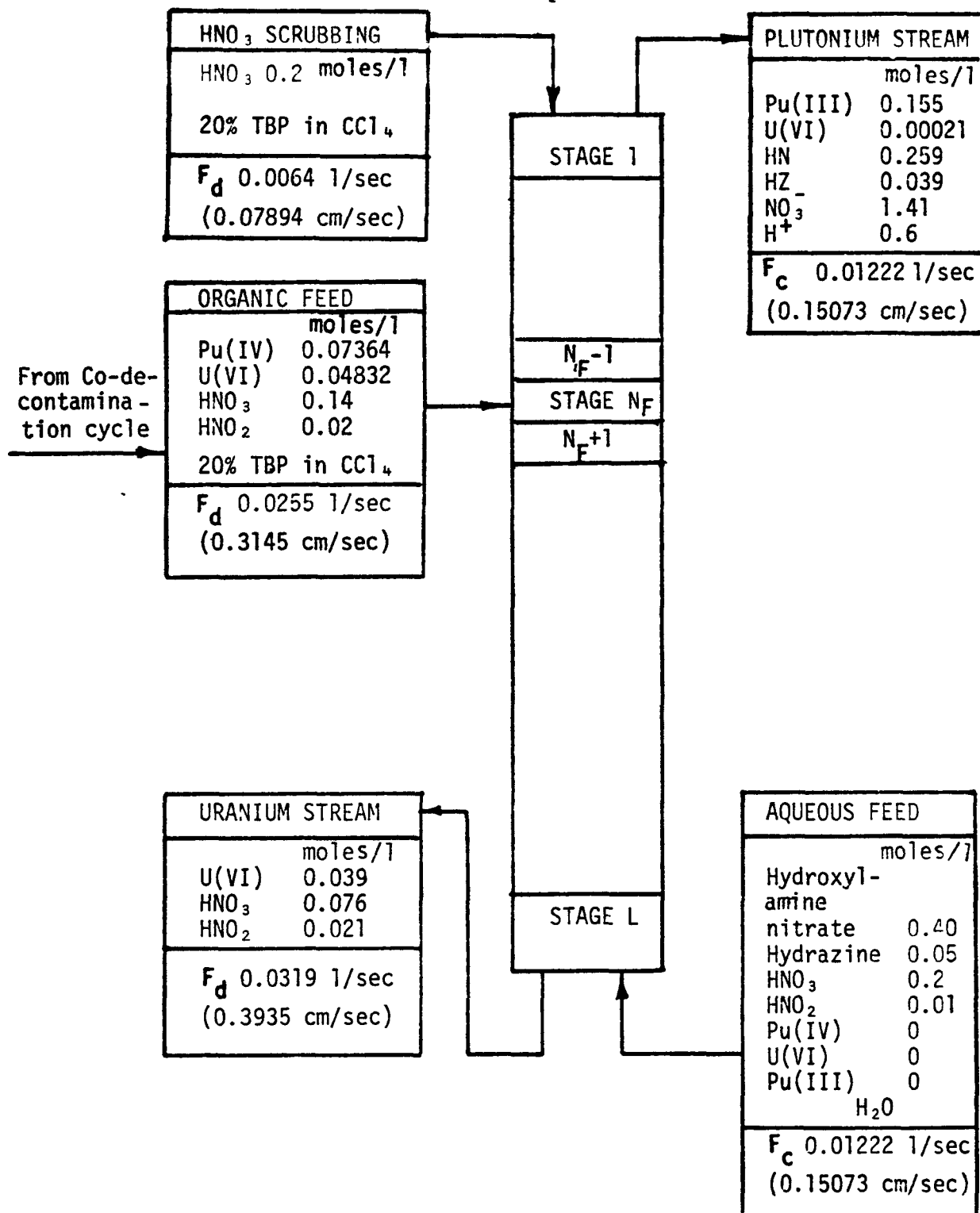


Figure 9. Flow sheet of U-Pu partitioning cycle. Initial conditions of the pulse column (from Pease).

Table 16. Pulse column simulation condition details

Column geometry	Column diameter	4.0 in	10.16 cm
	Column height	45.0 ft	1371.6 cm
	Plate spacing	2.0 in	5.08 cm
	Plate free area fraction	0.23	
	Cross section area	12.57 in ²	81.07 cm ²
	Total column volume	6788 in ³	1.1 x 10 ⁵ cm ³
System	Equilibrium stage volume	25.13 in ³	411.85 cm ³
	Dispersed phase	20% TBP in CCl ₄	
	Continuous phase	H ₂ O	
Physical properties	Interfacial surface tension	4.7x10 ⁵ lb/hr	16.5 dyne/cm
	Dispersed phase viscosity	2.68 lbm/ft hr	0.0111 poise
	Dispersed phase density	91.08 lb/ft ³	1.459 g/cm ³
Operating variables	Pulse amplitude	1.333 in/cyc	3.387 cm/cyc
	Pulse frequency	60.0 cyc/min	1.0 cyc/sec
	Dispersed phase flow rate	9.32 ^a 46.4 ft/hr	0.079 ^a 0.394 cm/sec
	Continuous phase flow rate	17.8 ft/hr	0.151 cm/sec
Column parameter	ψ	0.299	
	Dispersed phase holdup fraction, ϵ_d	0.0674 ^a	
	Continuous phase backflow ratio, α_c	20.95 ^a	
	Dispersed phase backflow ratio, α_d	18.06	
	Continuous phase backmixing coeff., E_c	2.387 ^a	
	Dispersed phase backmixing coeff., E_d	1.69	
		3.678 ^a	
		3.18 cm ² /sec	
		0.304 ^a	
		0.803 cm ² /sec	

^aValue for stages before feed stage.

$$- \frac{(1 - E_{U,i})}{H_i} [U(VI)]_{c,i} \frac{d}{dt} H_i \} \cdot \{ \Delta t / [1 + E_{U,i} \left(\frac{V_i - H_i}{H_i} \right)] \}$$

Equation for HNO_2

$$\begin{aligned} [HNO_2]_{c,i}^{t+\Delta t} = & [HNO_2]_{c,i}^t + \frac{F_c}{H_i} [(1 + \alpha_{c,i+1}) [HNO_2]_{c,i+1} + \alpha_{c,i-1} [HNO_2]_{c,i-1} \\ & - (1 + 2\alpha_{c,i}) [HNO_2]_{c,i}] + \frac{F_d}{H_i} [(1 + \alpha_{d,i-1}) [HNO_2]_{c,i-1} \\ & + \alpha_{d,i+1} E_{HNO_2,i+1} [HNO_2]_{c,i+1} - (1 + 2\alpha_{d,i}) E_{HNO_2,i} [HNO_2]_{c,i}] \\ & - \frac{1}{2} Rxn\ 2 - Rxn\ 4 - Rxn\ 5 - \frac{(1 - E_{HNO_2,i})}{H_i} [HNO_2]_{c,i} \frac{d}{dt} H_i \} \\ & \cdot \{ \Delta t / [1 + E_{HNO_2,i} \left(\frac{V_i - H_i}{H_i} \right)] \} \end{aligned}$$

Equation for hydroxylamine (only present in aqueous phase)

$$\begin{aligned} [NH_3OH^+]_{c,i}^{t+\Delta t} = & [NH_3OH^+]_{c,i}^t + \frac{F_c}{H_i} [(1 + \alpha_{c,i+1}) [NH_3OH^+]_{c,i+1} + \alpha_{c,i-1} [NH_3OH^+]_{c,i-1} \\ & - (1 + 2\alpha_{c,i}) [NH_3OH^+]_{c,i}] - 0.69 Rxn\ 1 - Rxn\ 5 \\ & - \frac{1}{H_i} [NH_3OH^+]_{c,i} \frac{d}{dt} H_i \} \Delta t \end{aligned}$$

Equation for hydrazine (only present in aqueous phase)

$$\begin{aligned} [N_2H_5^+]_{c,i}^{t+\Delta t} = & [N_2H_5^+]_{c,i}^t + \frac{F_c}{H_i} (1 + \alpha_{c,i+1}) [N_2H_5^+]_{c,i+1} + \alpha_{c,i-1} [N_2H_5^+]_{c,i-1} \\ & - (1 + 2\alpha_{c,i}) [N_2H_5^+]_{c,i}] - 0.25 Rxn\ 3 - Rxn\ 4 \\ & - \frac{1}{H_i} [N_2H_5^+]_{c,i} \frac{d}{dt} H_i \} \Delta t \end{aligned}$$

Equation for H^+

$$\begin{aligned}
 [H^+]_{c,i}^{t+\Delta t} = & [H^+]_{c,i}^t + \left[\frac{F_c}{H_i} \right] \left[(1 + \alpha_{c,i+1}) [H^+]_{c,i+1} + \alpha_{c,i-1} [H^+]_{c,i-1} \right. \\
 & - (1 + 2\alpha_{c,i}) [H^+]_{c,i} \left. + \frac{F_d}{H_i} \right] \left[(1 + \alpha_{d,i-1}) E_{HNO_3,i-1} [NO_3^-]_{c,i-1} \right. \\
 & + \alpha_{d,i+1} E_{HNO_3,i+1} [NO_3^-]_{c,i+1} \left. - (1 + 2\alpha_{c,i}) E_{HNO_3,i} [NO_3^-]_{c,i} \right] \\
 & + 1.75 \text{ Rxn 1} - 1.5 \text{ Rxn 2} + 1.25 \text{ Rxn 3} + \text{Rxn 4} + \text{Rxn 5} - ([H^+]_{c,i}^t \\
 & - E_{HNO_3,i} [NO_3^-]_{c,i}) \frac{1}{H_i} \frac{d}{dt} H_i \} \Delta t - \left(\frac{V_i - H_i}{H_i} \right) E_{HNO_3,i} ([NO_3^-]_{c,i}^{t+\Delta t} - [NO_3^-]_{c,i}^t)
 \end{aligned}$$

Equation for NO_3^-

$$\begin{aligned}
 [NO_3^-]_{c,i}^{t+\Delta t} = & [NO_3^-]_{c,i}^t + \left[\frac{F_c}{H_i} \right] \left[(1 + \alpha_{c,i+1}) [NO_3^-]_{c,i+1} + \alpha_{c,i-1} [NO_3^-]_{c,i-1} \right. \\
 & - (1 + 2\alpha_{c,i}) [NO_3^-]_{c,i} \left. + \frac{F_d}{H_i} \right] \left[(1 + \alpha_{d,i-1}) (E_{HNO_3,i-1} [NO_3^-]_{c,i-1} \right. \\
 & + 4E_{Pu,i-1} [Pu(IV)]_{c,i-1} + 2E_{U,i-1} [U(VI)]_{c,i-1}) \\
 & + \alpha_{d,i+1} (E_{HNO_3,i+1} [NO_3^-]_{c,i+1} + 4E_{Pu,i+1} [Pu(IV)]_{c,i+1} \\
 & + 2E_{U,i+1} [U(VI)]_{c,i+1}) \left. - (1 + 2\alpha_{d,i}) (E_{HNO_3,i} [NO_3^-]_{c,i} \right. \\
 & + 4E_{Pu,i} [Pu(IV)]_{c,i} + 2E_{U,i} [U(VI)]_{c,i}) \left. \right] - \frac{1}{2} \text{ Rxn 2} \\
 & - \left(\frac{1 - E_{HNO_3,i}}{H_i} \right) [NO_3^-]_{c,i} \frac{d}{dt} H_i \} \Delta t - 4E_{Pu,i} \frac{V_i - H_i}{H_i} \\
 & ([Pu(IV)]_{c,i}^{t+\Delta t} - [Pu(IV)]_{c,i}^t) - 2E_{U,i} \frac{V_i - H_i}{H_i} ([U(VI)]_{c,i}^{t+\Delta t} \\
 & - [U(VI)]_{c,i}^t) / (1 + \frac{V_i - H_i}{H_i} E_{HNO_3,i})
 \end{aligned}$$

RESULTS

Four programs, one for each combination of two holdup subroutines, each in turn with and without backmixing, were used. The results are shown in Table 17. According to the different holdup and backmixing correlations in the results obtained are discussed below.

The results of Run 1, listed in Table 17, show that the dispersed phase holdup fraction evaluated from the flow rate ratio approach is 0.34 above the feed stage and 0.73 below the feed stage. From the results of the literature survey and from comparison with the plant scale column (43), the dispersed phase holdup fraction calculated from this assumption appears to be much too high. In this run which followed the piston flow model with 20 equilibrium stages, the plutonium inventory in the column at steady state was 868.234 grams. This is lower than the value reported by Bruns (7) who estimated the amount to be about 2 kilograms. Although the output concentrations are in good agreement with Pease's actual column data the concentration profiles probably peak too much because backmixing has not been accounted for.

A second run made with the new holdup correlation gave a dispersed phase holdup fraction of 0.067 in those stages above feed stage and 0.196 in those stages below the feed stage. By comparison with the data of Rouyer et al. (43) and Arthayukti et al. (2) this value is reasonable. The plutonium inventory increased to 1147 grams. The output streams still show good agreement with Pease's data.

Backmixing was included in the third run in which the backflow ratios were calculated as $\alpha_i = Afe_i/F_i$. The holdup used to calculated the

Table 17. Comparison of the simulated models with the actual column

Variables	Dispersed phase holdup fraction	Aqueous back flow ratio	Organic back flow ratio	Plutonium stream			
				Pu(III) mole/l g/hr	U(VI) mole/l g/hr	HN	HNO ₃
Run	ϵ_d	α_c	α_d			M	M
A ^a				0.147 1619.2	0.0006 6.8	0.31	1.13
B ^b	0.067* 0.196	20.95* 18.06	2.887* 1.69	0.146 1534	0.0084 86.86	0.28	1.25
C ^c	0.064* 0.187	21.03* 18.27	2.75* 1.61	9.146 1534.6	0.0084 85.82	0.28	1.25
D ^d	0.067* 0.196	0	0	0.153 1614	0.0004 3.83	0.27	1.41
E ^e	0.344* 0.73	0	0	0.155 1634.2	0.0002 2.2	0.26	1.41
F ^f	0.067* 0.196	20.897* 17.99	2.886* 1.69	0.153 1609.3	0.00054 5.55	0.28	1.33

^aPease's actual column with 270 real stages, as cited by McCutcheon (30).

^bSimulated backflow model with holdup evaluated by using proposed correlation and equilibrium stages assumed as 20. (Run No. 3).

^cSimulated model with holdup evaluated by using Miyauchi's correlation and equilibrium stages assumed to be 20. (Run No. 4).

^dSimulated plugflow model with holdup evaluated by using proposed correlation and equilibrium stages assumed to be 20. (Run No. 2).

^eSimulated plugflow model with holdup evaluated by using pseudoflow ratio approach and equilibrium stages assumed to be 20. (Run No. 1).

^fSimulated backflow model with holdup evaluated by using proposed correlation and equilibrium stage assumed to be 90 (results of Yih (57)).

^gTracer quantity.

*Value for stages before feed stage.

Uranium stream						Flow rate			Pu(III) Inventory grams
H ⁺ M	HNO ₂ M	Pu(IV) mole/l g/hr	U(VI) mole/l g/hr	HNO ₃ M	HNO ₂ M	F _d 1/hr cm/sec	F _c 1/hr cm/sec		
0.77	-	0	0.0396 1050.9	0.012	-	113 0.387	46 0.157		
0.52	-9	-9	0.0354 955.4	0.137	0.002	114.84 0.393	44 0.151	1448.29	
0.52	-9	-9	0.0354 955.4	0.137	0.002	114.84 0.393	44 0.151	1443.95	
0.7	-9	0	0.0385 1056.7	0.076	0.004	114.84 0.393	44 0.151	1146.81	
0.6	0	0	0.0392 1052.3	0.076	0.021	114.84 0.393	44 0.151	868.23	
0.62	0	-9	0.0384 1036.3	0.104	0.023	114.84 0.393	44 0.151	2840.0	

backflow ratio was that obtained from the new holdup correlation. The dispersed phase holdup was thus the same as that in the second run, since the same correlation was used. Figures 10 through 15 show the comparison of the concentration profiles of this run with the second run which had no backmixing effects.

Figure 10 shows the plutonium concentration profiles from the backmixing and the piston flow models. The plutonium (III) and the uranium (VI) concentration profiles both have more of a flat profile than the corresponding curves for the piston flow model. The profiles from the backmixing run show a higher concentration present in each equilibrium stage and hence the plutonium inventory is higher. The plutonium inventory for this run was 1448.29 grams, which is closer to the value suggested by Bruns (7). This shows the importance of backmixing effects in the simulation work.

The plutonium (III) concentration at the bottom of the column is much higher for the backmixing run. In fact it indicates contamination of the uranium product stream since such a high concentration in the aqueous phase at the bottom of the column also means that there will be a significant amount of plutonium in the uranium product stream leaving the bottom of the column. An increased number of equilibrium stages is needed to meet the output concentration found experimentally.

Figure 11 shows the uranium concentration profiles. The backmixing effects on the uranium concentration profile are very severe in both phases. Therefore, the uranium concentration in the plutonium product stream at the top of the column will be contaminated with uranium.

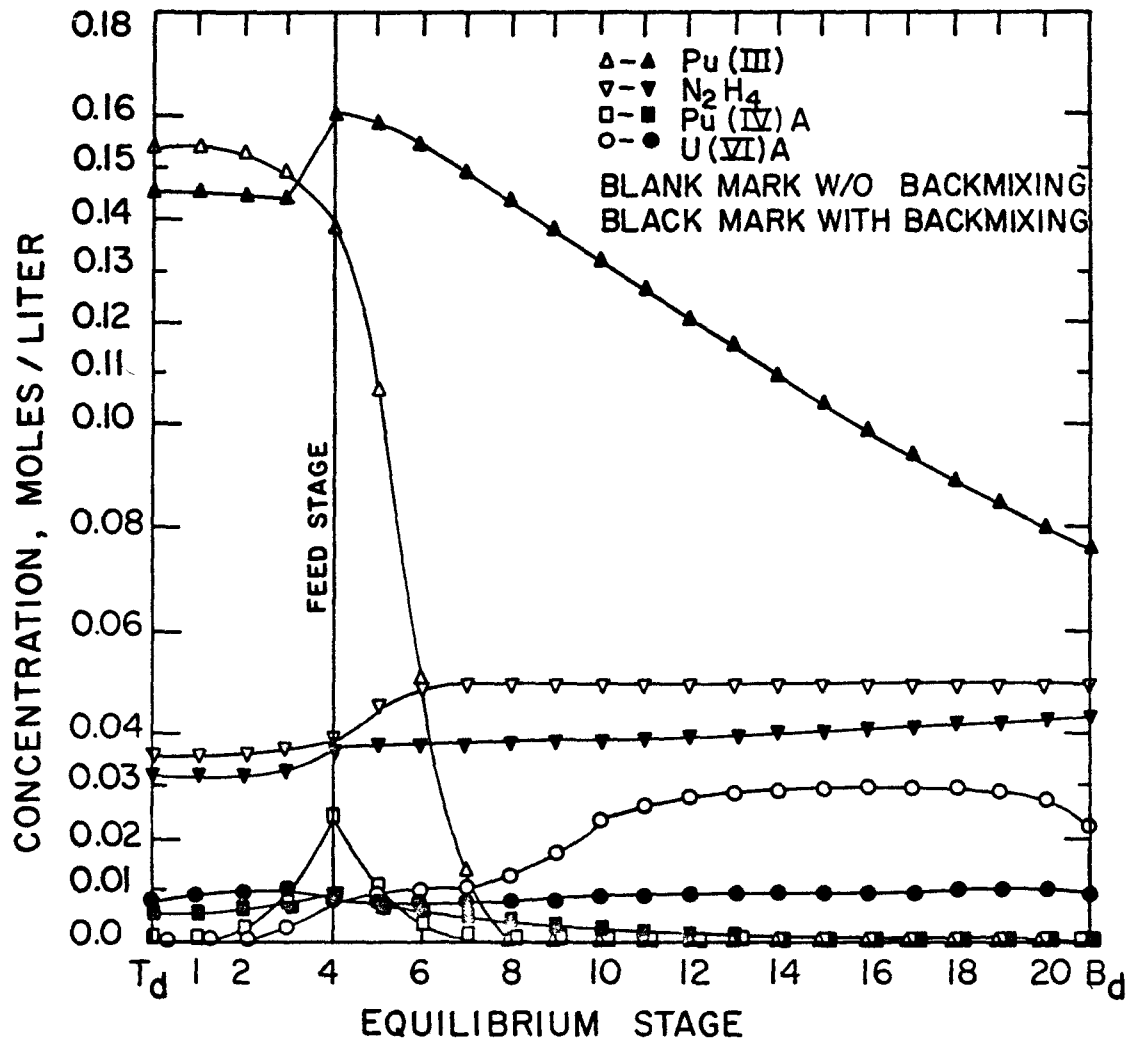


Figure 10. Comparison of plutonium stream profiles with and without backmixing effects (aqueous phase).

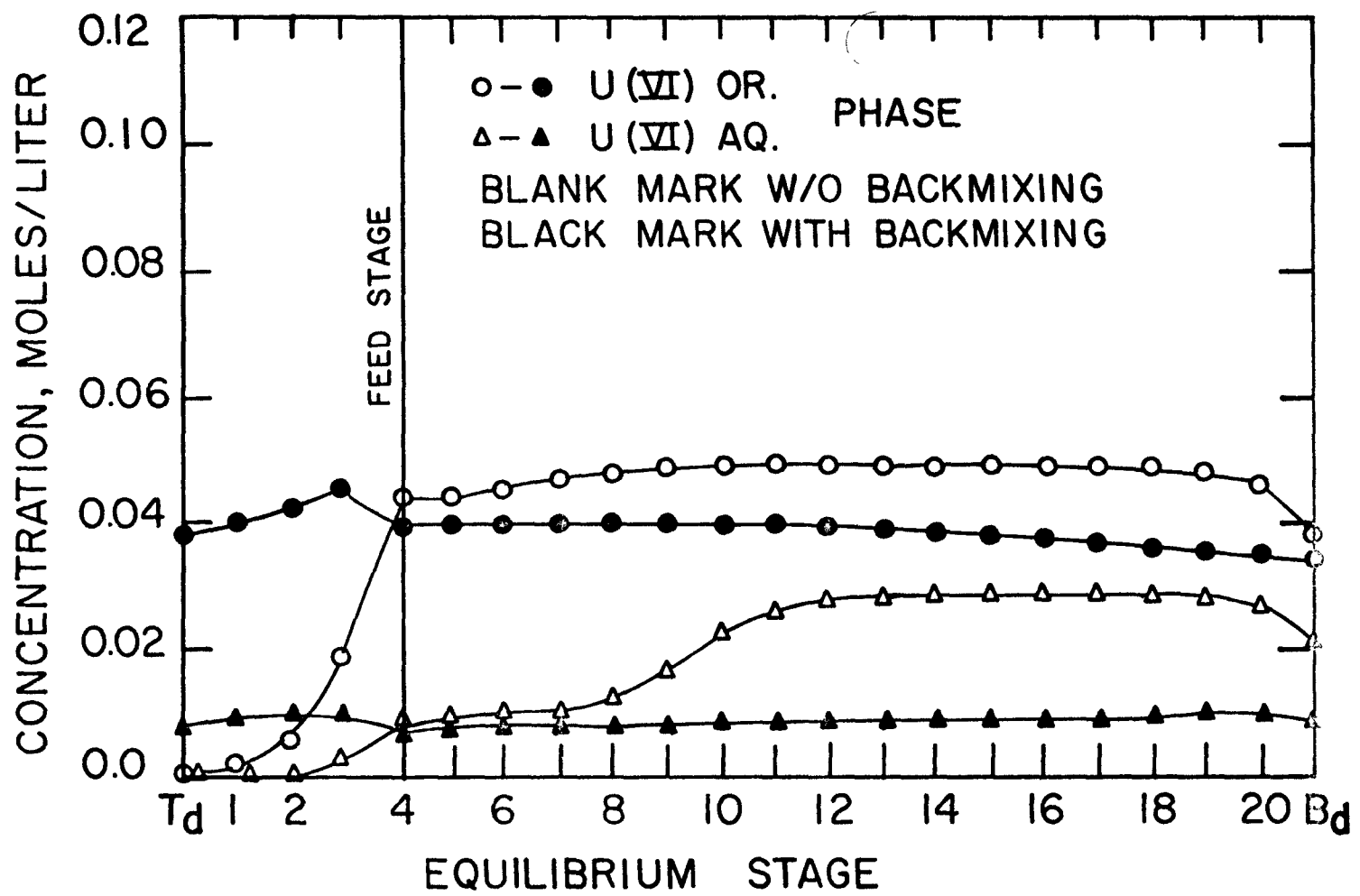


Figure 11. Comparison of uranium concentration profiles in both phases with and without backmixing.

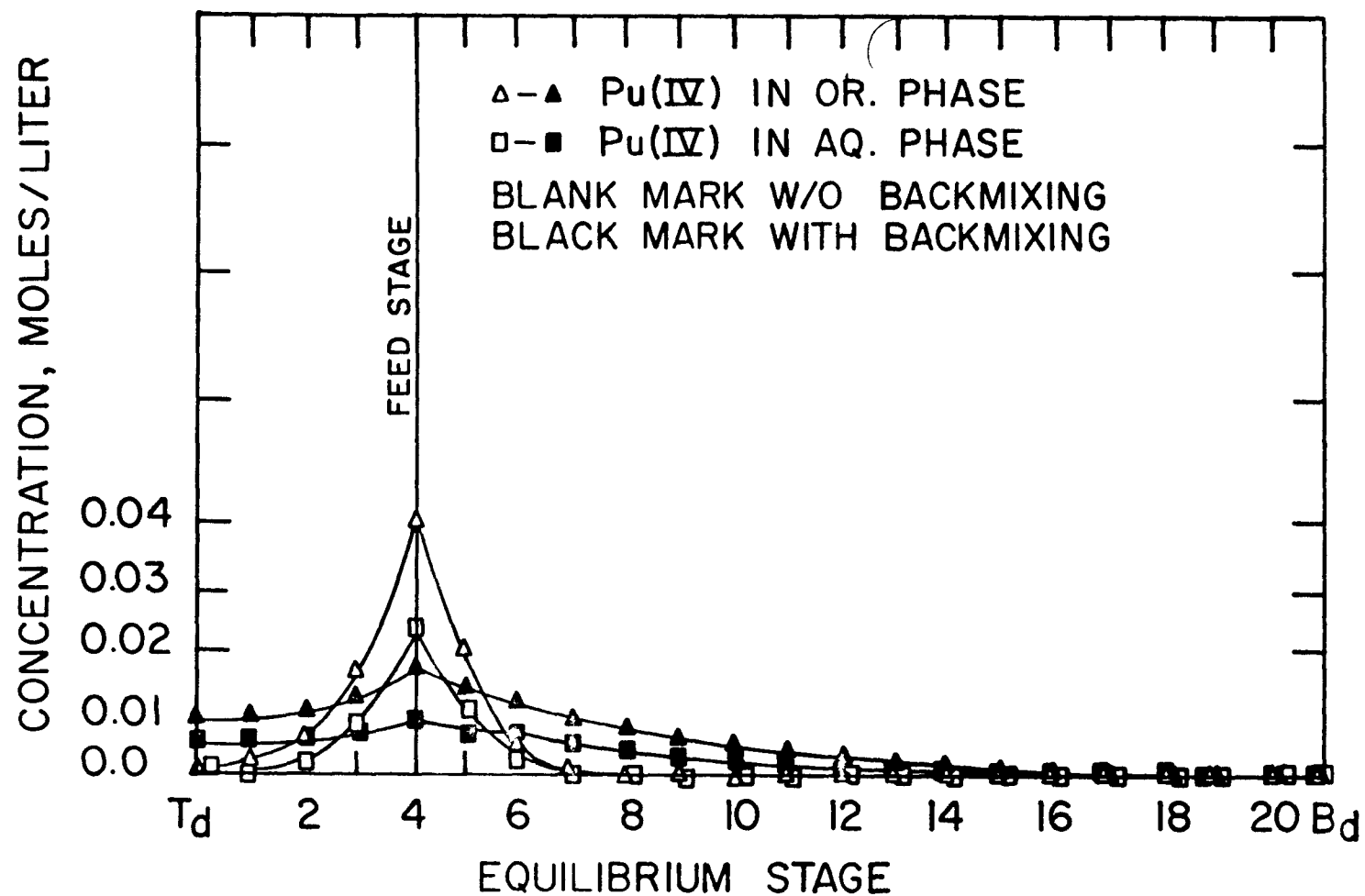


Figure 12. Comparison of plutonium (IV) concentration profiles in both phases with and without backmixing.

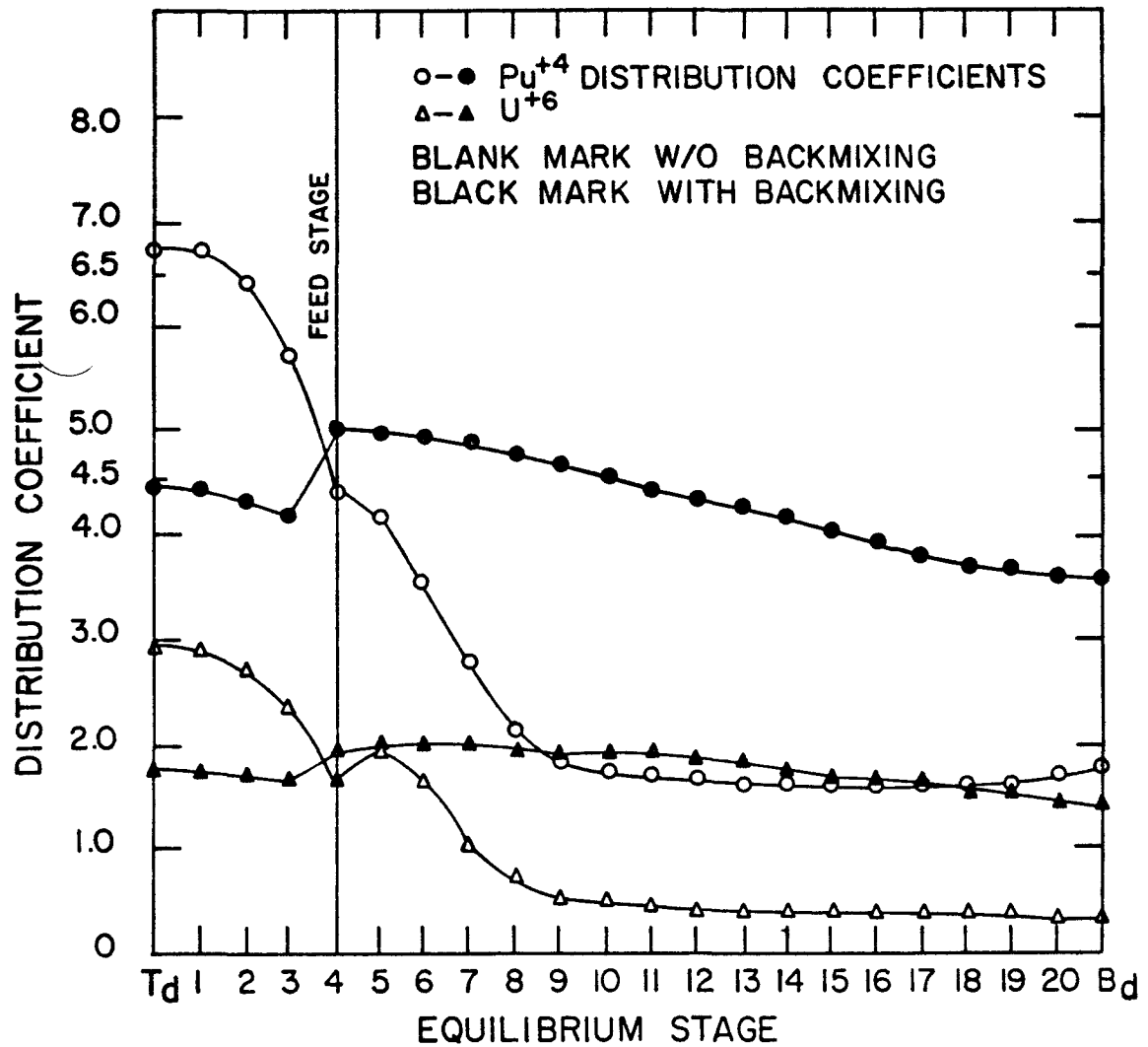


Figure 13. Comparison of distribution coefficients of uranium and plutonium (IV) with and without backmixing effect.

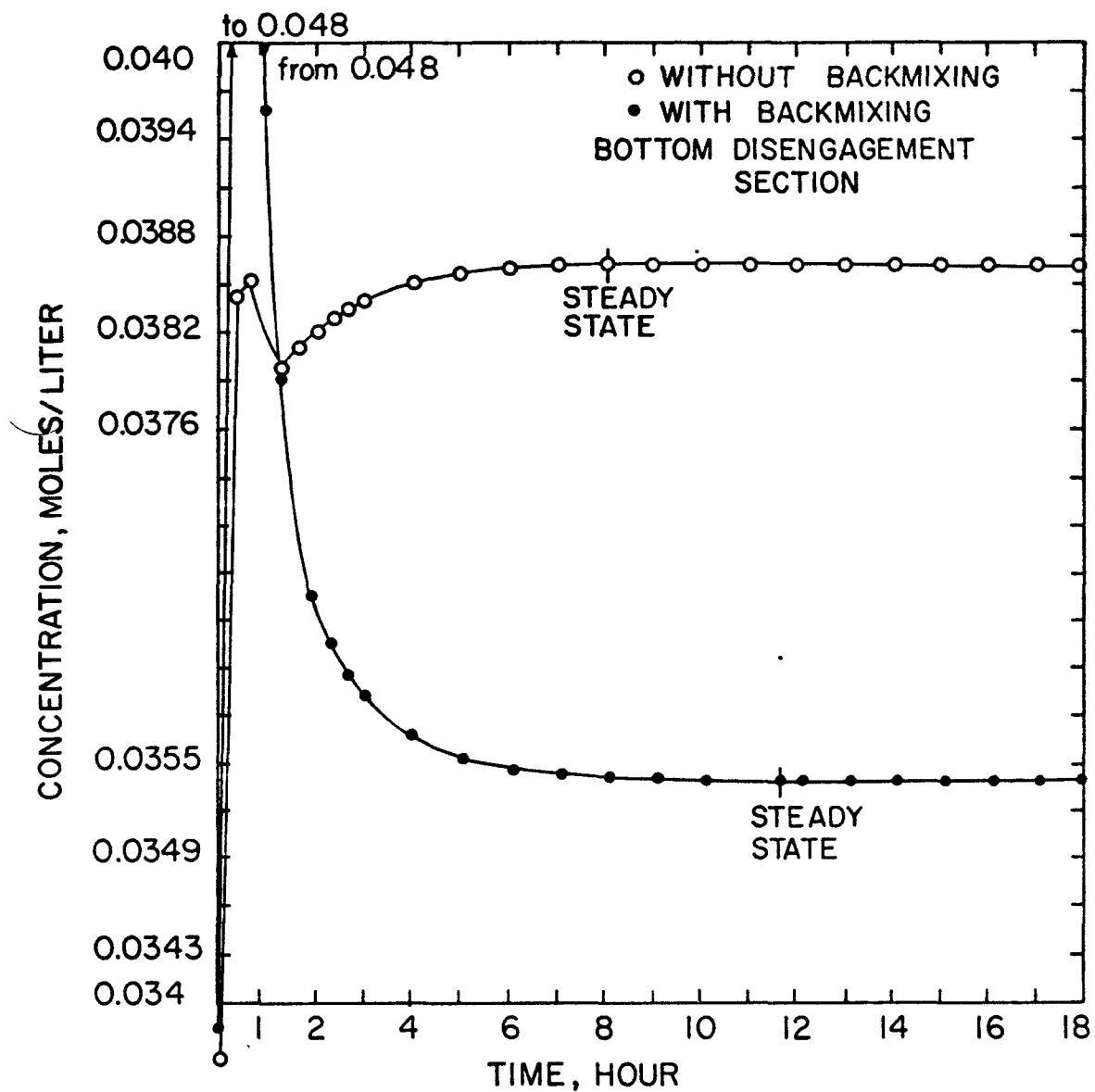


Figure 14. Comparison of transient concentration profiles of uranium in uranium stream with and without backmixing effect.

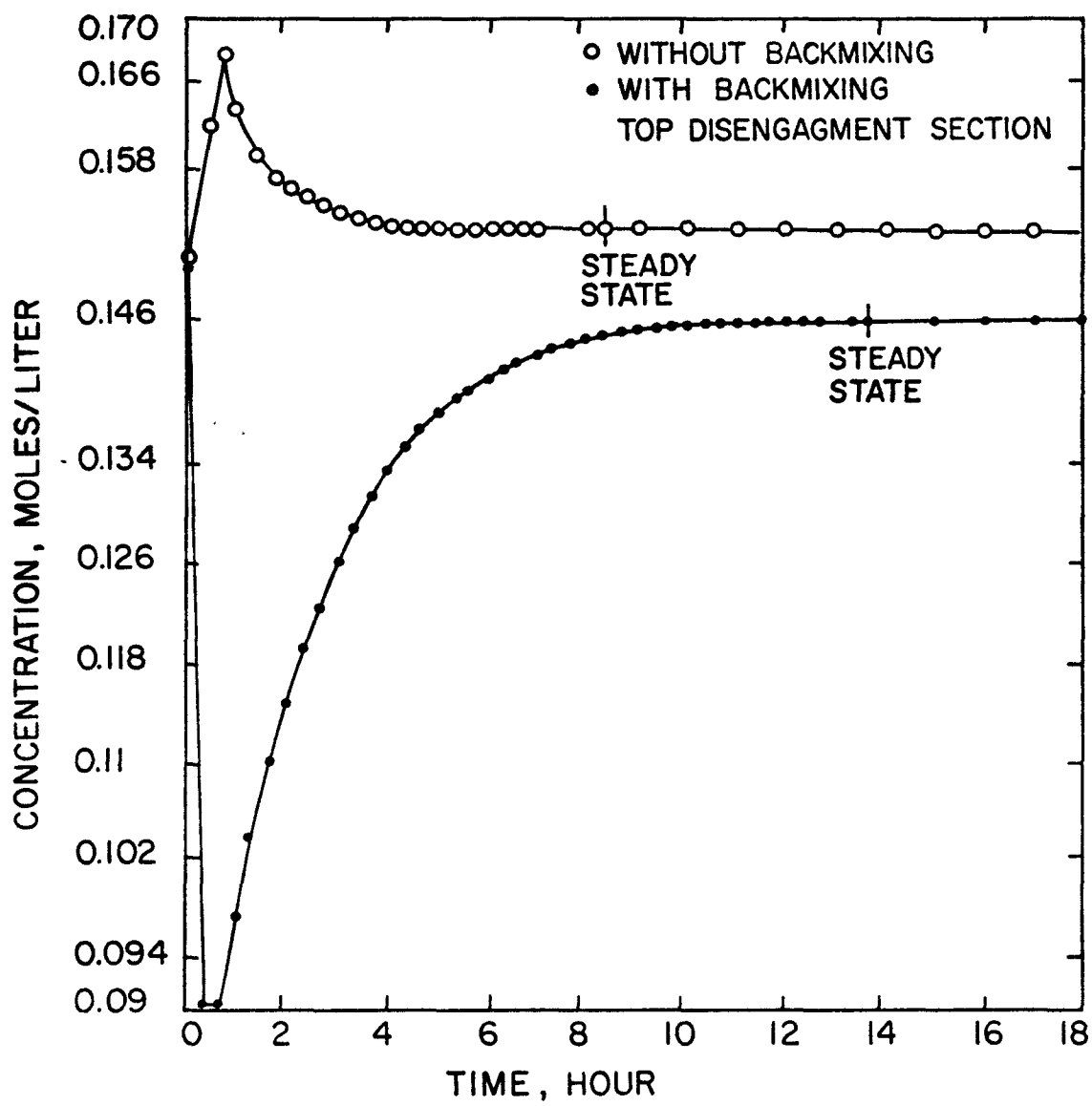


Figure 15. Comparison of transient concentration profiles of plutonium (III) with and without backmixing effect.

Plutonium (IV) concentration profiles are plotted in Figure 12. Backmixing effects can be seen in the characteristic flat concentration profile. The plutonium profile in the organic phase is higher than the plutonium profile in the aqueous phase because the plutonium (IV) in the aqueous phase is reduced to plutonium (III) by hydroxylamine and subsequently transferred to the aqueous phase. Pu(III) is essentially insoluble in the organic phase.

The distribution coefficients of plutonium and uranium are functions of ionic strength which, in turn, is a function of the concentration of each species in the column. Because backmixing affects the concentration distribution of each component, the distribution coefficients are also affected. The magnitude of the effect is shown in Figure 13.

The transient change in the uranium concentration in the uranium product stream leaving the bottom of the column is shown in Figure 14. The transient concentration in the piston flow model increases from a minimum point to steady state in 8 hours. But the uranium transient concentration under the influence of backmixing decreases from a maximum point to its steady state value. The time needed is 11 hours.

Figure 15 shows that the plutonium (III) transient concentration in the piston flow model decreases from the maximum point to steady state in 8 hours. The plutonium (III) transient concentration leaving the top of the column in the backmixing model increases from a minimum point to steady state in 13 hours, which is longer than the 8 hours required without backmixing. From this comparison it can be seen that backmixing increases the time needed to arrive at steady state.

The fourth run used the holdup equation of Miyauchi. The dispersed phase holdup fraction was 0.064 for the stages above the feed stage and 0.187 for the stages below the feed stage. The ψ value calculated for this simulation is 0.299 and at this value Miyauchi's correlation is very close to the new correlation. Hence the calculated values of holdup will be very similar. Therefore, the results of this run were not plotted, since the other effects were also similar to those found in the third run. The plutonium inventory for the fourth run was 1443.95 grams, a little lower than the value from third run.

Since the contamination of the uranium product stream and the plutonium product stream was very severe when backmixing effects were included in a 20 equilibrium stage model, an increase in the number of equilibrium stages is necessary in order to simulate the measured column performance.

This work has been done by Yih (57) in an independent study. The number of equilibrium stage was determined by trial and error based on the specifications for acceptable levels of uranium and plutonium contamination. The number of equilibrium stages needed to correct the backmixing effects was 90 which is 4.5 times the number used by McCutcheon. Figures 16 through 20 are the comparison of the concentration profiles of piston flow, 20 stage backmixing model and 90 stage backmixing model. The output concentrations are in good agreement to Pease's experimental data. The plutonium inventory is 2840 grams which is a little higher than Brun's suggested value. However the effect of extraction efficiency has not yet been accounted for even in the 90 stage simulation.

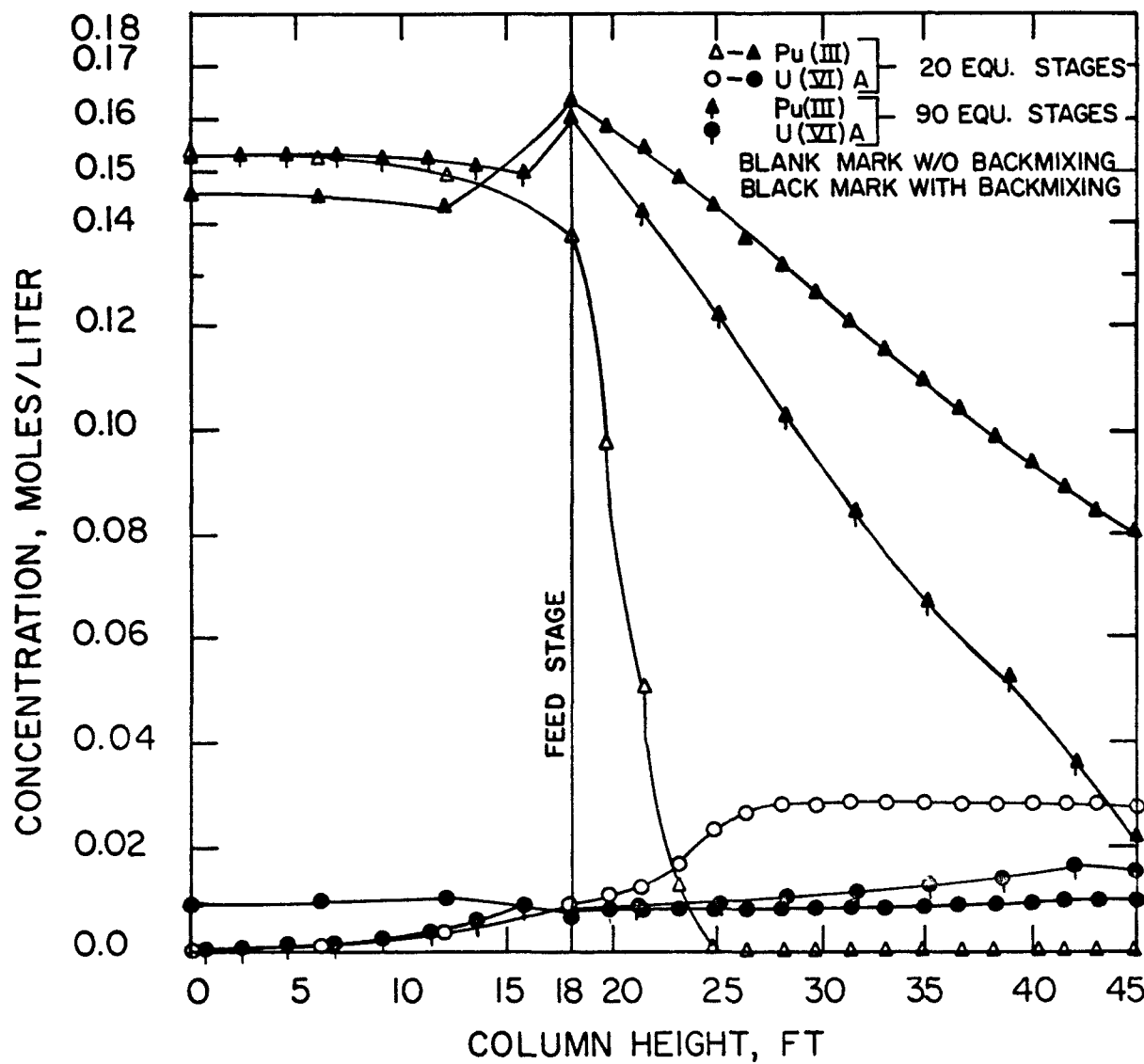


Figure 16. Comparison of plutonium stream concentration profiles in different equilibrium stage model with and without backmixing effect.

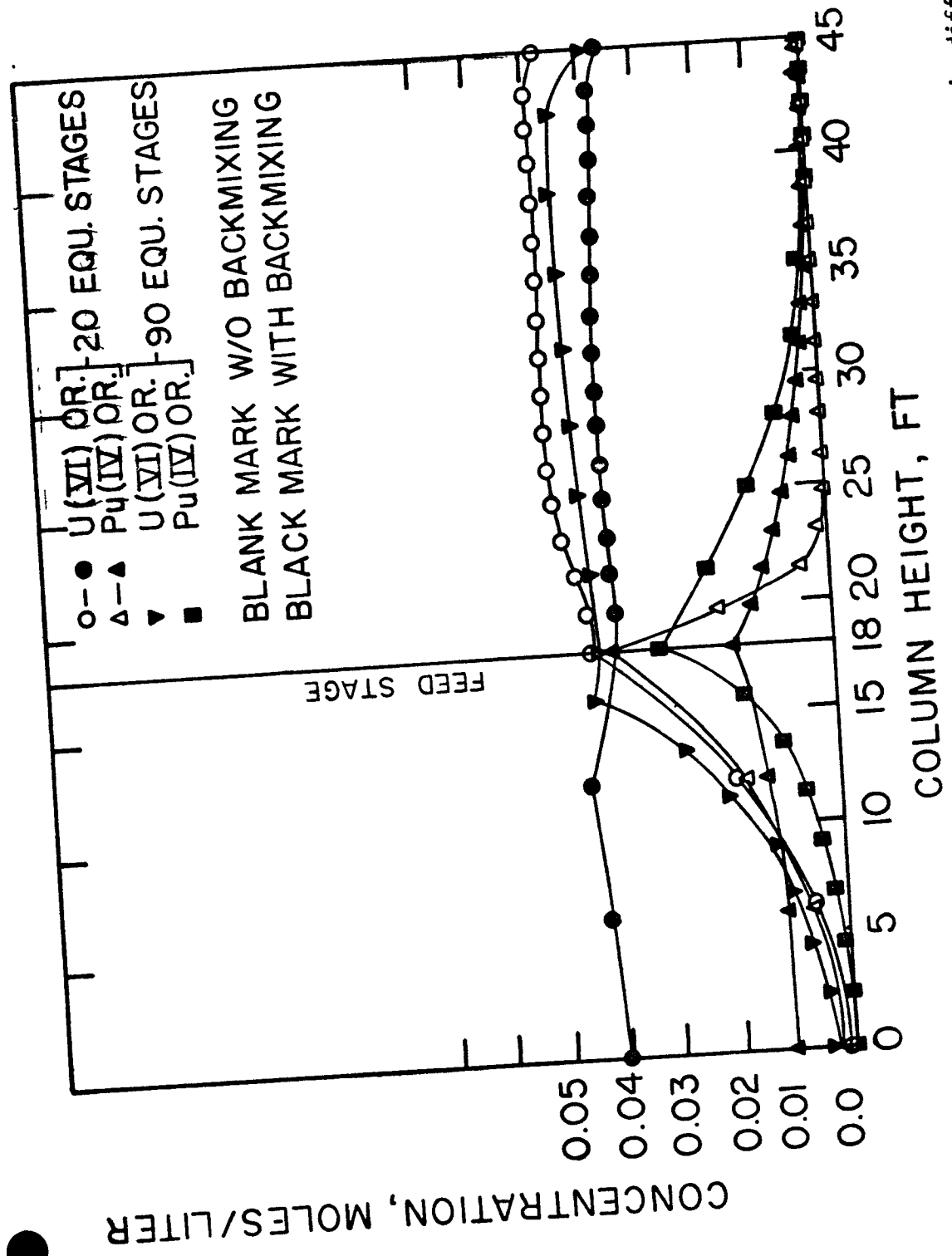


Figure 17. Comparison of uranium and plutonium concentration profiles in organic phase in different equilibrium stage model with and without backmixing effect.

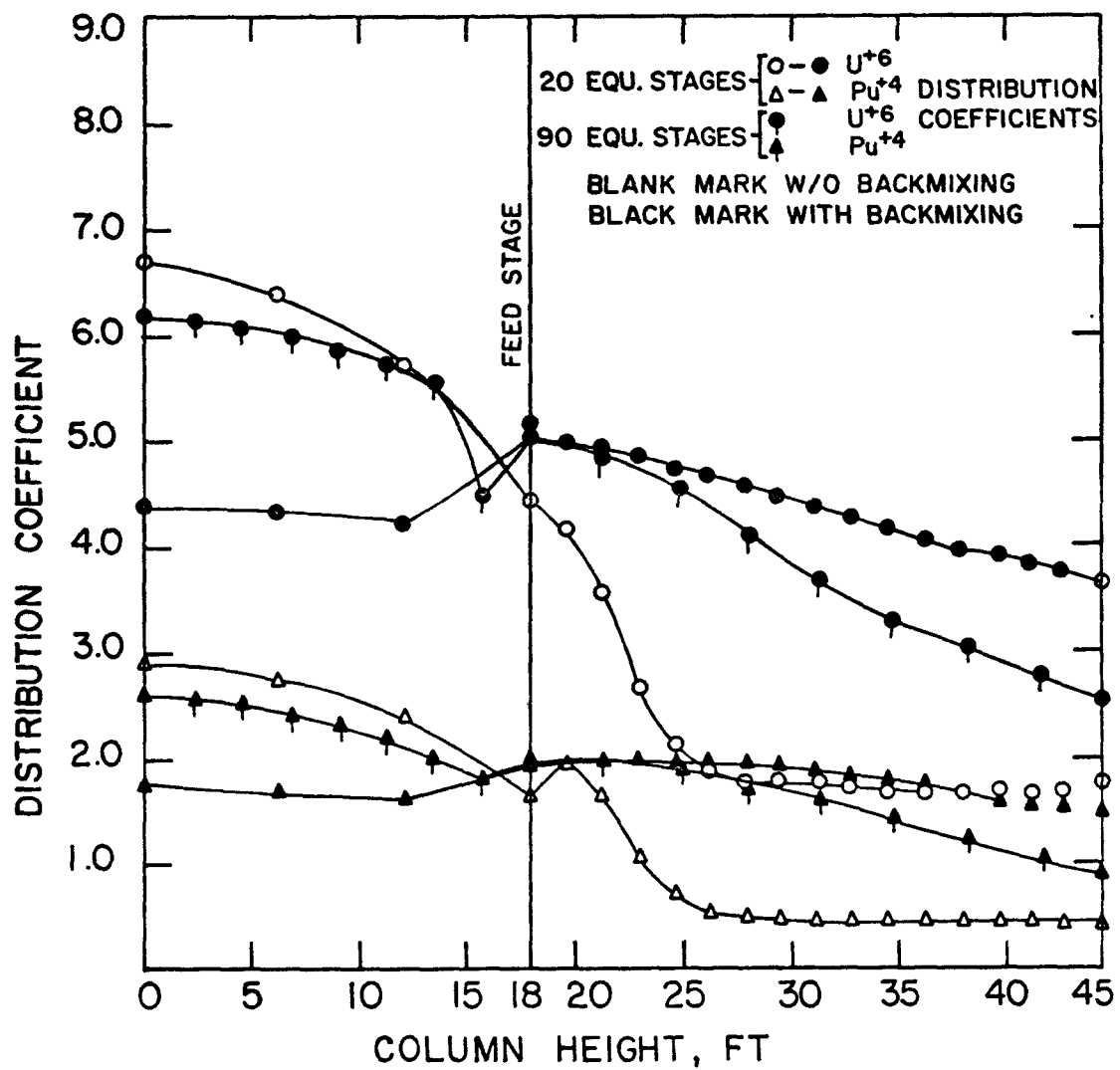


Figure 18. Comparison of distribution coefficients of uranium and plutonium in different equilibrium stage model with and without backmixing effect.

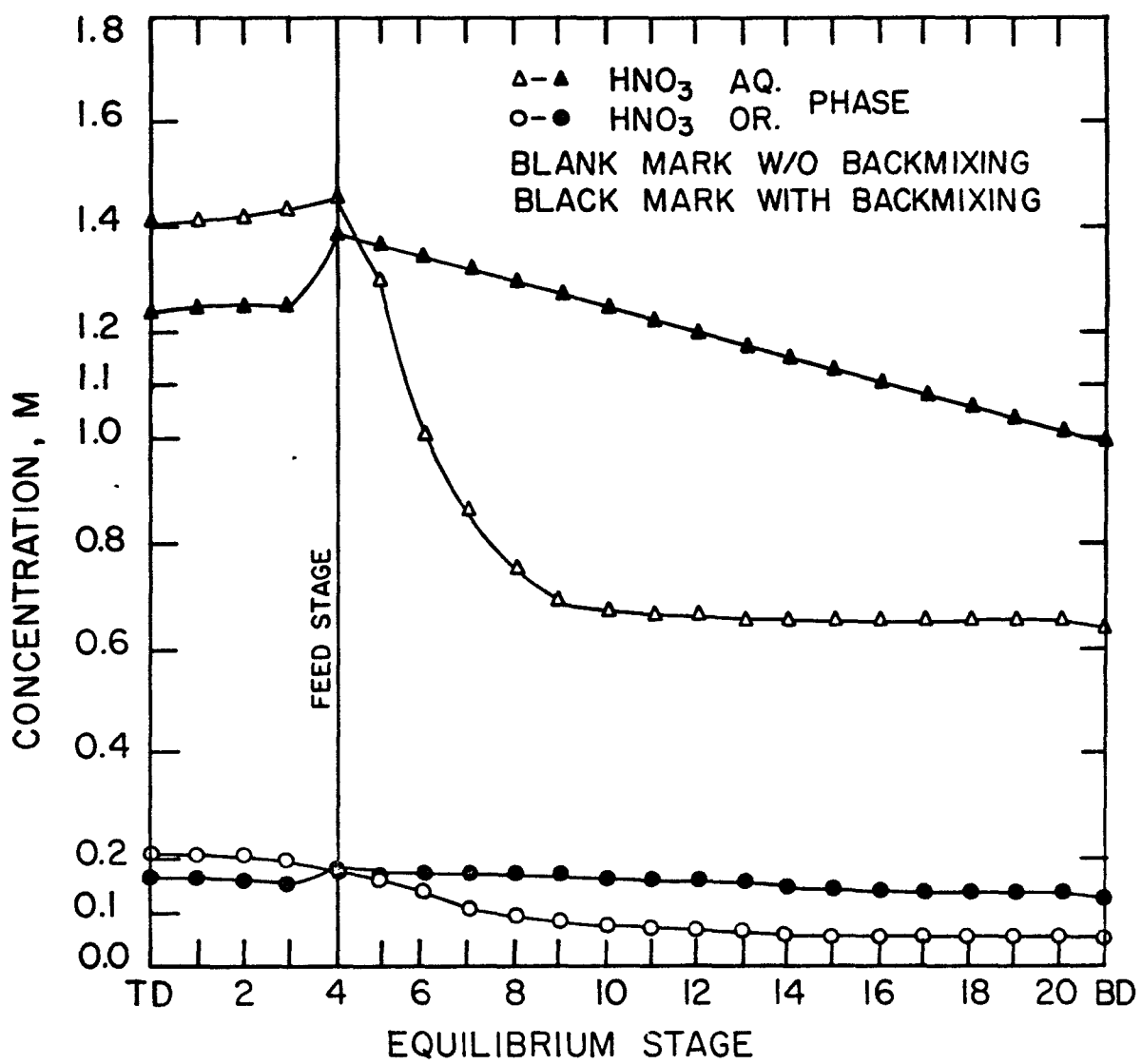


Figure 19. Comparison of hydroxylamine, hydrogen ion, and hydrazine concentration profiles in different equilibrium stage model with and without backmixing effect.

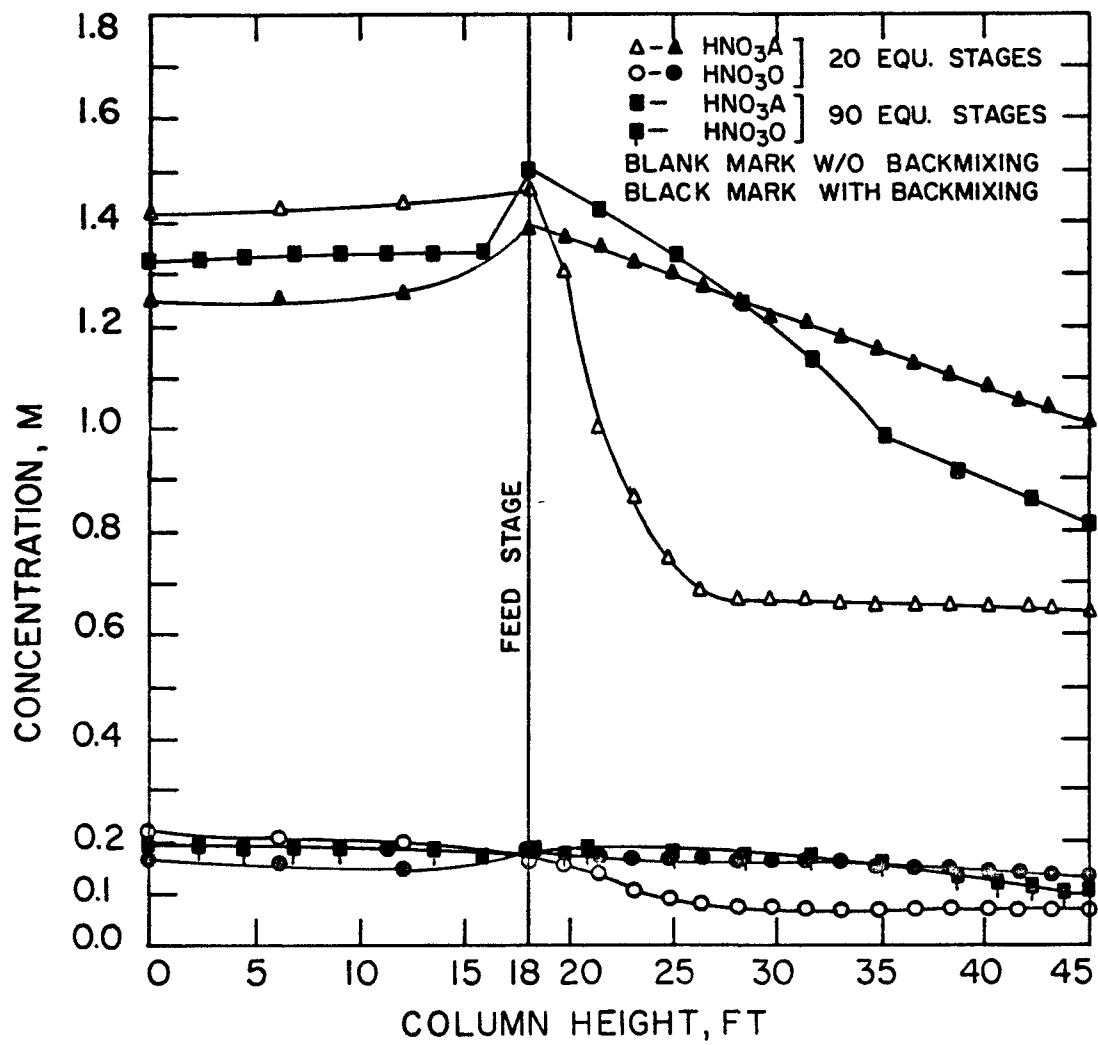


Figure 20. Comparison of nitric acid concentration profiles in both phases with and without backmixing effect.

Figure 16 shows that the profile for plutonium (III) in the 90 stage backmixing model has a slope between that of the piston flow model and the backmixing model, both with 20 equilibrium stages. This means that the backmixing effects are not so severe as in the 20 stage model. The uranium contamination is reduced by using the 90 stage backmixing model.

Table 17 shows that the 90 stage model is in good agreement with Pease's actual column data and a little higher than Bruns estimate (7). Only the nitric acid concentration in the uranium stream is too high to fit Pease's data. It is expected that even better agreement with experimental data will be obtained when the effects of extraction efficiency, or finite mass transfer rates, are included in the model.

CONCLUSIONS AND RECOMMENDATIONS

Backmixing effects on pulse column operation have been investigated by a critical survey of the literature and also by mathematical simulation of a plutonium-uranium partitioning column. A variety of conclusions can be drawn regarding holdup and backmixing phenomena.

(1) Holdup plays an important role in backmixing effects. A correct holdup estimate is needed to achieve a good simulation with backmixing. The newly proposed holdup correlation is an improvement over those which have already been proposed.

(2) Backmixing effects on the pulse column have been shown very clearly from the simulation work by the resulting flat concentration profiles, the elongation of the time required to arrive at steady state, and by the increase in number of equilibrium stages required in the simulation model.

(3) In pulse column design backmixing must be taken into account. A higher column is needed than that predicted from a model which does not include backmixing.

(4) In the present simulation work, the extraction efficiency was assumed to be 100% to investigate only the influence of backmixing. Since the extraction efficiency is also important, the interphase mass transfer coefficients must also be incorporated into the model.

(5) In simulation work with backmixing and extraction efficiency a correlation for H.T.U. is needed and experimental work in this area is recommended.

LITERATURE CITED

1. Aris, R. 1959. Notes on the diffusion type model for longitudinal mixing in flow. *Chem. Eng. Sci.* 9: 266-267.
2. Arthayukti, W., G. Muratet and H. Angelino. 1976. Longitudinal mixing in the dispersed phase in pulsed perforated-plate columns. *Chem. Eng. Sci.* 31: 1193-1197.
3. Bell, R. L. and A. L. Babb. 1969. Holdup and axial distribution of holdup in a pulsed sieve-plate solvent extraction column. I. and E. C. *Process Design and Development* 8(3): 392-400.
4. Biery, J. C. 1961. The transient startup behavior of a liquid-liquid extraction pulse column. Ph.D. dissertation. Iowa State University, Ames, Iowa.
5. Biery, J. C. and D. R. Boylan. 1963. Dynamic simulation of a liquid-liquid extraction column. I. and E. C. *Fund.* 2: 44.
6. Bischoff, K. B. and O. Levenspiel. 1962. Fluid dispersion-generalization and comparison of mathematical models-1 generalization of models. *Chem. Eng. Sci.* 17: 245-255.
7. Bruns, L. E. 1969. Plutonium-uranium processing in the plutonium reclamation facility by coextraction-partition. U.S. AEC ARH-1343.
8. Burger, L. L. and W. H. Swift. 1953. Backmixing in pulse columns II experimental values and effect of several variables. U.S. AEC HW-29010.
9. Burkhardt, L. E. 1956. Extraction efficiency of a pulse column of varied geometry. M.S. thesis. Iowa State University, Ames, Iowa.
10. Burkhardt, L. E. 1958. Pulse column design. Ph.D. dissertation. Iowa State University, Ames, Iowa.
11. Cohen, R. M. and G. H. Beyer. 1953. Performance of a pulse extraction column. *Chem. Eng. Progress* 49(6): 279-286.
12. Danckwerts, P. V. 1953. Continuous flow systems: Distribution of residence times. *Chem. Eng. Sci.* 2(1): 1-13.
13. Davies, O. L. 1954. Design and analysis of industrial experiments. Hafner Publication Co., New York.
14. Defives, D. G. Schneider. 1961. Retention of dispersed phase in a pulse column. *Genie Chim.* 85: 246-251.

15. Eguchi, W. and S. Nagata. 1959. Studies on the pulsed plate column. *Chem. Eng. Japan* 23(3): 146-152.
16. Endoh K. and Y. Oyama. 1958. On the size of droplet disintegrated in liquid-liquid contacting mixer. *J. Sci. Res. Inst.* 52(1496): 131-142.
17. Foster, H. R., Jr., R. E. McKee and A. L. Babb. 1970. Transient holdup behavior of a pulsed sieve plate solvent extraction column. *I. and E. C. Process Design and Development* 9(2): 272-278.
18. Geankoplis, C. J. and A. N. Hixson. 1950. Mass transfer coefficients in an extraction spray tower. *I. and E. C.* 42(6): 1141-1151.
19. Graham, H. V. 1960. Effect of pulse column variables on bubble diameter. *Ph.D. dissertation. Iowa State University, Ames, Iowa.*
20. Groenier, W. S., R. A. McAllister, and A. D. Ryon. 1966. Flooding perforated-plate pulsed extraction columns: A survey of reported experimental data and correlations, and the presentation of new correlations with physical properties operating variables, and column geometry. *U.S. AEC ORNL-3890.*
21. Hinze, J. O. 1955. Fundamentals of the hydrodynamic mechanism of splitting in dispersion processes. *Am. Ind. Chem. Eng.* 1(3): 289-295.
22. Jealous, A. C. and H. F. Johnson. 1955. Power requirements for pulse generation in pulse columns. *I. and E. C.* 47(6): 1159-1166.
23. Jones, S. C. 1963. *Ph.D. dissertation. University of Michigan, Ann Arbor, Mich.*
24. Joseph, C., J. Van Geel, E. Detilleux, and J. Centeno. 1971. Technological experience with extraction experience at Eurochemic. *Proc. Int. Solvent Extraction Conf. (The Hague)*. Vol. 1, p. 593. Society of the Chemical Industry, London.
25. Kagan, S. Z., M. E. Aerov, V. Lonik and T. S. Volkova. 1965. Some hydrodynamic and mass-transfer problems in pulsed sieved-plate extractors. *International Chem. Eng.* 5(4): 656-661.
26. Kagan, S. Z., B. A. Veisbein, V. G. Trukhanov and L. A. Muzychens. 1973. Longitudinal mixing and its effect on mass transfer in pulsed-screen extractors. *International Chem. Eng.* 13(2): 217-220.
27. Li, W. H. and W. M. Newton. 1957. Liquid-liquid extraction in a pulsed perforated-plate column. *Am. Ind. Chem. Eng.* 3(1): 56-62.

28. Logsdail, D. H. and J. D. Thornton. 1957. Liquid-liquid extraction part XIV: The effect of column diameter upon the performance and throughput of pulsed plate columns. *Trans. Inst. Chem. Engrs.* 35: 331-342.
29. Mar, B. W. and A. L. Babb. 1959. Longitudinal mixing in a pulsed sieve-plate extraction column. *I. and E. C.* 51(9): 1011-1014.
30. McCutcheon, E. B. 1975. Simulation and control synthesis for a pulse column separation system for plutonium-uranium recovery. Ph.D. dissertation. Iowa State University, Ames, Iowa.
31. McMullen, A. K., T. Miyauchi and T. Vermeulen. 1958. Longitudinal dispersion in solvent-extraction columns: Numerical table. U.S. AEC UCRL-3911 supp.
32. Misek, T. and V. Rod. 1971. Calculation of contactors with longitudinal mixing. Pages 197-236 in C. Hanson. *Recent advances in liquid-liquid extraction*. Pergamon Press, New York.
33. Miyauchi, T. 1957. Longitudinal dispersion in solvent-extraction column: Mathematical theory. U.S. AEC UCRL-3911.
34. Miyauchi, T. and T. Vermeulen. 1963. Longitudinal dispersion in two-phase continuous-flow operations. *I. and E. C. Fund.* 2(2): 113-125.
35. Miyauchi, T. and T. Vermeulen. 1963. Diffusion and backflow models for two-phase axial dispersion. *I. and E. C. Fund.* 2(4): 304-310.
36. Miyauchi, T. and H. Oya. 1965. Longitudinal dispersion in pulsed perforated plate columns. *Am. Ind. Chem. Eng.* 11(3): 395-402.
37. Morello, V. S. and N. Poffenberger. 1950. Commercial extraction equipment. *I. and E. C.* 42(6): 1021-1035.
38. Newman, M. L. 1952. Correspondence spray tower extraction. *I. and E. C.* 44(10): 2457-2458.
39. Nicholson, E. L. 1967. Preliminary investigation of processing fast-reactor fuel in an existing plant. U.S. AEC ORNL-TM-1784.
40. Pratt, H. R. C. 1975. A simplified analytical design method for differential extractors with backmixing: 1. Linear equilibrium relationship. *I. and E. C. Process and Development* 14(1): 74-80.
41. Purex Technical Manual. 1955. U.S. ERDA Report HW-31000(Del.).
42. Rod, V. 1964. Calculation of extraction columns with longitudinal mixing. *British Chem. Eng.* 9(5): 300-304.

43. Rouyer, H., J. Lebouhellec, E. Henry, and P. Michel. 1974. Present study and development of extraction pulsed columns. Proc. Int. Solvent Extraction Conf. (Lyon, France). Society of the Chemical Industry (London) 3: 2339-2364.
44. Rozen, A. M., Yu G. Rubezhnyy and B. V. Martynov. 1970. Longitudinal mixing in pulsation extraction columns. The Soviet Chem. Ind. 2: 66-73.
45. Sato, T., K. Sugihara and I. Taniyama. 1964. Performance characteristics of pulsed perforated plate columns. Kagaku Kogaku 2(1): 30-32.
46. Sege, G. and F. W. Woodfield. 1954. Pulse column variables. Chem. Eng. Progress 50: 396-402.
47. Sehmel, G. A. and A. L. Babb. 1963. Holdup studies in a pulsed sieve-plate solvent extraction column. I. and E. C. Process Design and Development 2(1): 38-42.
48. Sehmel, G. A. and A. L. Babb. 1964. Longitudinal mixing studies in a pulsed extraction column. I. and E. C. Process Design and Development 3(3): 210-214.
49. Shirotuka, T., N. Honda, and H. Oya. 1958. Extraction characteristics of and flow properties with pulsed extraction columns either packed or perforated. Kagaku Kogaku Chemical Engineering (Japan) 22 (11): 687-694.
50. Sleicher, C. A., Jr. 1959. Axial mixing and extraction efficiency. Am. Ind. Chem. Eng. 5(2): 145-149.
51. Sleicher, C. A., Jr. 1960. Entrainment and extraction efficiency of mixer-settler. Am. Ind. Chem. Eng. 6(3): 529-531.
52. Smoot, L. D. and A. L. Babb. 1962. Mass transfer studies in a pulsed extraction column. I. and E. C. Fund. 1(2): 93-103.
53. Stemerding, S., E. C. Lumb and J. Lips. 1963. Axial vermischung in einer Drehscheiben-Extraktions Kolonne. Chem. Ing. Tech. 35(12): 844-850.
54. Thornton, J. D. 1957. Liquid-liquid extraction part XIII: The effect of pulse wave-form and plate geometry on the performance and throughput of a pulsed column. Trans. Inst. Chem. Engrs. 35: 316-330.
55. Van Dijck, W. J. D. 1935. Extraction apparatus. U.S. Patent No. 2,011,186.

56. Van der Laan, E. T. 1958. Notes on the diffusion type model for the longitudinal mixing in flow. *Chem. Eng. Sci.* 7(3): 187-191.
57. Yih, S. M. Private communication.

ACKNOWLEDGMENTS

I wish to express my appreciation to Dr. L. E. Burkhart for his kindly help, guidance, encouragement, valuable criticisms and money support for simulation program running through this research effort.

To the other members of my graduate committee also go my thanks. These gentlemen are Dr. Ulrichson, Chemical Engineering, and Dr. Mathews, Mathematic Science.

Thanks to Dr. Vince Yih who has helped me to get through some conceptions of this research studying and Mr. Chuang's SAS help.

For their work in the preparation of the dissertation manuscript, I would like to thank Charmian Nickey for the typing and the drafting staff at the Ames Laboratory for preparation of the figures.

My father, who was blinded during the suffering of captive in Sino-Japan war of World War II. But he treats himself as a normal man; he can do everything which everybody can do, of course he needs to overcome a lot of difficulties. This impressed me the strength to face the difficult circumstances and frustrations in my life.

To my mother, who was dead before I start my back school studying, I would like to present this thesis as a memorial to her.

My beloved wife Shu-Lan takes care of my family during my abroad studying periods and a lots thanks to her in my heart.

Also, thanks to those people who encourage me as the studying driving forces and those who discourage me as the backmixing effects. Eventually, the driving forces overcome the backmixing effects and extraction can be performed. Thanks be to God.

APPENDIX: SIMULATION PROGRAM

Computer Program Variables List

A	Pulse amplitude, cm/cycle
AA	Intermediate symbol for calculating Psi, AA = (Af)/ ((BCxSP)**(1/3))
AP	Pseudoaqueous phase flow rate, liter/sec
AQ	Actual aqueous phase flow rate (does not vary from stage to stage)
AQN	New actual aqueous phase flow rate, liter/sec
A1 thru A9	Constant used in calculating U(VI) and Pu(IV) distribu- tion coefficient
ALPHA	Backflow ratio of aqueous phase; ALPHA = Af ϵ /F _i
ALPHO	Backflow ratio of dispersed phase
B1 thru B3	Constants used in calculating distribution coefficients for NO ₃
BC	Constant for calculating Psi, BC = S ² /(1 - S)(1 - S ²)
BB	Constant for calculating Psi, BB = Visd ²
C	Tributyl phosphate concentration used in calculating Pu(III), and U(VI) distribution coefficient; used in subroutine DISTRI
CC	Intermediate symbol for calculating Psi, CC = absolute (Dend-Denc)xGam
DATLAB	Label of plot data on plot
DDTAQ	Time derivative of pseudoaqueous phase flow rate
DDTHU	Time derivative of aqueous phase holdup
DDTOR	Time derivative of pseudoorganic phase flow rate
DDTORF	Time derivative of organic feed flow rate
DT	Time increment between integration steps; second
DENC	Continuous phase density, gram/cm ³

DEND	Dispersed phase density, gram/cm ³
DISTR1	Name for distribution coefficient subroutine
EH2	Distribution coefficient for nitrous acid
EH3	Distribution coefficient for nitric acid
ENH2	((Vol-HU)/HU)xEH2 or (Op/Ap)xEH2
ENH3	((Vol-HU/HU)xEH3 or (Op/Ap)xEH3
ENP	((Vol-HU)/HU)xEOAP or (Op/Ap)xEOAP
ENU	((Vol-HU)/HU)xEOAU or (Op/Ap)xEOAU
EOAP	Distribution coefficient for plutonium (IV)
EOAU	Distribution coefficient for uranium (VI)
F	Pulse frequency, cycle/sec
FD	Dispersed phase superficial flow rate, cm/sec
FIS	$10^{**}(0.91\bar{\mu}_j^{1/2} - 1.52)$ used in distribution coefficient calculation subroutine
FTBP	C", for TBP concentration used in calculating the distribution coefficient for HNO ₂
G	Conversion factor used for calculating linear flow rate from volume flow rate
GAM	Interfacial tension of liquid system; dyne/cm
H	H ⁺ , hydrogen ion concentration, aqueous phase, mole/liter
HF	Hydrogen concentration at time t+Δt
HN	(NH ₃ OH ⁺), hydroxylamine concentration, aqueous, mole/liter
HNF	(NH ₃ OH ⁺), hydroxylamine concentration at time t+Δt
HNO ₂	Nitrous acid concentration, aqueous, mole/liter
HNO ₂ F	Nitrous acid concentration, aqueous, at time t+Δt
HN020	Nitrous acid concentration, organic, mole/liter

HZ	$N_2H_5^+$, hydrazine concentration, aqueous, mole/liter
HZF	Hydrazine concentration, aqueous, at time $t+\Delta t$
HU	Aqueous phase volume holdup, liter
HUH	Aqueous phase holdup fraction
HOLDUP	Name for subroutine for calculating holdups and flow rate parameter
I	Subscript for stage number
IS	Aqueous phase ionic strength
J	Subscript or number index
KH	Ion strength function for hydrogen ion
KP	Ion strength function for plutonium (IV)
KU	Ion strength function for uranium (VI)
K1	Rate constant for reaction 1
K2	Constant used in TEM4 multiple RXN1 material balance calculation
K3	Rate constant for reaction 3
K4	Rate constant for reaction 2
K5	Rate constant for reaction 4
L	Last stage in the column
LL	Bottom disengagement section
M	Symbol for fictitious stage (LL+1), used to specify input and output at the bottom stage (LL)
MPK	Physical factor on calculating Psi, $MPK = (VISd^2/(GAM \times \text{Absolute (DENC-DEND)}))^{1/4}$
N	Number of iterations or time steps specified
NF	Feed stage number
NO ₃	NO ₃ ⁻ concentration in aqueous phase, mole/liter

NO3I	Nitric acid feed concentration, M
NO3O	Nitric acid concentration in organic phase, mole/liter
NO3F	Nitric acid at time $t+\Delta t$ of aqueous phase
NO3S	Nitric acid concentration in the scrub stream, mole/liter
OP	Pseudoorganic phase flow rate, liter/sec
OR	Actual organic phase flow rate (does not vary from stage to stage), liter/sec
ORF	Organic feed flow rate, liter/sec
OR1	Organic phase flow rate in scrubbing section, liter/sec
OR2	Organic phase flow rate in extraction section, OR2 = OR1 + ORF, liter/sec
PUORG	Plutonium (IV) organic phase outlet concentration, plutonium (IV) concentration in the uranium product stream, mole/liter
P3A	Plutonium (III) concentration in aqueous phase, mole/liter
P3AF	Plutonium (III) concentration at time $t+\Delta t$, aqueous phase
P4A	Plutonium (IV) concentration in aqueous phase, mole/liter
P4AF	Plutonium (IV) concentration at time $t+\Delta t$, aqueous phase
P4O	Plutonium (IV) concentration in organic phase, mole/liter
P4OF	Plutonium (IV) concentration in organic feed at feed stage, mole/liter
PSI	Holdup correlation constant
PUBAL	Residual from overall Pu material balance over the column
PUTOT	Total plutonium inventory in the column, grams
PUS	Plutonium inventory in each individual stage, gram
RXN1 thru RXN5	Incremental change in material gained or lost to reaction for each time step as determined by the kinetic rate equations, mole/liter sec

REACT	Name of subroutine for reaction rate models
S	Plate free area fraction
SP	Column plate spacing, cm
TAQ	Interstage time constant for pseudoaqueous flow rate, sec ⁻¹
TOR	Interstage time constant for pseudoorganic flow rate, sec ⁻¹
TEM1 thru TEM8	Intermediate variables used in material balance calculation, essentially these variables represent all terms except the accumulation terms in the material balance
TIME	Number of minutes of column operation
UA	Uranium (VI) concentration in the aqueous phase, mole/liter
UAF	Uranium (VI) concentration at time t+Δt, mole/liter
UBAL	Overall uranium material balance, gram
UO	Uranium (VI) concentration in the organic phase, mole/liter
UOF	Uranium concentration in feed stage, organic phase, mole/liter
VOL	Volume of a single theoretical stage, liter
VISC	Continuous phase viscosity, poise
VISD	Dispersed phase viscosity, poise
V1	Volume of disengagement section, liter
W	(NO ₃ ⁻) ² , square of nitrate concentration
XLAB	Label on X axis in plot
YLAB	Label on Y axis in plot

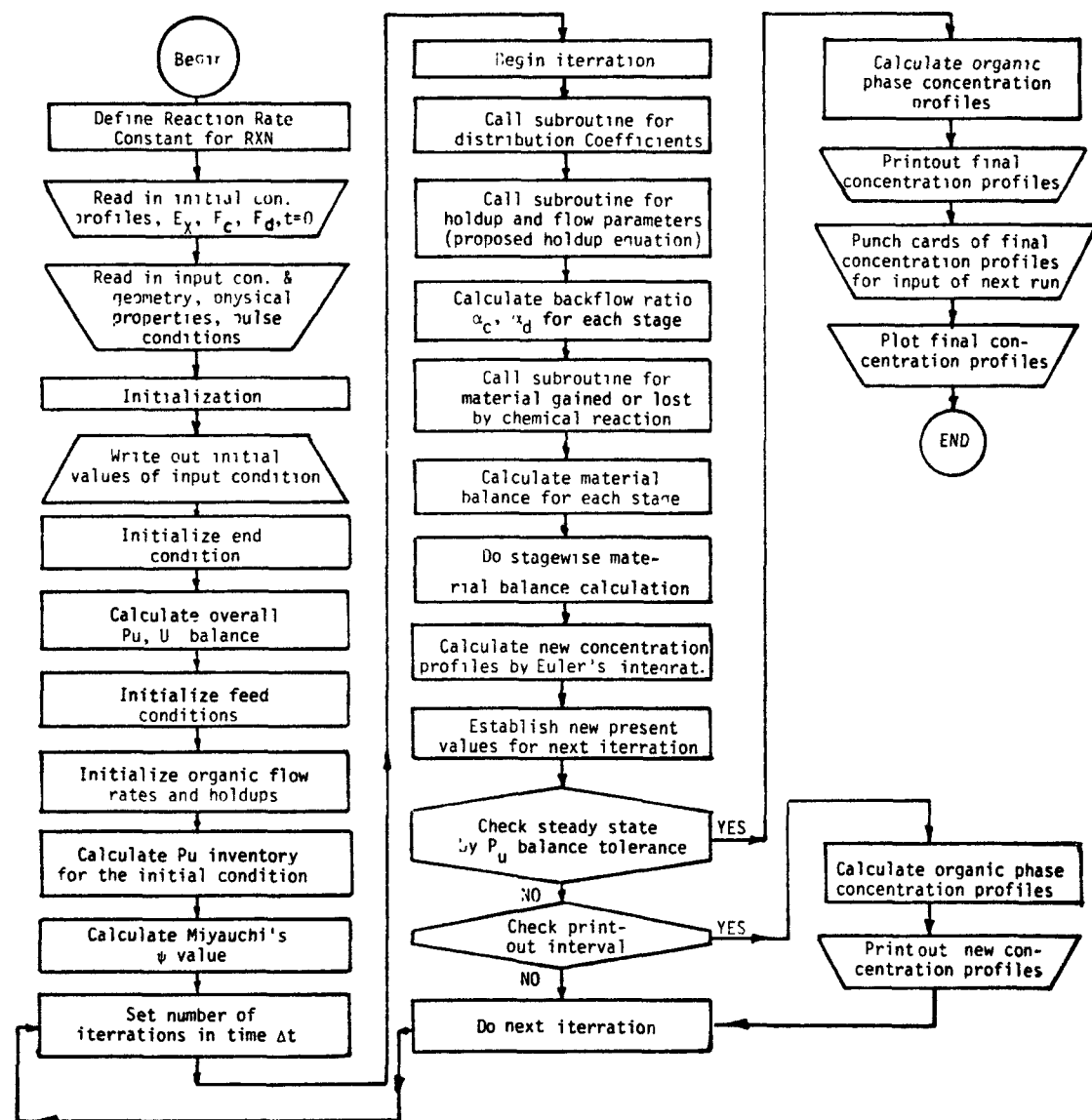


Figure 21. Simulation program flowsheet.

```
*****  
* SIMULATION ON URANIUM-PLUTONIUM PARTITIONING PULSE COLUMN WITH OR WITHOUT*  
* BACKMIXING EFFECTS  
* THE SIMULATION MODEL USED IS STAGewise BACKFLOW MODEL  
* MODEL PARAMETER ACCOUNTS FOR BACKMIXING IS ALPHA=A*F*HUh/FLOW RATE  
*****
```

```
*****  
* USING MCCUTCHEON'S HOLDUP RATIO EQUALS THE PSEUDO FLOW RATE RATIO:  
* HUh=OP^/(AQ^+OP^)  
*****
```

```
*****  
* USING MIYAUCHI'S HOLDUP CORRELATION: HUh=0.66*FD**2./3.*PSI**0.84  
* OR HUh=6.32*FD**2/3*PSI**2.4  
* IF PSI IS GREATER THAN 0.21  
* HUh=6.32*FD**2/3*PSI**2.4  
* IF PSI IS LESSER THAN 0.21  
* HUh=0.66*FD**2/3*PSI**0.84  
*****
```

```
*****  
* USING THE PROPOSED HOLDUP CORRELATION; HUh=1.4703*OP(I-1)**(2./3.)  
* *PSI**1.15149529  
* IF PSI IS GREATER THAN 0.09  
* HUh=1.4703*FD**(2./3.)*PSI**1.15149529  
* IF PSI IS LESSER THAN 0.09  
* HUh=0.0073*FD**(2./3.)*PSI**-0.9485  
*****
```

* THE PARTITIONING PULSE COLUMN IS 4 INCHES IN DIAMETER AND THE EFFECTIVE *
* HEIGHT IS 45 FEET ,REAL STAGES ARE 270,THE PLATE SPACING IS 2 INCHES. *
* THE FEED STAGE IS LOCATED AT 18 FEET HIGH OF THE PULSE COLUMN *
* THE DISPERSED PHASE IS CCL4 AND THE CONTINUOUS PHASE IS WATER *
* THE OPERATING AMPLITUDE IS 1.333 INCHES PER CYCLE AND THE FREQUENCY IS *
* 1 CYCLE PER SECOND *

THE MAIN PROGRAM CONSISTS OF INITIALIZATION FUNCTIONS, INTERSTAGE
BACKFLOW RATIO CALCULATION AND GENERAL MATERIAL BALANCES.
THE REACTION MODELS , DISTRIBUTION COEFFICIENTS , AND VARIABLE
HOLDUPS ARE WRITTEN IN SUBROUTINES.

112

```
REAL TOR,TAQ,A,F,VOL,V1,PUBAL,UBAL
REAL DRF,OR1,OR2,OR,AQ
REAL HZF(23),NO3S,NO3I
REAL P4AF(23),P3AF(23),UAF(23),HF(23),NO3F(23),HN02F(23),HNF(23)
REAL P4A(23),P4O(23),P3A(23),UA(23),UO(23),H(23),NO3(23),NO3O(23)
REAL HN02(23),HN02O(23),HN(23),HZ(23),PUORG(23),PUS,PUTOT
REAL EOAP(23),EOAU(23),EH3(23),EH2(23)
REAL ENP(23),ENU(23),ENH2(23),ENH3(23)
REAL HU(23),ALPHA(23),ALPH0(23),HUH(23)
REAL AP(23),OP(23),DDTOR(23),DDTAQ(23),DDTHU(23)
REAL K1,K2,K3,K4,K5,KU,KP,KH,IS,FIS(23)
REAL X(23),Y(23),XLAB(5),YLAB(5),GLAB(5),DATLAB(5)
REAL RXN1,RXN2,RXN3,RXN4,RXN5
REAL PSI,GAM,MPK
```

DEFINE REACTION RATE CONSTANTS FOR CHEMICAL REACTIONS

K1=0.0235
K2=0.68966
K3=0.0693
K4=1.5
K5=0.234

WRITE(6,5)

READ IN INITIAL VALUES OF CONCENTRATION PROFILE, DISTRIBUTION COEFFICIENTS, FLOW RATES AND FEED RATES, ETC. AT TIME=0

READ(5,15) TAQ,TOR,F,A
READ(5,25) DT
READ(5,35) NF,L
M=L+3.
READ(5,45) HZ(M),HNO2(M),NO3(M),HN(M),H(M),OR1,NO3S
READ(5,25) AQ
READ(5,25) AQNEW

113

READ IN INPUT FEED CONCENTRATION

READ(5,55) P4DF,U0F,HNO2I,ORF
READ(5,65) SP,S
READ(5,75) GAM,VISD,DENC,DEND
LL=L+2
DO 6 I=1,LL
READ(5,85) NO3(I),HNO2(I),HN(I),HZ(I)
6 READ(5,85) EOAP(I),EOAU(I),EH3(I),EH2(I)
READ(5,85) P4A(I),P3A(I),UA(I),H(I)

INITIALIZATION

```
N8=NF+1
N7=NF-1
VOL=((3.1415928*(4.*2.54)**2./4.)*(45.*30.48/1000.))/L
V1=VOL
OR2=ORF+OR1
TIME=0.0
N5=20
```

WRITE OUT INITIAL VALUES OF INPUT CONDITIONS

```
WRITE(6,75) P4DF,UDF,HN(M),HZ(M),NO3(M),NO3I,NO3S,HNO2(M),HNO2I,OR
*1,ORF,OR2,AQ,DT,L,NF,TAQ,TOR,N5,A,F
```

114

INITIALIZE PSEUDO FLOW RATES

```
DO 16 I=1,N7
AP(I)=AQ
OP(I)=OR1
DDTAQ(I)=0.0
16 DDTOR(I)=0.0
J=NF
DO 26 I=J,LL
AP(I)=AQ
OP(I)=OR2
DDTOR(I)=0.0
26 DDTAQ(I)=0.0
```

INITIALIZE END CONDITIONS

```
AP(M)=AQ
DDTAQ(M)=0.0
P4A(M)=0.0
P3A(M)=0.0
UA(M)=0.0
NO3(N)=NO3(M)+HN(M)
```

OVERALL PU AND U BALANCE

```
PUBAL=1.0-(AQ*(P4A(1)+P3A(1))+OR2*P4A(LL)*EOAP(LL))/(ORF*P4OF)
UBAL=1.0-(AQ*UA(1)+OR2*UA(LL)*EOAU(LL))/(ORF*UOF)
```

INITIALIZE FEED CONDITIONS

```
DDTDRF=0.0
WRITE(6,105) P4OF,UOF,HNO2I,ORF
WRITE(6,115) TIME,PUBAL,UBAL
```

INITIALIZE ORGANIC FLOW RATES AND HOLDUPS

```
HU(1)=V1/(1.+OR1/AQ)
HU(LL)=V1/(1.+OR2/AQ)
P4O(1)=EOAP(1)*P4A(1)
P4O(LL)=EOAP(LL)*P4A(LL)
DDTHU(LL)=0.0
DDTHU(1)=0.0
DO 36 J=2,N7
  HU(J)=VOL/(1.+OR1/AQ)
  P4O(J)=EOAP(J)*P4A(J)
36  DDTHU(J)=0.0
```

36 DDTHU(J)=0.0

```
K=NF
N2=LL-1.0
DO 46 I=K,N2
  HU(I)=VOL/(1.+DR2/AQ)
  P40(I)=EOAP(I)*P4A(I)
46  DDTHU(I)=0.0
    WRITE(6,125)
    DO 56 I=1,LL
56  WRITE(6,135)I,P4A(I),P40(I),P3A(I),UA(I),H(I),NO3(I)
    WRITE(6,145)
    DO 66 I=1,LL
66  WRITE(6,155)I,HNO2(I),HN(I),HZ(I),EOAP(I),EOAU(I),EH3(I),EH2(I)
    WRITE(6,165)
    DO 76 I=1,LL
76  WRITE(6,175) I,AP(I),OP(I),HU(I),DDTAQ(I),DDTOR(I),DDTHU(I)
```

116

CALCULATE THE TOTAL PLUTONIUM IN THE COLUMN

```
PUTOT=0.
DO 86 J=1,LL
  PUS=((P4A(J)+P3A(J))*HU(J)+P4A(J)*EOAP(J)*(VOL-HU(J)))*239.
86  PUTOT=PUTOT+PUS
    WRITE(6,185) PUTOT
    N=1
    WRITE(6,195)
```

G=1000./(3.1415928*(4.*2.54)**2./4.)

CONSTANT PSI CALCULATION
BC=(S*S)/((1.-S)*(1.-S*S))
AA=(A*F)/((BC*SP)**(1./3.))
BB=VISD*VISD
CC=(ABS(DENC-DEND))*GAM
MPK=(BB/CC)**(0.25)
PSI=AA*MPK
WRITE(6,205) SP,S,GAM,VISD,DEND,MPK,PSI

SET NUMBER OF ITERRATION
3 IF(N.EQ.32001) GO TO 13

AQ=AQNEW
BEGAIN ITERRATION
AP(M)=AQ
TIME=N*DT/60.

117

CALL SUBROUTINE FOR DISTRIBUTION COEFFICIENTS

CALL DISTRI(P4A,P3A,HN,H,N03,HN02,HZ,UA,FIS,EOAU,EOAP,EH3,EH2
1,LL,N)

CALL SUBROUTINE FOR HOLDUPS AND FLOW PARAMETERS

CALL HOLDUP(OP,AP,EOAU,EOAU,EH2,EH3,DDTOR,DDTAQ,HU,ENP,ENU,
1,ENH2,ENH3,DDTHU,N7,DDTORF,LL,NF,TOR,ORF,VOL,V1,
1,OR1,N8,MUH,OR2,TAQ,AQ,PSI,G)

```
BACKFLOW RATIO CALCULATION : ALPH=A*F*HUH/FLOW RATE
ALPHA(1)=A*F*HUH(1)/(AQ*G)
ALPHO(1)=A*F*(1-HUH(1))/(OP(1)*G)
DO 96 I=2,LL
ALPHA( I)=A*F*HUH( I)/(AQ*G)
ALPHO( I)=A*F*(1-HUH( I))/(OP( I-1)*G)
96 CONTINUE
ALPHA(NF)=A*F*HUH(NF)/(AQ*G)
ALPHO(NF)=A*F*(1-HUH(NF))/(OR2*G)

IF IN PISTON FLOW MODEL SET ALPH=0
DO 96 I=1,LL
ALPHA( I)=0.0
ALPHO( I)=0.0
96 CONTINUE
```

118

```
MATERIAL BALANCE CALCULATIONS FOR EIGHT COMPONENTS
DO 126 I=1,LL
CALL SUBROUTINE FOR REACTION MODELS
IF(I.EQ.1) GO TO 23
IF(I.EQ.LL) GO TO 33
CALL REACT(P4A,P3A,HN,H,NO3,HN02,HZ,F1S,RXN1,RXN2,RXN3,RXN4,
RXN5,K1,K2,K3,K4,K5,M,I)
GO TO 43
23 CONTINUE
```

CALCULATE THE UPPER DISENGAGEMENT SECTION ASSUME NO CHEMICAL REACTION OCCURS INSIDE

TEM1=(AQ/HU(1))*((1+ALPHA(2))*P4A(2)-(1+ALPHA(1))*P4A(1))
1+(OR1/HU(1))*(ALPH0(2)*EOAP(2)*P4A(2)-(1+ALPH0(1))*EOAP(1)*P4A(1))

TEM2=(AQ/HU(1))*((1+ALPHA(2))*UA(2)-(1+ALPHA(1))*UA(1))
1+(OR1/HU(1))*(ALPH0(2)*EOAU(2)*UA(2)-(1+ALPH0(1))*EOAU(1)*UA(1))

TEM3=(AQ/HU(1))*((1+ALPHA(2))*P3A(2)-(1+ALPHA(1))*P3A(1))

TEM4=(AQ/HU(1))*((1+ALPHA(2))*HN(2)-(1+ALPHA(1))*HN(1))

TEM5=(AQ/HU(1))*((1+ALPHA(2))*HZ(2)-(1+ALPHA(1))*HZ(1))

TEM6=(AQ/HU(1))*((1+ALPHA(2))*NO3(2)-(1+ALPHA(1))*NO3(1))
1+(OR1/HU(1))*(NO3S+ALPH0(2)*EH3(2)*NO3(2)-(1+ALPH0(1))*EH3(1)*NO3(1))
+(OR1/HU(1))*(4*ALPH0(2)*EOAP(2)*P4A(2)+2*ALPH0(2)*EOAU(2)*
1UA(2))-(OR1/HU(1))*(1+ALPH0(1))*(4*EOAP(1)*P4A(1)+2*EOAU(1)*UA(1))

TEM7=(AQ/HU(1))*((1+ALPHA(2))*HNO2(2)-(1+ALPHA(1))*HNO2(1))
1+(OR1/HU(1))*ALPH0(2)*EH2(2)*HNO2(2)-(OR1/HU(1))*(1+ALPH0(1))*
1EH2(1)*HNO2(1)

TEM8=(AQ/HU(1))*((1+ALPHA(2))*H(2)-(1+ALPHA(1))*H(1))
1+(OR1/HU(1))*(NO3S+ALPH0(2)*EH3(2)*NO3(2))-(OR1/HU(1))*(1+ALPH0(1))*
1EH3(1)*NO3(1)

GO TO 53

43 IF(I.NE.NF) GO TO 63

TEM1=(AQ/HU(NF))*(ALPHA(N7)*P4A(N7)+(1+ALPHA(N8))*P4A(N8)-(1+2*
1ALPHA(NF))*P4A(NF))+(ORF/HU(NF))*P40F+(OR1/HU(NF))*(1+ALPHO(N7))*
1EOAP(N7)*P4A(N7)+(OR2/HU(NF))*ALPHO(N8)*EOAP(N8)*P4A(N8)
1-(OR2/HU(NF))*(1+2*ALPHO(NF))*EOAP(NF)*P4A(NF)-RXN1+RXN2-RXN3

TEM2=(AQ/HU(NF))*(ALPHA(N7)*UA(N7)+(1+ALPHA(N8))*UA(N8)-(1+2*ALPHA
1(NF))*UA(NF))+(ORF/HU(NF))*U0F+(OR1/HU(NF))*(1+ALPHO(N7))*EOAU(N7)
1*UA(N7)+(OR2/HU(NF))*ALPHO(N8)*EOAU(N8)*UA(N8)-(OR2/HU(NF))*
1(1+2*ALPHO(NF))*EOAU(NF)*UA(NF)

TEM3=(AQ/HU(NF))*(ALPHA(N7)*P3A(N7)+(1+ALPHA(N8))*P3A(N8)-(1+2*
1ALPHA(NF))*P3A(NF))+RXN1-RXN2+RXN3

TEM4=(AQ/HU(NF))*(ALPHA(N7)*HN(N7)+(1+ALPHA(N8))*HN(N8)-(1+2*
1ALPHA(NF))*HN(NF))-K2*RXN1-RXN5

TEM5=(AQ/HU(NF))*(ALPHA(N7)*HZ(N7)+(1+ALPHA(N8))*HZ(N8)-(1+2*ALPHA
1(NF))*HZ(NF))-0.25*RXN3-RXN4

TEM6=(AQ/HU(NF))*(ALPHA(N7)*NO3(N7)+(1+ALPHA(N8))*NO3(N8)-(1+2*
1ALPHA(NF))*NO3(NF))+(ORF/HU(NF))*(NO3I+4*P40F+2*U0F)
1+(OR1/HU(NF))*(1+ALPHO(N7))*(NO3(N7)*EH3(N7)+4*P4A(N7)*EOAP(N7)
1+2*UA(N7)*EOAU(N7))+(OR2/HU(NF))*(ALPHO(N8))*(NO3(N8)*EH3(N8)
1+4*P4A(N8)*EOAP(N8)+2*UA(N8)*EOAU(N8))
1-(OR2/HU(NF))*(1+2*ALPHO(NF))*(NO3(NF)*EH3(NF)+4*P4A(NF)*EOAP(NF)
1+2*UA(NF)*EOAU(NF))-0.5*RXN2

TEM7=(AQ/HU(NF))*(ALPHA(N7)*HNO2(N7)+(1+ALPHA(N8))*HNO2(N8)-
1(1+2*ALPHA(NF))*HNO2(NF))+(ORF/HU(NF))*HNO2I+(OR1/HU(NF))*(1+
1ALPHO(N7))*EH2(N7)*HNO2(N7)+(OR2/HU(NF))*ALPHO(N8)*EH2(N8)*HNO2
1(N8)-(OR2/HU(NF))*(1+2*ALPHO(NF))*EH2(NF)*HNO2(NF)+0.5*RXN2-
1RXN4-RXN5

$TEM8 = (AQ/HU(NF)) * (\text{ALPHA}(N7) * H(N7) + (1 + \text{ALPHA}(N8)) * H(N8) - (1 + 2 * \text{ALPHA}(N7) * H(NF)) + (\text{ORF}/HU(NF)) * NO3I + (\text{OR1}/HU(NF)) * (1 + \text{ALPHO}(N7)) * EH3(N7) + NO3(N7) + (\text{OR2}/HU(NF)) * \text{ALPHO}(N8) * EH3(N8) * NO3(N8) - (\text{OR2}/HU(NF)) * (1 + 2 * \text{ALPHO}(N8)) * EH3(NF) * NO3(NF) + 1.75 * RXN1 - 1.5 * RXN2 + 1.25 * RXN3 + RXN4 + RXN5$
 GO TO 53

14 O=OR1
 P=OR1
 IF(I.EQ.N7) P=OR2
 IF(I.GT.NF) GO TO 73
 GO TO 83

73 O=OR2
 P=OR2
 IF(I.EQ.LL) GO TO 33

83 TEM1 = (AQ/HU(I)) * (\text{ALPHA}(I-1) * P4A(I-1) + (1 + \text{ALPHA}(I+1)) * P4A(I+1) - (1 + 2 * \text{ALPHA}(I)) * P4A(I)) + (O/HU(I)) * (1 + \text{ALPHO}(I-1)) * EOAP(I-1) * P4A(I-1) + (P/HU(I)) * \text{ALPHO}(I+1) * EOAP(I+1) * P4A(I+1) - (O/HU(I)) * (1 + 2 * \text{ALPHO}(I)) * EOAP(I) * P4A(I) - RXN1 + RXN2 - RXN3

$TEM2 = (AQ/HU(I)) * (\text{ALPHA}(I-1) * UA(I-1) + (1 + \text{ALPHA}(I+1)) * UA(I+1) - (1 + 2 * \text{ALPHA}(I)) * UA(I)) + (O/HU(I)) * (1 + \text{ALPHO}(I-1)) * EOAU(I-1) * UA(I-1) + (P/HU(I)) * \text{ALPHO}(I+1) * EOAU(I+1) * UA(I+1) - (O/HU(I)) * (1 + 2 * \text{ALPHO}(I)) * EOAU(I) * UA(I)$

$TEM3 = (AQ/HU(I)) * (\text{ALPHA}(I-1) * P3A(I-1) + (1 + \text{ALPHA}(I+1)) * P3A(I+1) - (1 + 2 * \text{ALPHA}(I)) * P3A(I)) + RXN1 - RXN2 + RXN3$

$TEM4 = (AQ/HU(I)) * (\text{ALPHA}(I-1) * HN(I-1) + (1 + \text{ALPHA}(I+1)) * HN(I+1) - (1 + 2 * \text{ALPHA}(I)) * HN(I)) - K2 * RXN1 - RXN5$

$TEM5 = (AQ/HU(I)) * (\text{ALPHA}(I-1) * HZ(I-1) + (1 + \text{ALPHA}(I+1)) * HZ(I+1) - (1 + 2 * \text{ALPHA}(I)) * HZ(I)) - 0.25 * RXN3 - RXN4$

```

TEM6=(AQ/HU(I))*ALPHA(I-1)*NO3(I-1)+(1+ALPHA(I+1))*NO3(I+1)-
1(1+2*ALPHA(I))*NO3(I)+(0/HU(I))*(1+ALPHO(I-1))*(EH3(I-1)*NO3(I-1)
1+4*EOAP(I-1)*P4A(I-1)+2*EOAU(I-1)*UA(I-1))+(P/HU(I))*ALPHO(I+1)
1*(EH3(I+1)*NO3(I+1)+4*P4A(I+1)*EOAP(I+1)+2*EOAU(I+1)*UA(I+1))
1-(0/HU(I))*(1+2*ALPHO(I))*(EH3(I)*NO3(I)+4*P4A(I)*EOAP(I)+2*EOAU(I)
1)*UA(I))-0.5*RXN2

```

```

TEM7=(AQ/HU(I))*(ALPHA(I-1)*HNO2(I-1)+(1+ALPHA(I+1))*HNO2(I+1)
1-(1+2*ALPHA(I))*HNO2(I))+(O/HU(I))*(1+ALPHO(I-1))*EH2(I-1)*
1HNO2(I-1)+(P/HU(I))*ALPHO(I+1)*EH2(I+1)*HNO2(I+1)-(O/HU(I))*(1+
12*ALPHO(I))*EH2(I)*HNO2(I)+0.5*RXN2-RXN4-RXN5

```

```

TEM8=(AQ/HU(I))*ALPHA(I-1)*H(I-1)+(1+ALPHA(I+1))*H(I+1)-(1+2*ALPHA(I))*H(I)+(O/HU(I))*(1+ALPHO(I-1))*EH3(I-1)*NO3(I-1)+(P/HU(I))*ALPHO(I+1)*EH3(I+1)*NO3(I+1)-(O/HU(I))*(1+2*ALPHO(I))*EH3(I)*NO3(I)+1.75*RXN1-1.5*RXN2+1.25*RXN3+RXN4+RXN5

```

GO TO 53

33 CONTINUE

```
TEM1=(AQ/HU(LL))*(P4A(M)+ALPHA(L+1)*P4A(L+1)-(1+ALPHA(LL))*  
1P4A(LL))+(OR2/HU(LL))*(1+ALPH0(L+1))*EOAP(L+1)*P4A(L+1)-(OR2/HU  
1LL))*(1+ALPH0(LL))*EOAP(LL)*P4A(LL)
```

```
TEM2=(AQ/HU(LL))*UA(M)+ALPHA(L+1)*UA(L+1)-(1+ALPHA(LL))*UA(LL)
1+(OR2/HU(LL))*((1+ALPHO(L+1))*EOAU(L+1)*UA(L+1)-(OR2/HU(LL))*(
1+ALPHO(LL))*EOAU(LL)*UA(LL))
```

```
TEM3=(AQ/HU(LL))*((P3A(M)+ALPHA(L+1)*P3A(L+1)-(1+ALPHA(LL))*P3A(LL))  
1)
```

TEM4=(AO/HU(LL))+((HN(H)+ALPHA(L+1)*HN(L+1)-(1+ALPHA(LL))*HN(LL))

TEM5=(AQ/HU(LL))*HZ(H)+ALPHA(L+1)*HZ(L+1)-(1+ALPHA(LL))*HZ(LL)

1(LL))+ (OR2/HU(LL))*(1+ALPH0(L+1))*(EH3(L+1)*NO3(L+1)+4*EOAP(L+1)
1*P4A(L+1)+2*EOAU(L+1)*UA(L+1))-(OR2/HU(LL))*(1+ALPH0(LL))*
2EH3(LL)*NO3(LL)+4*EOAP(LL)*P4A(LL)+2*EOAU(LL)*UA(LL))

TEM7=(AQ/HU(LL))*(HN02(M)+ALPHA(L+1)*HN02(L+1)-(1+ALPHA(LL))*
1HN02(LL))+ (OR2/HU(LL))*(1+ALPH0(L+1))*EH2(L+1)*HN02(L+1)
1-(OR2/HU(LL))*(1+ALPH0(LL))*EH2(LL)*HN02(LL)

TEM8=(AQ/HU(LL))*(H(M)+ALPHA(L+1)*H(L+1)-(1+ALPHA(LL))*H(LL))
1+(OR2/HU(LL))*(1+ALPH0(L+1))*EH3(L+1)*NO3(L+1)-(OR2/HU(LL))*
1(1+ALPH0(LL))*EH3(LL)*NO3(LL)

EULER INTEGRATION ROUTINE, CALCULATE NEW CONCENTRATION
PROFILE AT TIME T=T+DT

53 CONTINUE

P4AF(I)=P4A(I)+(TEM1-(1-EOAP(I))*P4A(I)*DDTHU(I)/HU(I))*DT/(1+ENP(I))
IF(P4AF(I).LE.0.0) P4AF(I)=0.0

UAF(I)=UA(I)+(TEM2-(1-EOAU(I))*UA(I)*DDTHU(I)/HU(I))*DT/(1+ENU(I))
IF(UAF(I).LT.0.0) UAF(I)=0.0

P3AF(I)=P3A(I)+(TEM3-P3A(I)*DDTHU(I)/HU(I))*DT
IF(P3AF(I).LT.0.0) P3AF(I)=0.0

HNF(I)=HN(I)+(TEM4-HN(I)*DDTHU(I)/HU(I))*DT
IF(HNF(I).LT.0.0) HNF(I)=0.0

HZF(I)=HZ(I)+(TEM5-HZ(I)*DDTHU(I)/HU(I))*DT
IF(HZF(I).LT.0.0) HZF(I)=0.0

NO3F(I)=NO3(I)-(4*(P4AF(I)-P4A(I))*ENP(I)+2*(UAF(I)-UA(I))*ENU(I)-
(TEM6-(1-EH3(I))*NO3(I)*DDTHU(I)/HU(I))*DT)/(1+ENH3(I))
IF(NO3F(I).LT.0.0) NO3F(I)=0.0

```
HN02F(I)=HN02(I)+(TEM7-(I-EH2(I))*HN02(I)*DDTHU(I)/HU(I))*DT/(I+EN
*H2(I))
IF(HN02F(I).LT.0.0) HN02F(I)=0.0
```

```
HF(I)=H(I)+(TEM8-(H(I)-EH3(I)*NO3(I))*DDTHU(I)/HU(I))*DT-ENH3(I)*
*(NO3F(I)-NO3(I))
IF(HF(I).LT.0.0) HF(I)=0.0
```

```
126 CONTINUE
```

OVERALL PLUTONIUM AND URANIUM CALCULATION

```
PUBAL=1.0-(AQ*(P4AF(I)+P3AF(I))+OR2*P4AF(LL)*EOAP(LL))/(ORF*P4OF)
UBAL=1.0-(AQ*UAF(I)+OR2*UAF(LL)*EOAU(LL))/(ORF*UOF)
```

CALCULATE THE TOTAL PLUTONIUM IN THE COLUMN

```
PUTOT=0.
DO 136 I=1,LL
PUS=((P4A(I)+P3A(I))*HU(I)+P4A(I)*EOAP(I)*(VOL-HU(I)))*239
PUTOT=PUTOT+PUS
```

```
136 CONTINUE
```

ESTABLISH NEW PRESENT VALUES

```
DO 146 I=1,LL
AP(I)=AP(I)+DDTAQ(I)*DT
OP(I)=OP(I)+DDTOR(I)*DT
P4A(I)=P4AF(I)
P3A(I)=P3AF(I)
UA(I)=UAF(I)
HZ(I)=HZF(I)
HN(I)=HNF(I)
```

124

```
HNO2(I)=HNO2F(I)
NO3(I)=NO3F(I)
H(I)=HF(I)
146 CONTINUE
```

```
*****+
* CHECK THE STEADY STATE BY TOLERANCE OF PLUTONIUM BALANCE
* IF(PUBAL.LE.0.001) GO TO 13
*****+
```

```
*****+
* PRINT OUT INTERVAL CONTROL
* IF(MOD(N,800).EQ.0) GO TO 93
* N=N+1
* GO TO 3
* 93 CONTINUE
*****+
```

CALCULATE CONCENTRATIONS IN ORGANIC PHASE

```
DO 156 I=1,LL
HNO2O(I)=HNO2(I)*EH2(I)
NO3O(I)=NO3(I)*EH3(I)
UO(I)=UA(I)*EOAU(I)
PUORG(I)=P4A(I)*EOAP(I)
156 CONTINUE
```

SUCCESSIVE PRINTOUTS OF CONC. AND DISTRIBUTION COEF. PROFILES

```
WRITE(6,225) TIME,PUBAL,UBAL
WRITE(6,235) TIME
```

```
DO 166 I=1,LL
166 WRITE(6,245) I,PUORG(I),P4A(I),UO(I),UA(I),P3A(I),H(I)
      WRITE(6,255)
      DO 176 I=1,LL
176 WRITE (6,265)I,NO30(I),NO3(I),HNO20(I),HNO2(I),HN(I),HZ(I)
      WRITE(6,275)
      DO 186 I=1,LL
186 WRITE(6,285)I,EOAP(I),EOAU(I),EH3(I),EH2(I)
      N=N+1
      GO TO 3
```

PRINT FINAL STEADY STATE PU & U PROFILESC DISTRIBUTION COEF. PROFILES

```
13  WRITE(6,295) N1,TIME
      WRITE(6,305) PUBAL,UBAL
      DO 196 I=1,LL
      P40(I)=EUAP(I)*P4A(I)
      UO(I)=EOAU(I)*UA(I)
      HNO20(I)=HNO2(I)*EH2(I)
      NO30(I)=NO3(I)*EH3(I)
196 CONTINUE
      WRITE(6,315)
      WRITE CONCENTRATION PROFILES
      DO 206 I=1,LL
206 WRITE(6,325) I,P4A(I),P40(I),P3A(I),UA(I),UO(I),NO3(I)
      WRITE(6,335)
      DO 216 I=1,LL
216 WRITE(6,325) I,NO30(I),H(I),HN(I),HZ(I),HNO2(I),HNO20(I)
      WRITE DISTRIBUTION COEFFICIENTS
      DO 226 I=1,LL
226 WRITE(6,355) I,EOAP(I),EOAU(I),EH3(I),EH2(I)
      WRITE TOTAL PLUTONIUM INVENTORY
      WRITE(6,185) PUTOT
      WRITE BACKFLOW RATIO AND HOLDUPS
```

```
      WRITE(6,365)
      DO 236 I=1,LL
236 WRITE(6,375) I,HU(I),HUH(I)
      DO 246 I=1,LL
246 WRITE(6,385) I,ALPHA(I),I,ALPH0(I)

***** PLOT THE PROFILES *****

      DO 256 I=1,LL
      X(I)=I
256 Y(I)=P4A(I)
      PLOT PLUTONIUM PROFILE
      K=1
      CALL GRAPH(LL,X,Y,K,107, 8.,12.,3.,1.,0.,0.,"STAGE NUMBER;","CON
      IN MOLE/LITER;","SPECIES NOTE;","PU(IV)A;")
      DO 266 I=1,LL
266 Y(I)=P40(I)
      K=2
      CALL GRAPHS(LL,X,Y,K,107,"PU(IV)0;")
      PLOT URANIUM CONCENTRATION PROFILE
      DO 276 I=1,LL
276 Y(I)=UA(I)
      K=3
      CALL GRAPHS(LL,X,Y,K,107,"U(VI)A;")
      DO 286 I=1,LL
286 Y(I)=U0(I)
      K=4
      CALL GRAPHS(LL,X,Y,K,107,"U(VI)0;")
      PLOT PLUTONIUM(VI) CONCENTRATION PROFILE
      DO 296 I=1,LL
296 Y(I)=P3A(I)
      K=5
      CALL GRAPHS(LL,X,Y,K,107,"PU(III);")
      PLOT HNO3 PROFILE
      DO 306 I=1,LL
```

```
306 Y(I)=NO3(I)
K=6
CALL GRAPH(LL,X,Y,K,107, 8.,12.,3.,1.,0.,0.,"STAGE NUMBER;","CON
IN MOLE/LITER;","SPECIES NOTE;","NO3A;")
DO 316 I=1,LL
316 Y(I)=NO30(I)
K=7
CALL GRAPHS(LL,X,Y,K,107,"NO30;")
PLOT HYDRAZINE CONCENTRATION PROFILE
DO 326 I=1,LL
326 Y(I)=HZ(I)
K=8
CALL GRAPH(LL,X,Y,K,107, 8.,12.,3.,1.,0.,0.,"STAGE NUMBER;","CON
IN MOLE/LITER;","SPECIES NOTE;","HYDRAZINE;")
PLOT HYDROXYLAMINE CONCENTRATION PROFILE
DO 336 I=1,LL
336 Y(I)=HN(I)
K=9
CALL GRAPHS(LL,X,Y,K,107,"HYDROXYLAMINE;")
PLOT H+ CONCENTRATION PROFILE
DO 346 I=1,LL
346 Y(I)=H(I)
K=10
CALL GRAPHS(LL,X,Y,K,107,"HYDROGEN ION H+;")
PLOT HNO2 CONCENTRATION PROFILE
DO 356 I=1,LL
356 Y(I)=HNO2(I)
K=11
CALL GRAPH(LL,X,Y,K,107, 8.,12.,3.,1.,0.,0.,"STAGE NUMBER;","CON
IN MOLE/LITER;","SPECIES NOTE;","HNO2 IN AQ;")
DO 366 I=1,LL
366 Y(I)=HNO20(I)
K=12
CALL GRAPHS(LL,X,Y,K,107,"HNO2 IN OR PHASE;")
```

```
*****
* PUNCH DATA CARDS FOR NEXT RUNS INPUT IF STEADY STATE DID NOT ARRIVE
* DO 376 I=1,LL
* WRITE(7,65) P4A(I),P3A(I),UA(I),H(I)
* WRITE(7,65) NO3(I),HNO2(I),HN(I),HZ(I)
* WRITE(7,65) EOAP(I),EOAU(I),EH3(I),EH2(I)
* 376 CONTINUE
*****
FORMATS
```

```
5  FORMAT(//,.5X, ' ASSUME THE VOLUME OF UPPER AND BOTTOM DISENGAGE
1MENT SECTION IS THE SAME AS THE EQUILIBRIUM STAGE VOLUME')
15 FORMAT(4F12.7)
25 FORMAT(F12.7)
35 FORMAT(2I5)
45 FORMAT(8F9.4)
55 FORMAT(4F10.5)
65 FORMAT(2F4.2)
75 FORMAT(4F6.3)
85 FORMAT(4E14.5)
95 FORMAT(10X, 'ORIGINAL SYSTEM PARAMETERS',/10X,
1' PLUTONIUM FEED CONC  ',F9.5,/,10X,
2' URANIUM FEED CONC   ',F9.5,/,10X,
3' HN EXTRACT CONC    ',F9.5,/,10X,
4' HZ EXTRACT CONC    ',F9.5,/,10X,
5' HNO3 EXTRACT CONC  ',F9.5,/,10X,
6' HNO3 FEED CONC    ',F9.5,/,10X,
7' HNO3 SCRUB CONC   ',F9.5,/,10X,
8' HNO2 STRIP CONC   ',F9.5,/,10X,
8' HNO2 FEED CONC    ',F9.5,/,10X,
9' ORGANIC FLOW: SCRUB ',F9.5,/,10X,
A'          FEED      ',F9.5,/,10X,
B'          EXTRACT   ',F9.5,/,10X,
```

C'AQUEOUS FLOW',10X,F9.5,/,10X,'TIME STEP SEC',8X,F4.1,/,10X,
E'NUMBER OF EQUIL STAGES',I4,/,10X,'FEED AT STAGE 'I4,/,1
GOX,'INTERSTAGE TCS: AQ,OR',F9.2,F9.2,/,10X,
H'PRINT, MIN ',I4,/,10X,
I'AMPLITUDE CM/CYCLE ',F9.5,/,10X,'FREQUENCY CYCLES/SEC',F9.5,/
105 FORMAT(10X,'INPUT CONDITIONS IMPOSED AT TIME = 0.0',/,10X,
 '' PLUTONIUM FEED CONC',F9.5,/,10X,
 '' URANIUM FEED CONC ',F9.5,/,10X,
 '' HNO2 FEED CONC ',F9.5,/,10X,
 '' OR FEED FLOW RATE ',F9.5,/
115 FORMAT(/,15X,'TIME = ',F5.1,/,12X,'ORIGINAL OVERALL PU AND U MATER
'ERIAL BALANCES: (INPUT - OUTPUT)/INPUT',/,12X,'PLUTONIUM...',E14.
',10X,'URANIUM...',E14.6,/
125 FORMAT(/,5X,'STAGE NUMBER OUTPUTS: PU(IV)A PU(IV)0
 1 PU(III) UA(VI) H+ NO3-')
135 FORMAT(/,13X,I2,12X,E12.5,5X,E12.5,5X,E12.5,5X,E12.5,5X,E12.5,5X,
 1E12.5)
145 FORMAT(/,5X,'STAGE NUMBER OUTPUTS: HN02 HN H
 1Z EOAP EDAU EH3 EH2')
155 FORMAT(/,13X,I2, 5X,E12.5,2X,E12.5,2X,E12.5,2X,E12.5,2X,E12.5,2X,
 1E12.5,2X,E12.5)
165 FORMAT(/,5X,'STAGE NUMBER OUTPUTS: AP OP
 1 HU DDTAQ DDTOR DDTHU')
175 FORMAT(/,13X,I2,12X,E12.5,5X,E12.5,5X,E12.5,5X,E12.5,5X,E12.5,5X
 1.E12.5)
185 FORMAT(/,5X,'THE TOTAL PLUTONIUM IN THE COLUMN IS',2X,F16.8)
195 FORMAT(/,5X,'INITIAL CONDITIONS PRINTOUTS END',50('*'),//////)
205 FORMAT(/,5X,'MIYAUCHI HOLDUP CORRELATION PHYSICAL AND GEOMETRY
 1CONSTANTS ARE LISTED BELOW',/,5X,'SPACING=',F6.3,2X,'PLATE FREE
 1AREA FRACTION=',F6.3,/,5X,'INTERFACIAL SURFACE TENSION=',F6.3,
 1'DISPERSED PHASE VISCOSITY=',F6.3,'DISPERSED PHASE DENSITY=',F6.3,
 1/,5X,'MIYAUCHIS PHYSICAL CONSTANT=',F10.7,2X,'MIYAUCHIS GEOMETRY
 1CONSTANT=',F10.7)
215 FORMAT(/,5X,'ALPHA',1X,I2,2X,F10.7,3X,'ALPH0',1X,I2,2X,F10.7)

```

225 FORMAT('1',15X,'TIME=',F10.5,/,20X,'OVERALL MATERIAL BALANCES: (I
  'INPUT - OUTPUT)/INPUT',/,20X,'PLUTONIUM...',E14.6,10X,'URANIUM...
  '',E14.6,/)
235 FORMAT (/,10X,'AT TIME=',F10.5,/,16X,'PU(IV)',12X,'PU(IV)',1
  1 13X,'U(VI)',13X,'U(VI)',9X,'PU(III)',10X,'H+',/,16X,'ORGANIC',
  111X,'AQUEOUS',12X,'ORGANIC',11X,'AQUEOUS',/)
245 FORMAT (/,5X,'STAGE',12,2X,6(E12.5,5X))
255 FORMAT ('--',/,16X,'NO3-',14X,'NO3-',15X,'HNO2',14X,'HNO2',12X,
  1'HN',14X,'HZ',/,16X,
  4'ORGANIC',11X,'AQUEOUS',12X,'ORGANIC',11X,'AQUEOUS',/)
265 FORMAT(5X,'STAGE',12,2X,6(E12.5,5X))
275 FORMAT('--',/,15X,'EPU(IV)',14X,'EU(VI)',13X,'EHN03',13X,'EHN02',/)
285 FORMAT(5X,'STAGE',12,2X,4(E12.5,7X))
295 FORMAT(/,5X,'NUMBER OF ITERRATION',16,5X,'AT TIME',F9.4,/,10X,
  1' THE FINAL CONCENTRATION PROFILES ARE LISTED BELOW')
305 FORMAT(/,5X,'PUBAL=',E12.5,10X,'UBAL=',E12.5)
315 FORMAT(/,5X,'STAGE NUMBER  OUTPUTS:    PU(IV)          PUO(IV)
  1 PU(III)          U(VI)A          U(VI)O          NO3-',/)
325 FORMAT(/,6X,12,19X,E12.5,3X,E12.5,2X,E12.5,2X,E12.5,1X,E12.5,2X,E1
  12.5)
335 FORMAT(/,5X,'STAGE NUMBER  OUTPUTS:    NO3O          H+
  1   HN          HZ          HNO2          HNO2O',/)
345 FORMAT(/,5X,'STAGE NUMBER  OUTPUTS:    EOAP          EOAU
  1   EH3          EH2',/)
355 FORMAT(6X,12,19X,E12.5,3X,E12.5,2X,E12.5,2X,E12.5)
365 FORMAT(/,5X,'STAGE NUMBER',12X,'HOLD UP',13X,'HOLD UP FRACTION',/)
375 FORMAT(/,11X,12,16X,F10.6,10X,F10.6)
385 FORMAT(/,10X,'ALPHA',2X,12,2X,F9.6,10X,'ALPHO',2X,12,2X,F9.6)
*****STOP
END

```

LISTING OF SUBROUTINES USED IN MAIN PROGRAM

DISTRIBUTION COEFFICIENTS EVALUATION SUBROUTINE

```
SUBROUTINE DISTRI(P4A,P3A,HN,H,N03,HNO2,HZ,UA,
1F IS,EOAU,EOAP,EH3,EH2,LL,N)
REAL P4A(23),P3A(23),HN(23),H(23),N03(23),HNO2(23),HZ(23)
1,FIS(23),NO30(23)
REAL K1,K2,K3,K4,K5,KH,KP,KU,IS,N03S,N03I,INTERR
REAL UA(23),EOAU(23),EOAP(23),EH3(23),EH2(23)
DO 386 I=1,LL
W=N03(I)**2
IS=0.5*(N03(I)+H(I)+HN(I)+HZ(I))+2*UA(I)+8*P4A(I)+4.5*P3A(I)
KP=12.163-9.033*IS+2.23*IS*IS-0.163*IS**3
KU=8.791+6.071*IS-6.176*IS*IS+1.579*IS**3
KH=0.385-0.155*IS+0.024*IS*IS
FIS(I)=10** (0.91*SQRT(IS)-1.521)
C=0.731
A1=1+KH*H(I)*N03(I)
A2=UA(I)+KP*P4A(I)*W/KU
A3=P4A(I)+KU*UA(I)/(KP*W)
A4=(A1/N03(I))**2
A5=A4/W
A6=A1/(4*SQRT(KU)*N03(I)*A2)
A7=A1/(4*SQRT(KP)*W*A3)
A8=1-SQRT(1+8*C*KU*A2/A4)
A9=1-SQRT(1+8*C*KP*A3/A5)
EOAU(I)=(A6*A8)**2
EOAP(I)=(A7*A9)**2
B1=KH*H(I)+1/N03(I)
B2=UA(I)*KU+W*P4A(I)*KP
B3=1-SQRT(1+8*C*B2/(B1*B1))
EH3(I)=-B1*KH*B3/(4*B2)
FTBP=0.731-EH3(I)*N03(I)-2*EOAP(I)*P4A(I)-2*EOAU(I)*UA(I)
```

133
IF(FTBP.LT.0.0) FTBP=0.0
EH2(I)=18.5*FTBP
386 CONTINUE
RETURN
END

HOLDUP EVALUATION SUBROUTINE
I. BY USING MCCUTCHEON'S HOLDUP ASSUMPTION: HUH=OR/(1+AQ)

FOR UPPER DISENGAGEMENT STAGE

DDTOR(1)=(1./TOR)*(OR1-OP(1))
DDTAQ(1)=(1./TAQ)*(AP(2)-AP(1))
HU(1)=V1/(1.+OR1/AP(2))
HUH(1)=HU(1)/V1
ENP(1)=OR1*EOAP(1)/AP(2)
ENU(1)=OR1*EOAU(1)/AP(2)
ENH2(1)=OR1*EH2(1)/AP(2)
ENH3(1)=OR1*EH3(1)/AP(2)

FOR STAGE BETWEEN FEED STAGE AND UPPER DISENGAGEMENT SECTION

DO 416 J=2,LL
IF(J.NE.NF) GO TO 43
DDTOR(NF)=(1./TOR)*(OP(N7)-OP(NF)+ORF)
GO TO 416
43 DDTOR(J)=(1./TOR)*(OP(J-1)-OP(J))
416 DDTAQ(J)=(1./TAQ)*(AP(J+1)-AP(J))
DO 426 I=2,N7
HU(I)=VOL/(1.+OR1/AP(I+1))
HUH(I)=HU(I)/VOL
ENP(I)=OP(I-1)*EOAP(I)/AP(I+1)

426
ENU(I)=OP(I-1)*EOAU(I)/AP(I+1)
ENH2(I)=OP(I-1)*EH2(I)/AP(I+1)
426 ENH3(I)=OP(I-1)*EH3(I)/AP(I+1)

FOR FEED STAGE

HU(NF)=(AP(N8)*VOL)/(AP(N8)+OP(N7)+ORF)
HUH(NF)=HU(NF)/VOL
ENP(NF)=(OP(N7)+ORF)*EOAP(NF)/AP(N8)
ENU(NF)=(OP(N7)+ORF)*EOAU(NF)/AP(N8)
ENH3(NF)=(OP(N7)+ORF)*EH3(NF)/AP(N8)
ENH2(NF)=(OP(N7)+ORF)*EH2(NF)/AP(N8)

FOR STAGE BELOW FEED STAGE BUT BOTTOM DISENGAGEMENT SECTION

K=N8
LLL=LL-1
DO 436 I=K,LLL
HU(I)=VOL/(1+OR2/AP(I+1))
HUH(I)=HU(I)/VOL
ENP(I)=OR2*EOAP(I)/AP(I+1)
ENU(I)=OR2*EOAU(I)/AP(I+1)
ENH2(I)=OR2*EH2(I)/AP(I+1)
436 ENH3(I)=OR2*EH3(I)/AP(I+1)

134

FOR BOTTOM DISENGAGEMENT SECTION

DDTAQ(LL)=(1./TAQ)*(AP(LL+1)-AP(LL))
DDTOR(LL)=(1./TOR)*(OP(LL-1)-OP(LL))

```

        HU(LL)=V1/(1+OR2/AP(LL+1))
        HUH(LL)=HU(LL)/V1
        ENP(LL)=OR2*EOAP(LL)/AP(LL+1)
        ENU(LL)=OR2*EOAU(LL)/AP(LL+1)
        ENH2(LL)=OR2*EH2(LL)/AP(LL+1)
        ENH3(LL)=OR2*EH3(LL)/AP(LL+1)
        DDTHU(1)=(V1+OR1*DDTAQ(2))/((AP(2)+OR1)**2.)
        DO 446 I=2,N7
 446 DDTHU(I)=(VOL*OR1*DDTAQ(I+1)-VOL*AP(I+1)*DDTOR(I-1))/((AP(I+1)
 1+OR1)**2.)
        DDTHU(NF)=(VOL*(OP(N7)+ORF)*DDTAQ(N8)-VOL*AP(N8)*(DDTOR(N7)+DDT
 1ORF))/((AP(N8)+OP(N7)+ORF)**2.)
        DO 456 I=K,LLL
 456 DDTHU(I)=(VOL*OR2*DDTAQ(I+1)-VOL*AP(I+1)*DDTOR(I-1))/((AP(I+1)
 1+OR2)**2.)
        DDTHU(LL)=(V1*OR2*DDTAQ(LL+1)-V1*AP(LL+1)*DDTOR(LL-1))/(
 1((AP(LL+1)+OR2)**2.))
        RETURN
        END

```

135

II.USING MIYAUCHIS HOLDUP CORRELATION TO EVALUATE THE HOLDUP

```

        DO 476 I=2,LL
        IF(PSI.GT.0.21) GO TO 636
        HUH(I)=1-0.66*(OP(I-1)*G)**(2./3.)*PSI**(0.84)
        HU(I)=HUH(I)*VOL
        GO TO 476
 636 HUH(I)=1-6.32*(OP(I-1)*G)**(2./3.)*PSI**(2.4)
        HU(I)=HUH(I)*VOL
 476 CONTINUE
        IF(PSI.GT.0.21) GO TO 616
        HUH(1)=1-0.66*(OR1*G)**(2./3.)*PSI**(0.84)

```

```

HU(1)=HUH(1)*VOL
HUH(NF)=1-0.66*(OR2*G)**(2./3.)*PSI**(.84)
HU(NF)=HUH(NF)*VOL
GO TO 626
616 HUH(1)=1-6.32*(OR1*G)**(2./3.)*PSI**(.4)
HU(1)=HUH(1)*VOL
HUH(NF)=1-6.32*(OR2*G)**(2./3.)*PSI**(.4)
HU(NF)=HUH(NF)*VOL
626 CONTINUE
DDTOR(1)=(1./TOR)*(OR1-OP(1))
DDTAQ(1)=(1./TAQ)*(AP(2)-AP(1))

DO 416 J=2,LL
IF(J.NE.NF) GO TO 43
DDTOR(NF)=(1./TOR)*(OP(N7)-OP(NF)+ORF)
DDTAQ(NF)=(1./TAQ)*(AP(N7)-AP(NF))
GO TO 416
43 DDTOR(J)=(1./TOR)*(OP(J-1)-OP(J))
DDTAQ(J)=(1./TAQ)*(AP(J+1)-AP(J))
416 CONTINUE
IF(PSI.GT.0.09) GO TO 866
DDTHU(1)=-(2./3.)*0.66*(OR1*G)**(-1./3.)*VOL*DDTOR(1)*PSI**(.84)
GO TO 876

866 DDTHU(1)=-(2./3.)*6.32*PSI**(.4)*(OR1*G)**(-1./3.)*VOL*DDTOR(1)
876 CONTINUE
DO 596 I=2,LL
IF(PSI.GT.0.21) GO TO 526
DDTHU(I)=-0.66*(2/3)*(OP(I-1)*G)**(-1/3)*PSI**(.84)*VOL*DDTOR(I-1)
1)
DDTHU(NF)=-0.66*(2./3.)*(OR2*G)**(-1./3.)*PSI**(.84)*VOL*DDTOR(NF
1)
GO TO 596

```

```

526 DDTHU(I)=-(2./3.)*6.32*PSI**(2.4)*(OP(I-1)*G)**(-1/3)*VOL*DDTOR(I-
    I)
    DDTHU(NF)=-(2./3.)*6.32*PSI**(2.4)*(OR2*G)**(-1/3)*VOL*DDTOR(NF)
596 CONTINUE
DO 606 I=1,LL
ENP(I)=(VOL-HU(I))*EOAP(I)/HU(I)
ENU(I)=(VOL-HU(I))*EOAU(I)/HU(I)
ENH2(I)=(VOL-HU(I))*EH2(I)/HU(I)
ENH3(I)=(VOL-HU(I))*EH3(I)/HU(I)
606 CONTINUE
RETURN
END

```

III.USING THE PROPOSED HOLDUP CORRELATION TO EVALUATE THE HOLDUP

SUBROUTINE HOLDUP(OP,AP,EOAP,EOAU,EH2,EH3,DDTOR,DDTAQ,HU,ENP,
 1ENU,ENH2,ENH3,DDTHU,N7,DDTORF,LL,NF,TOR,ORF,VOL,
 1VI,OR1,N8,HUH,OR2,TAQ,AQ,PSI,G)

```

REAL      OP(23),AP(23),EOAP(23),EOAU(23),EH2(23),EH3(23),
1DDTOR(23),DDTAQ(23),HU(23)
REAL ENP(23),ENU(23),ENH2(23),ENH3(23),DDTHU(23)
REAL NO3,NO3F,NO3O(23),HUH(23),OR,OR1,OR2,ORF

```

```

REAL PSI
CALCULATE HOLDUPS AND FLOW PARAMETERS

```

USING THE PROPOSED CORRELATION TO EVALUATE THE HOLDUP

```

HUH(I)=(1-(1.4703*(OP(I)*G)**(2./3.)*PSI**(1.15149529)))

```

```
HU(1)=HUH(1)*VOL
DO 396 I=2,LL
  HUH(I)=1-(1.4703*(OP(I-1)*G)**(2./3.)*PSI**(1.15149529))
  HU(I)=HUH(I)*VOL
396 CONTINUE
  HUH(NF)=1-(1.4703*(OR2*G)**(2./3.)*PSI**(1.15149529))
  HU(NF)=HUH(NF)*VOL
  DDTOR(1)=(1/TOR)*(OR1-OP(1))
  DDTAQ(1)=(1./TAQ)*(AP(2)-AP(1))

DO 406 J=2,LL
  IF(J.NE.NF) GO TO 103
  DDTOR(NF)=(1./TOR)*(OP(N7)-OP(NF)+ORF)
  DDTAQ(NF)=(1./TAQ)*(AP(N7)-AP(NF))

  GO TO 406
103 DDTOR(J)=(1./TOR)*(OP(J-1)-OP(J))
  DDTAQ(J)=(1./TAQ)*(AP(J+1)-AP(J))
406 CONTINUE
  IF(PSI.GT.0.09) GO TO 113
  DDTHU(1)=-0.004867*(OP(1)*G)**(-1./3.)*VOL*DDTOR(1)*PSI**(-0.9485)
  GO TO 123
113 DDTHU(1)=-(2./3.)*1.4703*PSI**(1.15149529)*(OR1*G)**(-1./3.)*VOL
  *DDTOR(1)
123 CONTINUE
  DO 143 I=2,LL
  IF(PSI.GT.0.09) GO TO 133
  DDTHU(I)=-0.004867*(OP(I-1)*G)**(-1./3.)*PSI**(-0.9485)*VOL*DDTOR
  I(I-1)
  DDTHU(NF)=-0.004867*(OR2*G)**(-1./3.)*PSI**(-0.9485)*VOL*DDTOR(NF)
  GO TO 143
133 DDTHU(I)=-(2./3.)*1.4703*PSI**(1.15149529)*(OP(I-1)*G)**(-1./3.)*
  IVOL*DDTOR(I-1)
```

```
DDTHU(NF)=- (2./3.)*1.4703*PSI** (1.15149529)*(OR2*G)** (-1./3.)*VOL*
1DDTOR(NF)
143 CONTINUE
DO 416 I=1,LL
ENP(I)=(VOL-HU(I))*EOAP(I)/HU(I)
ENU(I)=(VOL-HU(I))*EOAU(I)/HU(I)
ENH2(I)=(VOL-HU(I))*EH2(I)/HU(I)
ENH3(I)=(VOL-HU(I))*EH3(I)/HU(I)
416 CONTINUE
RETURN
END
```

CHEMICAL REACTION MATERIAL BALANCE EVALUATION SUBROUTINE

SUBROUTINE REACT(P4A,P3A,HN,H,N03,HNO2,HZ,FIS,RXN1,RXN2,RXN3,RXN4
1,RXN5,K1,K2,K3,K4,K5,M,I)

139

```
REAL      TOR,TAQ,OR1,DRF,OR2,N8,NF,VOL,AQ,OR
REAL      P4A(23),P3A(23),HN(23),H(23),N03(23),HNO2(23),HZ(23)
1,FIS(23),N030(23)
REAL K1,K2,K3,K4,K5
REAL RXN1,RXN2,RXN3,RXN4,RXN5

RXN1=K1*(HN(I)**2)*(P4A(I)**2)/(P3A(I)**2*(H(I)**4)*(0.19+N03(I))
1**2)
RXN2=K4*P3A(I)*HNO2(I)*H(I)*N03(I)
RXN3=K3*P4A(I)*HZ(I)
RXN4=K5*HZ(I)*HNO2(I)*H(I)*H(I)
RXN5=FIS(I)*HNO2(I)
IF(HN(I).LE.0) RXN5=0
RETURN
END
```

INPUT DATA LISTED
//GO.SYSIN DD *
INTERSTAGE TIME CONSTANT, FREQUENCY, AMPLITUDE
750.0 750.0 1.0 3.387
TIME INTERVAL FOR EULER'S INTERGATION
1.5
FEED STAGE, TOTAL STAGE NUMBER
5 20
FEED CONCENTRATION
0.05 0.01 0.2 0.4 0.2 0.14 0.0064 0.2
AQUEOUS PHASE FLOW RATE
0.0122222
0.0122222
FLOW RATE AND FEED CONCENTRATIONS: FD1,U(VI)F,HNO2F,FD2
0.07364 0.04832 0.02 0.0255
COLUMN GEOMETRY: SPACING, FREE AREA FRACTION
5.080.23
CCL4 PHYSICAL CONSTANT: INTERFACIAL TENSION ,VISCOSITY,H2O DENSITY, CCL4
DENSITY
16.5 0.011 1.0 1.459
PEASE'S ORIGINFL PROFILES CLOSE TO STEADY STATE
1.49600E-03 1.50800E-01 2.11100E-04 6.50900E-01 140
1.42100E 00 1.83700E-10 2.28000E-01 3.73800E-02
3.14400E 00 6.81100E 00 1.57400E-01 9.15500E 00
1.49600E-03 1.50800E-01 2.11100E-04 6.50900E-01
1.42100E 00 1.83700E-10 2.28000E-01 3.73800E-02
3.14400E 00 6.81100E 00 1.57400E-01 9.15500E 00
5.18800E-03 1.49500E-01 9.66300E-04 7.66400E-01
1.44500E 00 2.37200E-08 2.28100E-01 3.76700E-02
2.65200E 00 6.21800E 00 1.45500E-01 8.89900E 00
1.43200E-02 1.45200E-01 3.38000E-03 7.51600E-01
1.46000E 00 3.24900E-06 2.29200E-01 3.87000E-02
2.17400E 00 5.37100E 00 1.32400E-01 8.11900E 00
3.73400E-02 1.31700E-01 9.99000E-03 7.06200E-01
1.49300E 00 4.76500E-04 2.39500E-01 4.16700E-02

1.47500E 00	4.16700E 00	1.10600E-01	6.88000E 00
2.30300E-02	1.15100E-01	1.01100E-02	6.51800E-01
1.40100E 00	1.13200E-04	3.03800E-01	4.55500E-02
1.72700E 00	4.14600E 00	1.20100E-01	7.38200E 00
1.31300E-02	8.53000E-02	1.10900E-02	6.02200E-01
1.25400E 00	3.42100E-05	3.29800E-01	4.79000E-02
1.78700E 00	3.88600E 00	1.28100E-01	8.08500E 00
5.46700E-03	5.32400E-02	1.29800E-02	5.27700E-01
1.08000E 00	1.24400E-05	3.50700E-01	4.92700E-02
1.57700E 00	3.46400E 00	1.33200E-01	8.87400E 00
9.02300E-04	2.12700E-02	1.70200E-02	4.29600E-01
8.99300E-01	5.28400E-06	3.71700E-01	4.98500E-02
1.12200E 00	2.76900E 00	1.31300E-01	9.55400E 00
5.31600E-05	3.76500E-03	2.24100E-02	3.32300E-01
7.66800E-01	2.52600E-06	3.83700E-01	4.99500E-02
7.43300E-01	2.16500E 00	1.24000E-01	9.96600E 00
0.0	7.05000E-04	2.60700E-02	2.67200E-01
7.04700E-01	1.28400E-06	3.85900E-01	4.99500E-02
5.80500E-01	1.88700E 00	1.19000E-01	1.01500E 01
9.22000E-08	8.80600E-05	2.79400E-02	2.36200E-01
6.78500E-01	6.70900E-07	3.86400E-01	4.99500E-02
5.17200E-01	1.77300E 00	1.16600E-01	1.02200E 01
0.0	1.14300E-05	2.88000E-02	2.23400E-01
6.67500E-01	3.53900E-07	3.86400E-01	4.99500E-02
4.91600E-01	1.72500E 00	1.15500E-01	1.02500E 01
1.08900E-10	4.35800E-06	2.91700E-02	2.18100E-01
6.63000E-01	1.87400E-07	3.86400E-01	4.99500E-02
4.81100E-01	1.70500E 00	1.15000E-01	1.02700E 01
0.0	4.33800E-06	2.93300E-02	2.15900E-01
6.61100E-01	9.94600E-08	3.86500E-01	4.99500E-02
4.76700E-01	1.69700E 00	1.14800E-01	1.02700E 01
7.32600E-13	4.33800E-06	2.93900E-02	2.15000E-01
6.60300E-01	5.28100E-08	3.86500E-01	4.99500E-02
4.74900E-01	1.69300E 00	1.14700E-01	1.02700E 01
4.65100E-13	4.34100E-06	2.94000E-02	2.14600E-01
6.59900E-01	2.81300E-08	3.86500E-01	4.99500E-02

4.74200E-01	1.69200E 00	1.14700E-01	1.02800E 01
4.43100E-13	4.38800E-06	2.93300E-02	2.14500E-01
6.59600E-01	1.94300E-08	3.86500E-01	4.99500E-02
4.73900E-01	1.69200E 00	1.14700E-01	1.02800E 01
3.74800E-12	4.74300E-06	2.90000E-02	2.14500E-01
6.58900E-01	2.25100E-07	3.86500E-01	4.99500E-02
4.73800E-01	1.69400E 00	1.14800E-01	1.03000E 01
0.0	6.44700E-06	2.77100E-02	2.14800E-01
6.56400E-01	9.24600E-06	3.86900E-01	4.99600E-02
4.73800E-01	1.70200E 00	1.15300E-01	1.03700E 01
2.44400E-09	9.90500E-06	2.25000E-02	2.14400E-01
6.46000E-01	3.17200E-04	3.88700E-01	4.99600E-02
4.70200E-01	1.72100E 00	1.16600E-01	1.06900E 01
2.44400E-09	9.90500E-06	2.25000E-02	2.14400E-01
6.46000E-01	3.17200E-04	3.88700E-01	4.99600E-02
4.70200E-01	1.72100E 00	1.16600E-01	1.06900E 01

/*
//GO.FT14F001 DD DSNAME=&SM,UNIT=SC3TCH,DISP=(NEW,PASS),
// SPACE=(800,(120,15)),DCB=(RECFM=FB, LRECL=796, BLKSIZE=800)
//SMPLTTR EXEC PLOT,PLOTTER=PRINTER
//

142
SMPLT1/3
SMPLT2/3
SMPLT3/3